CIV5000W: DISSERTATION FOR THE DEGREE OF MASTER OF SCIENCE

Effectiveness of high strength repair mortars in structural patch repairs of concrete members under axial compression.

Prepared by:

Vafa Naraghi

Supervised by:

Prof Hans Beushausen

Dissertation submitted in fulfilment of the requirements for the degree of "MSc in Civil Engineering specialising in Structural Engineering"

Department of Civil Engineering

University of Cape Town, Private Bag X3, Rondebosch,

South Africa, 7701

Declaration

I, Vafa Naraghi, know the meaning of plagiarism and declare that all the work in this document, save for that which is properly acknowledged, is my own.

Signed: Signed by candidate Date: 2 December 2021

Acknowledgements

First, and foremost, I would like to acknowledge The Almighty God for the abundance, aid and assistance throughout all my endeavours. As well as the Baha'i Faith, for creating a strong sense of purpose in my life to be of service to mankind.

Marina and Sefidvash. My beloved parents and the funniest humans I know. Thank you for being ever-supportive and patient with your unmarried eldest child. I do not take it for granted.

To my future wife, wherever you are. Good luck and all the best.

Safa and Sama, my younger brothers. Thank you for always being there for me. I look up to you guys for reasons other than me being the shortest amongst the three of us.

My supervisor, Professor Hans Beushausen. A remarkable academic with an above-average sense of humour for a German. Thank you for your continual support and guidance through this journey.

Mr Nicholas Jarratt (eventually to be Doctor). Thank you for availing yourself on countless occasions for our discussions, reviews, re-reviews, remarks and comments on my work. Concrete repair brothers for life.

To the staff at the University of Cape Town Civil Engineering laboratories. Nooredien Hassen and the late Taahir Mukaddam, may his soul rest in peace, as well as Messrs. Charles May, Christopher Caesar, Elvino Witbooi and Leonard Adams. Thank you for all the assistance as well as imparting your priceless knowledge and experience.

Chris Mapane, my stand-up comedy mentor and dear friend. Thank you for getting us over the line. Your contribution has been monumental.

Siyamthanda Songca, Jesse Twum-Boafo, Baraka Msulwa, Oscar Mokhele, Sesethu Simelela, Lusanele Magwa and Candice Foot. Thank you for your ever-present friendship and support as well as the countless distractions, without which I would have completed this work a year earlier.

Lastly to Jurgen Klopp and Liverpool Football Club. Thank you for delivering the Champions League, FIFA Club World Cup and English Premier League trophies in the time I took to complete this degree. Top drawer stuff.

Vafa Naraghi
Master of Science in Civil Engineering specialising in Structural Engineering
University of Cape Town, South Africa

Abstract

There is a dearth of knowledge and research into the performance and efficacy of repair materials used in structural concrete patch repair applications. The repercussions of this have led to the development of repair standards and guidelines that fail to adequately cover requirements for structural repair, often poor repair material choice, and ultimately concrete repair failure. This research set out to determine the efficacy of high strength cement-based materials in structural patch repair of concrete elements under axial compression. This was determined with respect to the ability of the repair material to contribute to load sharing in the repaired element under service loads. Three commercially available high strength cement-based repair materials were tested for their strength, elastic modulus, shrinkage and creep properties. The tested repair material properties were then used as inputs into an analytical model to determine the distribution of stress in the repaired element over-time. The research has shown that the repair materials do not contribute to load sharing in the long term for patch repaired concrete elements under axial compression. Thus, ‘structural’ repair materials and ‘structural’ patch repairs are considered ineffective in the context of the simulations conducted in this research. The analytical model may be used to inform repair material choice as well as a basis for future research within the field of structural concrete patch repairs.

Table of contents

List of tables

List of figures

1. Introduction

1.1 General introduction

Concrete is the most utilised construction material in the world (Acker & Ulm, 2001; Baldwin & King, 2003). Steel Reinforced Concrete (RC), in most structures, works to distribute and support loads and stresses in an effective and safe manner. Throughout a RC structure's service life, the structure undergoes deterioration and damage due to environmental or imposed conditions. Repair and rehabilitation of RC structures has become a common requirement in modern construction (Mangat & O'Flaherty, 2000). The most significant cause of deterioration in RC structures is the corrosion of steel reinforcement (Glass, 2003). In the repair of such RC structures, often part of the concrete requires restoration. Concrete patch repair techniques are commonly used in such restoration applications.

Concrete patch repairs are broadly categorised into structural and cosmetic repairs. Structural patch repairs are expected to carry loads or stresses and contribute to load sharing in the repaired concrete element.

In structural patch repairs, it is desirable that both the substrate concrete and repair material are dimensionally compatible (Emberson & Mays, 1990a; Emmons & Vaysburd, 1994; Cusson & Mailvaganam, 1996; Morgan, 1996; Decter & Keeley, 1997). Premature failure of structural patch repair is often as a result of differential stresses and strains between the repair material and substrate concrete. The stress and strain distribution in a repaired concrete system is dependent on the properties of the substrate concrete and the repair material, as well as their interaction with each other, in response to environmental conditions and imposed loads.

The modulus of elasticity, Poisson's ratio, shrinkage, creep, coefficient of thermal expansion and contraction, are the main material properties that significantly affect dimensional compatibility (Emberson & Mays, 1990a; Emmons & Vaysburd, 1994; Cusson & Mailvaganam, 1996; Morgan, 1996; Decter & Keeley, 1997). Emberson & Mays (1990a) recommended a set of general requirements for patch repair materials for structural compatibility, which are presented in Table 1-1. Several other researchers have made similar recommendations (Wood, King & Leek, 1990; Mays & Barnes, 1995; Morgan, 1996; Decter & Keeley, 1997).

High strength cement-based mortars are often used in structural patch repair applications. During curing and hardening, the physical material properties of cement-based materials develop. The development of compressive strength and elastic modulus properties occur, while creep and shrinkage strain developments are more sensitive to the environment and loading conditions. In the long-term, most physical material properties become more stable as development rates plateau; However, creep, and to an extent shrinkage strains, may still continue for several years. High strength repair mortars are particularly favoured for their rapid early-age compressive strength development, reaching and often surpassing the strength of the substrate concrete. Much emphasis is given to the compressive strength of the repair mortar, with a

common misconception that higher strength equates to high quality (Beushausen & Arito, 2018). Emphasis on rapid early-age strength development is often done at the expense of other properties such as crack resistance, durability, creep and shrinkage. Differential shrinkage and creep strains in the repair material cause the shedding of stress from the repair material to the substrate concrete overtime, resulting in little to no load sharing contribution from the repair material (Mangat & Limbachiya, 1994; Oluokun, Burdette & Deatherage, 2010; Pan & Meng, 2016). There remains a dearth of research into the efficacy of high strength repair mortars with respect to load sharing and carrying capacity of repaired concrete elements, when used in structural patch repair applications.

Table 1-1: General requirements of patch repair materials for structural compatibility adopted from Emberson & Mays (1990a)

Property	Relationship of repair material (R) to concrete substrate (C)
Strength in compression, tension and flexure	$R \geq C$
Modulus in compression, tension and flexure	$R \approx C$
Poisson's ratio	Dependant on modulus and type of repair
Coefficient of thermal expansion	$R \approx C$
Adhesion in tension and shear	$R \geq C$
Curing and long term shrinkage	$R \leq C$
Strain capacity	$R \geq C$
Creep	Dependent on whether creep causes desirable or undesirable effects
Fatigue performance	$R \geq C$

1.2 Background and previous research projects

Emberson & Mays (1990a) carried out material characterisation tests to measure the physical properties of nine generic types of repair systems which included resin-based and cement-based repair materials. Their findings included the following:

- All the repair materials tested are suitable for structural patch repair based on compressive strength values;
- The modulus values of resin-based repair materials are significantly lower than in cement-based repair materials and the substrate concrete;

- Thermal coefficients of resin-based repair materials are significantly higher than in cement-based repair materials and the substrate concrete and;
- Most of the repair materials underwent shrinkage and creep strain.

Emberson & Mays (1990b) carried out experimental methods and Finite Element Method (FEM) techniques to elucidate the axial load transfer in a repaired concrete element under axial tensile loading, focussing on the effects of varying modulus of elasticity and Poisson's ratio properties of the repair material. They found that for effective load transfer and avoidance of stress concentrations in the repaired member, the modulus of elasticity and Poisson's ratio of the repair material should not be significantly different (i.e. in the order of 10 GPa) from the substrate concrete. Emberson & Mays (1996) conducted a follow up study on repaired concrete elements under flexural loading and found the importance matching repair material and substrate concrete elastic modulus properties. Shambira & Nounu (2000, 2001) conducted laboratory experiments and FEM techniques on repaired RC columns under axial compressive loading. The authors found that the transfer of stresses from the repair material to the substrate concrete, over a six week period, to be attributed to the shrinkage and creep strain properties of the repair material. Mangat & O'Flaherty (1999a,b, 2000) conducted a series of experimental work on the strain distribution in patch repairs on columns and abutments of an existing concrete bridge in use, over an initial period of 12 months. They found that repair materials with elastic modulus higher than the substrate material, as well as having low creep characteristics, were most effective in attracting external applied loads in the long term.

The modulus of elasticity, shrinkage and creep properties of the repair material were found to be the most influential in the long-term stress and strain distribution in repaired concrete elements (Shambira & Nounu, 2000). However, the aforementioned studies had limitations in quantifying the global effect of all these properties on the stress and strain distribution in repaired concrete elements under axial compression. According to Canisus & Waleed (2004), researchers have considered different problems or only a limited number of influencing parameters in their studies, thus limiting the universal applicability of their recommendations. The modulus of elasticity, shrinkage and creep properties and their respective influence on stress and strain mechanisms in repaired concrete elements under axial compression are briefly discussed below. Refer to the literature review (Chapter 2) for a comprehensive review of the material properties and their mechanisms.

The elastic modulus of a material is a measure of its stiffness and determines the degree to which it deforms under a given stress. This property also influences the distribution of stresses in the cross section of the repaired concrete element. The material with the higher elastic modulus will attract more stress in the cross-section of the repaired element. Repair materials undergo more shrinkage strains as their physical properties develop, compared to the more stable substrate concrete, which undergoes negligible shrinkage strain. Differential shrinkage strain between the repair material and the substrate concrete inhibits the repair material in attracting compressive loads and thus causes a redistribution of stress into the substrate concrete of the repaired member.

Under sustained compressive stress, repair materials undergo viscoelastic compressive creep strain over time, compared to negligible creep strain in the aged substrate concrete. Similar to the action of differential shrinkage strain in the repaired concrete element, differential compressive creep strain between the repair mortar and the substrate concrete results in compressive stresses being shed from the repair material to the substrate concrete.

The International Organization for Standardization (ISO), European Standards (ENs) and American Concrete Institute (ACI) have developed documents to standardize and regulate the repair and maintenance of concrete structures. The ISO 16311 (2014) series outlines high level concrete repair principles but has not been fully developed to be used as a code of practice for repair design and repair material selection; for which the ISO series references EN and ACI documents. The EN and ACI documents provide guidelines and recommendations for repair design and repair material selection, however they have their limitations.

With respect to structural patch repair of concrete elements under axial compression, the limitations in the existing standards and guidelines include: not considering all the net influences of the different material properties on the stress and strain distribution in the repaired concrete system and; containing material property testing methods that are not representative of actual repair conditions. The EN 1504-3: 2005, for structural and non-structural repairs, characterizes repair materials based on their compressive strength and modulus of elasticity properties among other factors. Less significance is given to shrinkage and viscoelastic creep properties of the repair materials which have a greater effect on the long-term stress and strain distribution in structurally repaired concrete elements. The ACI guide equivalent for repair material selection, ACI 546.3R-14, provides a general overview of the important material properties of the different types of repair materials, without guidance to their effect on stress and strain distribution in the repaired system. The EN and ACI documents contain material characterization testing standards which are not representative of actual repair conditions; these testing standards are often adopted from existing standards for new structures.

The absence of an authority documentation with representative material characterization testing methods, allows proprietary material manufacturers and suppliers to modify existing material property testing methods or use non-standard testing methods in order to present their products more favorably. This makes it difficult for the specifier to select between similar repair materials, with reported properties based on different test methods. The limitations with the existing standards, guidelines and recommendations puts greater responsibility on the repair designer in understanding structural concrete patch repairs and the implication of the various repair material properties on the repair itself.

1.3 Problem statement

Research on the effectiveness of structural patch repairs has largely been focused on evaluating the static ultimate load carrying capacity of repaired elements (Mays & Barnes, 1995; Emberson & Mays, 1996; Río et al., 2005; Pellegrino, Porto & Modena, 2009; Pellegrino, Da Porto &

Modena, 2011; Da Porto, Stievanin & Pellegrino, 2012; Ortega et al., 2018a; Kristiawan et al., 2019). Experimental methods and non-linear finite element modelling (FEM) techniques have been used to evaluate the ultimate load carrying capacity of repaired concrete beams, columns and frames. The findings of such studies are useful in understanding the effects of repair material properties in the distribution of stresses and strains to failure loading in a structurally repaired concrete element at a given point in time. However, they do not sufficiently describe the effects of repair material properties on the stress and strain distribution in the repaired concrete element over time, under service loading conditions.

There is a dearth of research and resources available to determine the stress and strain distribution over time in structural patch repairs subjected to service loads, and thus no practical method in determining their structural effectiveness in sharing load in a repaired concrete member.

1.4 Research aim

The aim of this dissertation is to determine the efficacy of high strength repair mortars in structural patch repairs of concrete elements under axial compression, with respect to load sharing when subjected to service loads over time.

1.5 Research objectives

The research objectives of this dissertation are to:

i. Identify, through a review of literature, the key repair material properties, the substrate material properties, various structural mechanisms, environmental and imposed conditions that determine stress and strain distribution in a patch-repaired concrete element over time.

ii. Characterise proprietary high strength repair mortars for compressive strength, elastic modulus, shrinkage and creep properties and their development over time through experimental methods.

iii. Develop an analytical model of a repaired concrete element under axial compressive loading representing the multi-aspect effects identified in (i) as well as incorporating the material properties characterised in (ii).

iv. Determine, using the analytical model developed in (iii), the distribution of stress and strain in the repaired concrete element under different dimensional characteristics and loading conditions.

v. Determine the efficacy of the use of high strength repair mortars used in structural concrete patch repairs of concrete elements under axial compression.

1.6 Research questions

The key research questions in conducting this research are:

i. What are the strength, elastic modulus, shrinkage and creep properties of high strength cement based mortars?

ii. How do these properties develop at early ages?

iii. What is the effect early age loading on the creep properties of such materials?

iv. Can high strength cement-based repair mortars achieve dimensional compatibility with the substrate concrete?

v. How is time-dependent stress distributed in a repaired concrete member under axial compression?

vi. What are the effects of elastic modulus, shrinkage and creep properties on the distribution of stress within the concrete member in the short term?

1.7 Limitations

The distribution of stresses and strains in a repaired system is dependent on several inter-dependent aspects. For the purpose of this research some of these aspects have been simplified. These simplifications are briefly discussed below, refer to the literature review (Chapter 2) and model development (Chapter 5) for more details on the implications of such simplifications.

In modelling the repaired concrete element, the magnitude of stress and strain in each of the materials, i.e. the substrate concrete and repair mortar, is taken as uniform throughout the respective cross-sections. This research is concerned with the global stress distribution between the substrate concrete and the repair mortar and thus a uniform model for stress distribution will suffice.

In this research, the effects of force eccentricity and bending were ignored in the modelling of stress and strain distribution in the repaired element under axial compression. The repaired elements were assumed to have “short column” characteristics.

In the analytical model, the strain due to shrinkage was measured and modelled as one-dimensional, i.e. the direction parallel to the application of axial loading. Although shrinkage is a three-dimensional phenomenon, in the case of an axially loaded element the shrinkage in the two directions perpendicular to axial loading have negligible bearing on the structural mechanism of the element.

The bond at the interface between the substrate concrete and the repair mortar is assumed to be perfect, i.e. the two materials behave monolithically. In reality, the bond between the two materials is not perfect and is dependent on various factors. This may cause discontinuities in transferring load from one material to the other. Modelling of the bond requires more research and the use of non-linear numerical methods which is beyond the scope of this dissertation.

The model ignores the effects due to thermal expansion/contraction, inclusion of reinforcing steel in the repair, and the materials' Poisson's ratio. The material and mechanism testing for the above was not carried out in the experimental work in this dissertation.

The experimental research is limited to the testing and analysis of high strength cement-based proprietary repair mortars. Resin-based and polymer modified repair materials were not examined.

1.8 Research framework and dissertation layout

The layout of the dissertation and respective chapters follow the framework detailed in Figure 1-1.

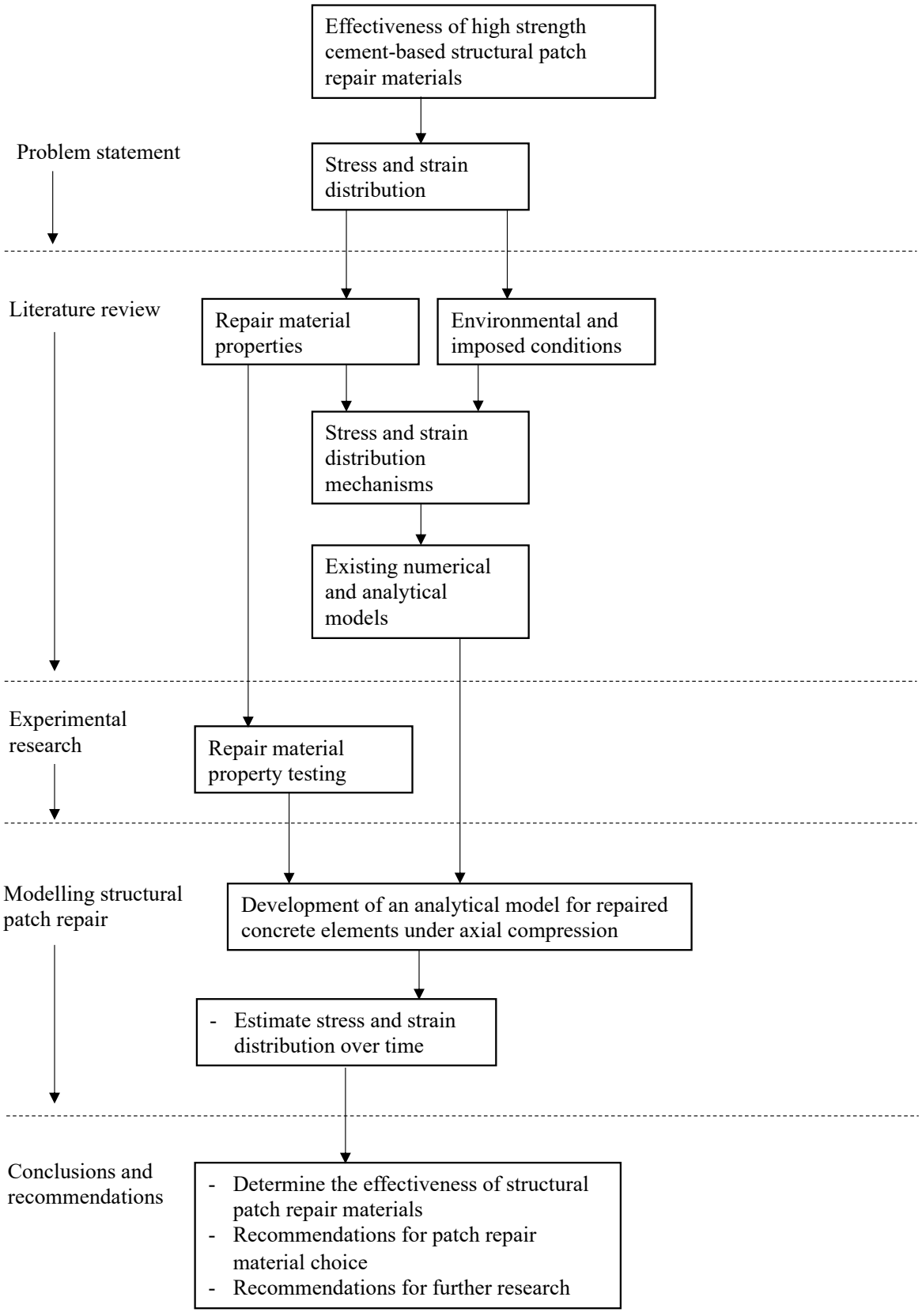

Figure 1-1: Research framework and dissertation layout

2. Literature Review

The following chapter provides a critical review of literature on structural patch repairs of concrete elements, with a focus on the repair materials properties and their influence on stress and strain distribution in the repair element. Structural patch repairs and repaired concrete elements under axial compressive loading form the focal point, however reference to other loading and non-loading conditions are made where applicable. The cause of damage to concrete elements, type of patch repairs as well as common modes of failure of concrete repairs are presented to provide context and background. The current standards, codes of practice and guidelines governing the application of patch repairs, as well as a review of literature on key properties of repair materials and their influence on patch repairs are presented. Aspects of material property interaction due to various imposed loading and environmental conditions in a repaired system are reviewed. Finally, models and theorems used to describe and estimate the load bearing capacity and stress-strain behaviour in repaired elements are presented.

2.1 Repair of reinforced concrete structures

Concrete is the most utilised construction material in our built environment (Acker & Ulm, 2001; Baldwin & King, 2003). As concrete structures age, they undergo deterioration and damage due to environmental and imposed conditions. The repair and rehabilitation of concrete structures has become a common requirement in modern construction (Mangat & O'Flaherty, 2000). Considering that most existing concrete structures built in the 1960s and 1970s have exceeded their design life, the demand and need for repair and maintenance of concrete structures has increased.

The need for, and the associated cost of, repair and maintenance of infrastructure is high in modern construction. The American Society of Civil Engineers (ASCE) (2017) reported an overall D+ (Poor, At Risk) rating on the condition infrastructure in the USA, estimating a budgetary requirement of USD 4.59 trillion to be spent over 10 years between 2016 and 2025 in repairing and maintaining current infrastructure. The South African Institute of Civil Engineers (SAICE) (2017) reported a similar condition rating of D+ (At risk of failure) of infrastructure in South Africa during their 2017 infrastructure report card. The primary function of most structures is to support and distribute imposed loads in an effective and safe manner, failure of which may result in damage to property and life.

In structures, steel reinforced concrete (RC) is a composite material that works to distribute and support loads and stresses in an effective and safe manner. The most significant cause of deterioration in RC structures is the corrosion of steel reinforcement (Glass, 2003).

2.1.1 Brief insight into concrete deterioration and reinforcement corrosion

It is important to understand the cause of damage to RC structures prior to conducting a repair. Deterioration of RC may result from a number of influences, including incorrect design, poor

workmanship, poor quality of materials, environmental influences and imposed loading conditions on the structure. Reinforcement steel corrosion is found to be the dominant degradation mechanism in 70-90% of cases where RC structures have undergone premature deterioration (Angst, 2018). A combination of insufficient concrete cover, poor concrete quality and exposure of harsh environments is a common cause leading to the corrosion of steel reinforcement in RC structures.

Corrosion is defined as the attack of a metal through a chemical or electrochemical reaction with its surrounding environment (Revie & Uhlig, 2008). The term "rusting" is associated with the corrosion of ferrous metals like iron and its alloys. When metals rust, corrosion products are formed from the electrochemical reaction, consisting largely of hydrous ferric oxides.

The electrochemical reaction that takes place during corrosion involves the formation of corrosion cell. A corrosion cell is formed when there is a flow of electric current between two electrodes (i.e. the anode and cathode) with different electric potentials. The electric current flow is facilitated through a conducting environment (i.e. electrolyte) allowing for the movement of ions and an electrical link between the anode and the cathode to enable the flow of electrons. Figure 2-1 shows the electrochemical reaction and components of a typical corrosion cell in a RC structure undergoing corrosion.

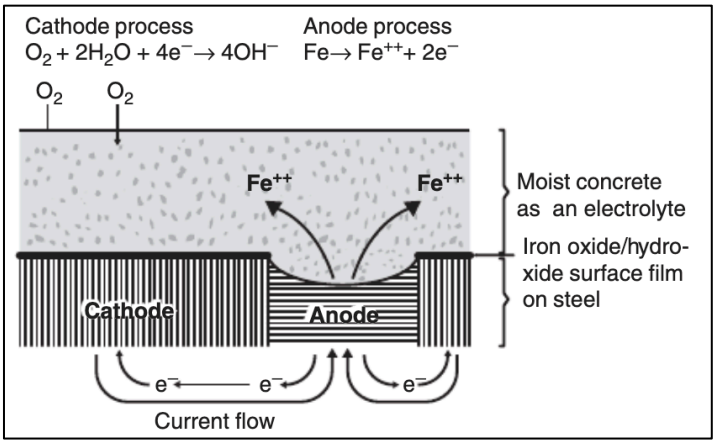

Figure 2-1: Typical RC concrete corrosion cell adopted from Mehta & Monteiro (2014)

The difference in electrochemical potentials needed to form a corrosion cell may be developed in two ways. This may be developed by either the connection of two dissimilar metals embedded in the concrete or; differences in the concentration of dissolved ions in the concrete in the vicinity of the reinforcement steel. The corrosion cell in Figure 2-1 represents the latter scenario. In the formation of the corrosion cell, one of the metals (or part of the same metal in the case of a single type of metal being present) becomes anodic and the other cathodic. A typical chemical reaction at the anode and cathode of an iron corrosion cell is shown in Figure 2-2.

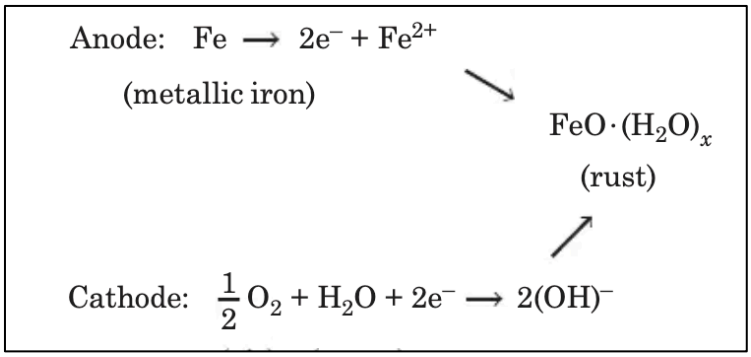

Figure 2-2: Anode and cathode reaction of an iron corrosion cell adopted from Mehta & Monteiro (2014)

Once the corrosion cell is formed, both the cathodic and anodic reactions need to be maintained for corrosion to progress. The cathodic reaction is dependent on the presence of air and water and the anodic reaction involving the ionisation of the metallic iron needs to be maintained by ensuring that the electrons are allowed to flow to the cathode through a constant link. Iron and metal products are covered with a film of iron-oxide which becomes impermeable in alkaline environments, such as concrete. The presence of this film prevents the anodic reaction from taking place and thus rendering the reinforcement steel passive to corrosion. This phenomenon is known as the passivation of steel in concrete (Mehta & Monteiro, 2014).

Reinforcement steel passivation in concrete, due to the iron-oxide film, is attributed to the alkalinity of the electrolyte in the concrete pores. The alkalinity of the hydrated cement paste, a saturated solution of calcium hydroxide in the pore solution, is high, with a pH typically above 12.5. A pH of 11.5 is reported to be sufficient to keep the protective iron-oxide film intact in the absence of chloride ions. The presence of chloride ions in the vicinity of the reinforcement steel are reported to destroy the protective film (Mehta & Monteiro, 2014). The protective film may also be destroyed through the ingress of cardon dioxide in the concrete paste, as the alkalinity of the pore solution is reduced to a pH below 11.5. The concrete cover plays a critical role in preventing the ingress of aggressive agents such as carbon dioxide and chloride ions. The cover depth, permeability of the concrete, pH of the pore solution and the presence of cracks in the concrete cover are some of the factors that determine the passivation of steel in concrete and thus protect the steel from corrosion. In the event that the passivity of the embedded steel is removed, the availability of oxygen, water and electrical resistivity determine the rate at which corrosion occurs.

Once corrosion occurs, products such as iron oxides, iron hydroxides or iron oxyhydroxides form on the surface of the metal. These products are referred to as rust in ferrous metals. Metallic irons are transformed to rust, often accompanied by a change in volume. In some cases, the volume change translates to more than 6 times the original volume. Figure 2-3 compares the volume of typical corrosion products to the volume of the original metallic iron.

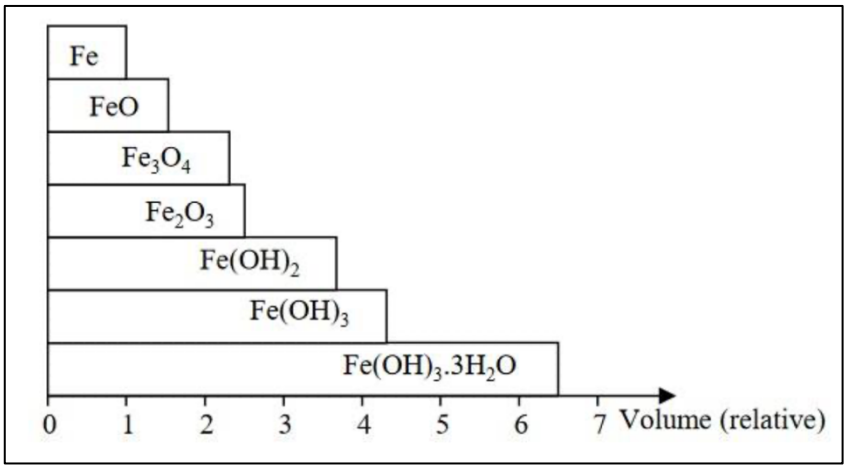

Figure 2-3: Volume of corrosion products in comparison to metallic iron adopted from Mehta & Monteiro (2014)

The increase in volume occupied by the corrosion products causes stresses to develop in the concrete cover leading to cracking, delamination and eventually spalling of the concrete. The damage to the RC structure as a result of corrosion of the embedded reinforcement steel may include damage to the concrete, loss of the bond between steel and concrete and loss of reinforcement cross-sectional area. The implications of such damage may result in a decrease in load bearing capacity of the RC structure, compromising the safety of the structure.

2.1.2 Concrete repair process

Mays (1999) outlined a process to be taken to for appropriate design for the protection and repair of concrete structures. The process outlined involves a number of steps:

- assessment of the condition of the structure;
- identification of the causes of deterioration;
- deciding the objectives of protection and repair;
- selection of the appropriate principles for protection and repair;
- selection of methods;
- definition of properties of products and systems;
- specification of maintenance requirements following protection and repair.

The above process formed the foundation to which the European Standards were designed. Several other guidelines and standards follow a similar process of development, for the design and implementation of concrete repairs.

2.1.3 Standards, guidelines and specifications

Towards the end of the 20th century, research within the field of concrete repair had pointed towards the need to develop a standard design for concrete repairs. Till that point, design of repairs was usually left to the discretion and experience of the design engineer or specialist contractor. Emberson & Mays (1990a), Emmons & Vaysburd (1994) and Mangat & Limbachiya (1994) were among the early researchers advocating for the development of engineering principles or a code of practice to inform concrete repair design and application. It was Emmons & Sordyl (2006) who spearheaded the drive towards the development of a code of practice in a "Vision 2020".

Since the early 2000s, significant progress has been made in developing standards, guidelines and recommendations to inform concrete repair design and application. The International Organization for Standardization (ISO), European Standards (ENs) and American Concrete Institute (ACI) have developed documents to standardize and regulate the repair and maintenance of concrete structures. These documents are, however, limited in providing information and guidance for appropriate structural patch repair design and repair material selection. The organization, principles and limitations of these documents are briefly reviewed in the sections below.

2.1.3.1 European Standard EN 1504

The European Standard EN 1504, products and systems for the protection and repair of concrete structures, consists of 10 main standards, with reference to 61 testing standards. Parts 2 to 7, of the standard, are the basis to regulate the products and systems used for protection and repair of concrete structures, supported by the 61 test method standards. Parts 1, 8, 9 and 10 provide support and guidelines to the use of the standards. The structure of the European Standard EN 1504 is represented in Figure 2-4 below.

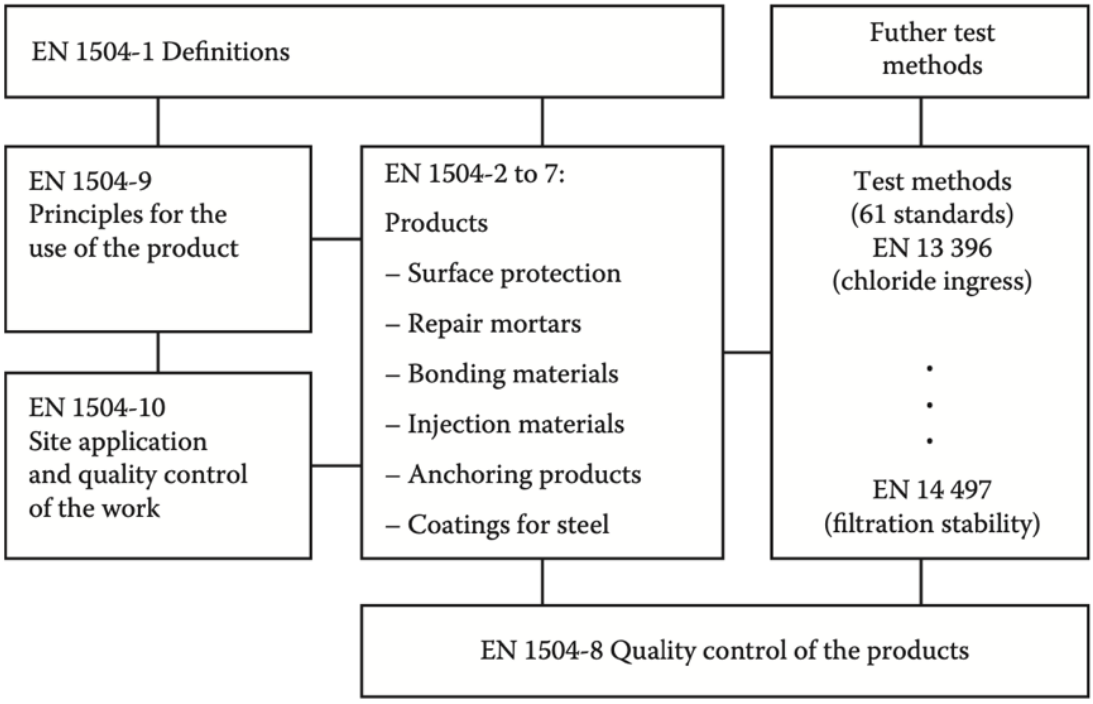

Figure 2-4: Structure of European Standards EN 1504-1 to -10, for protection and repair of concrete structures - adopted from Raupach & Büttner (2014)

The system of planning and executing a repair to a concrete structure, using the European Standard EN 1504 series, consists of a hierarchy of levels, namely, options, principles and methods. The options are a list of appropriate actions to be taken to ensure the structure meets its intended performance for the remainder of its service life. These include the following:

- do nothing;
- re-analyse the structural capacity;
- prevent or reduce further deterioration;
- strengthen or repair;
- reconstruct or replace or;
- demolish all or part of the concrete structure.

Principles for the repair and protection of the concrete structure are divided into two main categories, principles for defects in concrete and principles for protection against reinforcement corrosion. The eleven principles defined in EN 1504-9 are summarised in Table 2-1 and Table 2-2, for the two respective categories. These principles may be used separately or in combination in the protection and repair of the concrete structure. EN 1504-9 prescribes 43 methods by which the above principles for the protection and repair of concrete structures can be met. Several methods can be used in combination to meet the requirements of the principles. However,

EN 1504 does not cover all 43 methods listed, with some methods covered in other standards and others yet to be standardised. Each repair method is expected to meet certain performance requirements, detailed in EN 1504-9. Further to this, the performance requirements of products used in each method, are contained in EN 1504-2 to -7.

Table 2-1: Principles and methods related to defects in concrete (EN 1504-9: 2008)

Principle Number	Principle and definition
Principle 1 [PI]	Protection against ingress
Principle 2 [MC]	Moisture control
Principle 3 [CR]	Concrete restoration
Principle 4 [SS]	Structural strengthening
Principle 5 [PR]	Physical resistance
Principle 6 [RC]	Resistance to chemicals

Table 2-2: Principles and methods related to reinforcement corrosion (EN 1504-9: 2008)

Principle Number	Principle and definition
Principle 7 [RP]	Preserving or restoring passivity
Principle 8 [IR]	Increasing resistivity
Principle 9 [CC]	Cathodic control
Principle 10 [CP]	Cathodic protection
Principle 11 [CA]	Control of anodic areas

Principles 3 and 4 in Table 2-1 are applicable to structural patch repairs. The repair materials used under these principles, both for structural and non-structural applications, are expected to meet performance requirements listed in Part 3 of the EN series, EN 1504-3: 2005. Structural repair materials are classified as either type R3 or R4 under the code, primarily characterized by their compressive strength and modulus of elasticity properties. Table 2-3 represents a reduced list of the performance requirements for structural repair materials, mostly comprised of the mechanical performance requirements.

Table 2-3: Reduced list of performance requirements for structural repair products (EN 1504-3: 2005)

Performance characteristic	Testing method	Class R4	Class R3
Compressive strength	EN 12190	≥ 45 MPa	≥ 25 MPa
Adhesive bond	EN 1542	≥ 2,0 MPa	≥ 1,5 MPa
Restrained shrinkage	EN 12617-4	≥ 2,0 MPa	≥ 1,5 MPa
Elastic modulus	EN 13412	≥ 20 GPa	≥ 15 GPa

The repair material properties for the performance requirements in Table 2-3 are determined through various test methods. The compressive strength and elastic modulus properties are tested using conventional test methods for such material properties. The adhesive bond and restrained shrinkage test methods are similar in some respects. In both test methods, parent substrate concrete slab are cast and left to dry for a 6 month period, after which the surface is prepped before the repair material is cast over it. The test specimens are then allowed to cure in a water bath for 28 days. For the adhesive bond test, cores are drilled into the specimen after the curing period. Pull-off tests are conducted on the core samples to determine the strength of the bond. In the case of the restrained shrinkage test, after the 28-day water curing, the test specimens are inspected for any cracks or delamination before being left to air-dry for a 6 month period. The specimens are again inspected for any cracks or delamination before core samples are drilled. Pull-off tests are conducted to determine the strength of the bond after the extent of restrained shrinkage has occurred.

For structural repairs, it is expected that the repair material contributes towards the distribution of stress and/or enhance the load bearing capacity of the repaired element. The material properties of the substrate concrete and repair material that are most significant to the distribution of stresses in the repaired member are the elastic modulus, shrinkage and creep properties. The mechanisms and significance of these material properties are reviewed in more detail in Section 2.2. EN 1504-3: 2005 lists values for the elastic modulus properties of the repair material, however, less mention is given to shrinkage and viscoelastic creep properties of the repair materials. The performance requirement related to restrained shrinkage is a closer measure of resistance to crack development and propagation, which is not a direct measure of the material's performance in structural applications. Material manufacturers may be encouraged to produce repair materials that meet the requirements as per the code, as opposed to material that are suitable for structural patch repairs.

The test methods referenced in the EN 1504 series, with respect to repair material characterization, are similar to those for concrete used in normal construction. The environmental and loading conditions of these tests do not necessarily represent those that the repair material may be subjected to in application. For example, the repair material may be subjected to loading

prior to 28 days after application. In this case the material would not have achieved the compressive strength as characterized by the material tests. In cases where the test methods have yet to the standardized in the code, material manufacturers and suppliers may be led to modify existing test methods or use non-standard test methods in order to present their products more favorably.

The European Standard EN 1504 series has a good hierarchy of levels to guide concrete repairs conceptually; however, it lacks detail in the methods and performance characteristics for application of the repair. The series may be able to guide repair philosophy but requires refinement in order to be used as an effective tool to inform structural patch repair design and repair material selection.

2.1.3.2 ACI repair code and guidelines

The American Concrete Institute (ACI) has developed documents to guide the design and construction of concrete repairs. The documents range from providing guidance on assessment of damaged concrete structures and repair design, to repair material selection and application of concrete repairs.

The ACI 562, *Code Requirements for Assessment, Repair, and Rehabilitation of Existing Concrete Structures and Commentary*, was developed to provide a code for the assessment of concrete damage and deterioration and the design of appropriate repair strategies, for professionals involved with concrete repair. Since the inception of the code in 2013, there have been two successive revisions of the code, the most recent being ACI 562-19. The code provides minimum requirements for the assessment and repair of concrete structures. According to Kesner & Conroy (2017), the ACI 562 is a performance-based code that provides repair design professionals with a level of structural reliability, while allowing creativity and flexibility in repair assessment and design. This differs from traditional concrete design codes, which offer a more prescriptive framework.

A key provision to the use of ACI 562 is to select a design basis code. This design code will form the basis for which the structure will be evaluated. The ACI 562 was the first code developed by the ACI to work with the International Existing Building Code (IEBC). However, it may be adapted to be used in conjunction with local building design codes or older versions of the International Building Code (IBC) or IEBC. In regions where the use of the IEBC has not been adopted, the ACI may act as a stand-alone code providing guidance on conducting structural concrete repair assessments and designs (Kesner, Conroy & Kahn, 2014).

Once the design basis code is selected, the ACI guides the assessment and design of concrete repairs through a sequence of steps. The key steps set out in the 10 chapters cover the entire life cycle of the concrete repair process and include: the assessment and evaluation of the existing structure; design of the repair; the requirements for construction; quality control and; recommendations for repair maintenance. Details of the code's approach to the key steps in the concrete repair process are outlined below.

Evaluation of the existing structure is based on the in-situ conditions and material properties of the structure. The dimensions and significant material properties, like the compressive strength of the concrete and yield strength of the reinforcing steel, are required for the evaluation. The code recommends in-situ concrete and steel testing to obtain material property data. However, where this is not possible and the structure's materials are in good condition, the ACI 562 makes provision for the use of historical material property data provided in the code. The data provided is generally conservative and used as a means for preliminary analysis. ACI 562 also makes provision for load testing of the existing structure, in accordance to ACI 437.2, as an alternative or supplement to typical structural analysis.

The design of the structural concrete repairs, when using ACI 562, is expected to satisfy the strength and serviceability requirements typically required for the construction of new structures. These requirements are typically those of the initially established basis design code. The ACI 318, Building Code Requirements for Structural Concrete, is the most suitable choice of a basis design code, however, other design codes may be used in conjunction with ACI 562. ACI 562 includes provisions for interface bond evaluation; detailing to minimize cracking; sequence of repairs; and repair and substrate material interactions, which are unique to concrete repairs (Kesner & Conroy, 2017). Great significance is put on the interfacial bond between the repair material and the substrate concrete. The revision of bond strength evaluation and bond design, have formed the bulk of amendments in subsequent editions of the ACI 562 (Nahlawi & Paul, 2017).

Achieving durability of concrete repairs is a key objective of ACI 562, as durability issues in concrete structures are often the dominant cause of deterioration. Durability design of concrete repairs is complex in comparison to the design for strength. ACI 562 requires the designer to consider the durability of the repair area, as well as the entire structure, taking into consideration their independent durability characteristics and the effects resulting from their interactions. The code mainly provides commentary and references for durable design and detailing. In addition to durability design, the code requires that information on the maintenance needs of the repaired structure be provided to the owner.

The final components of the code include aspects pertaining to the construction and quality assurance of the concrete repair. The focus on the construction is mainly involved with ensuring stability and avoiding damage to any of the components or mechanisms of the existing structure. This includes the provisions for stability and shoring, temporary works and environmental conditions. The quality assurance of the repairs are similar to those specified for new construction but with adjusted frequencies and quantity of materials tested, mainly due to the smaller scale of material used in repair applications.

As a supplement to ACI 562, the ACI provides guidelines that may be used in conjunction with the code. Of particular importance are the ACI 546R, *Concrete Repair Guide*, and ACI 546.3R, *Guide to Materials Selection for Concrete Repair*, which guidelines for repair application methods and repair material selection respectively. The latter document, provides a

discussion around the material property aspects to be considered when selecting a repair material, without giving any measurable guidance on what the material properties ought to be. This may be considered as a limitation to use of these documents, as the decision of material selection is highly dependent on the experience and discretion of repair designer or applicator.

The ACI 562 provides a comprehensive framework for concrete repair design, implementation and management. Similar to the EN 1504, this is sufficient to guide concrete repairs conceptually at a high level. The code, however, has limitations in providing measurable guidance on repair material selection to designers and applicators. The varying experience and discretion of designers and applicators may lead to inconsistent application of the code. The code needs considerable refinement in the area of repair material selection, to ensure effective, practical and consistent application of the code.

2.1.3.3 ISO 16311

The ISO 16311 is standard for the repair and maintenance of concrete structures developed by the International Organization for Standardization (ISO). ISO 16311 contains four parts that cover various aspects of the concrete repair process: Part 1 – general principles of repair; Part 2 – assessment of existing concrete structure; Part 3 – design of repairs and prevention and; Part 4 – execution of repairs and prevention. The information and topics of concrete repair covered in the ISO code are similar to those covered by its European and ACI counterparts. The ISO 16311-3 published in 2014, bears significant similarities to the EN 1504-9 (2008) with respect to the principles and methods for the protection and repair of concrete.

The ISO 16311 bears similar limitations to the EN 1504 and ACI 562 with respect to being used as an effective and practical tool to inform concrete repairs. One of the significant shortcomings of the ISO 16311-3 is the lack of provision for repair material selection and specification criteria. Mihashi (2013), in developing guidelines for assessment of existing concrete structures for the Japanese Concrete Institute (JTI), found the ISO 16311 to contain various repair frameworks, however, lacks sufficient detail to act as an independent code. The code is considerably less detailed in comparison to EN 1504 and ACI 562. Mihashi (2013) believes the ISO 16311 is better suited as a model or reference code for national code writers.

2.1.4 Repair failures

In spite of the improvements in repair materials and methods to address infrastructure repair and maintenance needs, concrete repairs continue to fail prematurely (Zewdu, Sistonen & Taffese, 2013). According to Zewdu et al. (2013) the degradation process in repaired structures is far more complex than in new “unrepaired” structures. There are a number of factors to consider, in determining the service life of the repaired concrete structure. In addition to current and future environmental and imposed conditions on the structure, one has to take into account the pre-repair condition of the structure, the cause of initial damage, the appropriateness of the repair system employed as well as the degree of workmanship in carrying out the repair. The increase

in variables affecting the durability of concrete repairs may result in overestimating the service life of the repair or even premature failure of the structure.

In the early 2000s, it was estimated that over 50% of Europe's annual construction budget was spent on rehabilitation and repair of existing structures, including concrete structures (Matthews, 2007). The European Commission financially supported the CONREPNET, a network of companies and research groups, for a period of 4 years (2002-2006) to investigate performance-based rehabilitation of RC structures. This was done with the aim to provide building and infrastructure owners with more certainty on the service life of their repaired structures.

A study by Tilly & Jacobs (2007), as part of CONREPNET, examined the performance of concrete repairs conducted on 229 concrete structures across Europe. Of the cases examined they found that about 50% of concrete repairs showed signs of failure within the first 5 years of repair. The subsequent failure of the concrete repairs occurred at the following intervals: 25% within the first 5 years; 75% within the first 10 years and; 95% within the first 25 years after repair. The concrete repairs were found to have failed due to various reasons which include: inappropriate repair design (38%); poor repair workmanship (19%); incorrect diagnosis of the cause of the initial damage or deterioration (16%); inappropriate choice or specification of repair material (15%) and; other factors (12%). A breakdown of the cause of repair failure is shown in Figure 2-5.

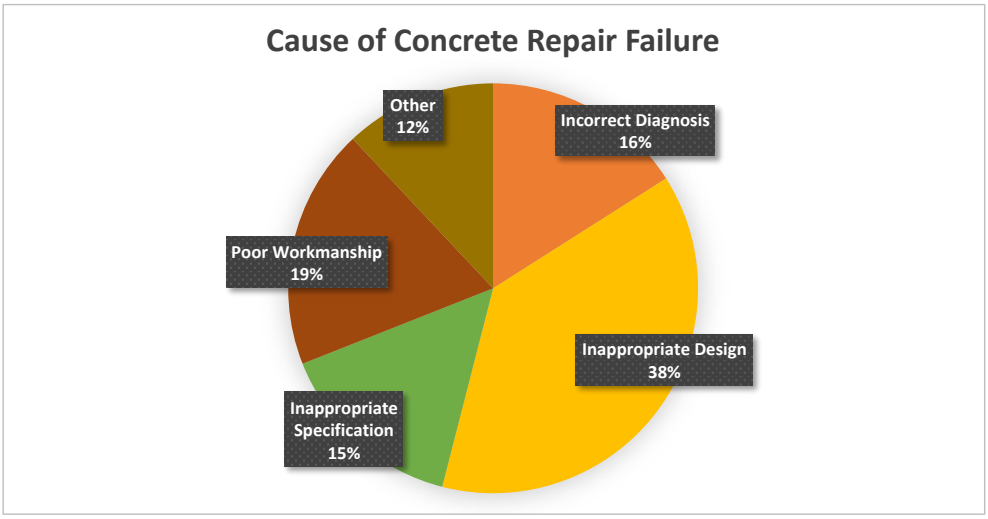

Figure 2-5: Cause of repair failure in concrete structures (Tilly & Jacobs, 2007)

Of the concrete structures investigated, the leading initial cause of failure in 54% of the structures was attributed to reinforcement steel corrosion (Tilly & Jacobs, 2007). Cracking and corrosion were found to be the most common modes of failure in concrete repairs at 36% and 37% respectively, giving a high indication that corrosion in the reinforcement steel was not prevented from perpetuating. Kim et al. (2016) shows that cracking and failure of patch repairs is sensitive to patch repair design and dimensions, in RC members still undergoing corrosion. They found

that patch repair depths which go beyond the corroded steel resist up to 30% more internal pressure, i.e. pressures arising from continued expansion of corroded steel, than those limited to the depth of the corroded steel. The other modes of failure of the concrete repairs reported by Tilly & Jacobs (2007) are found in Figure 2-6.

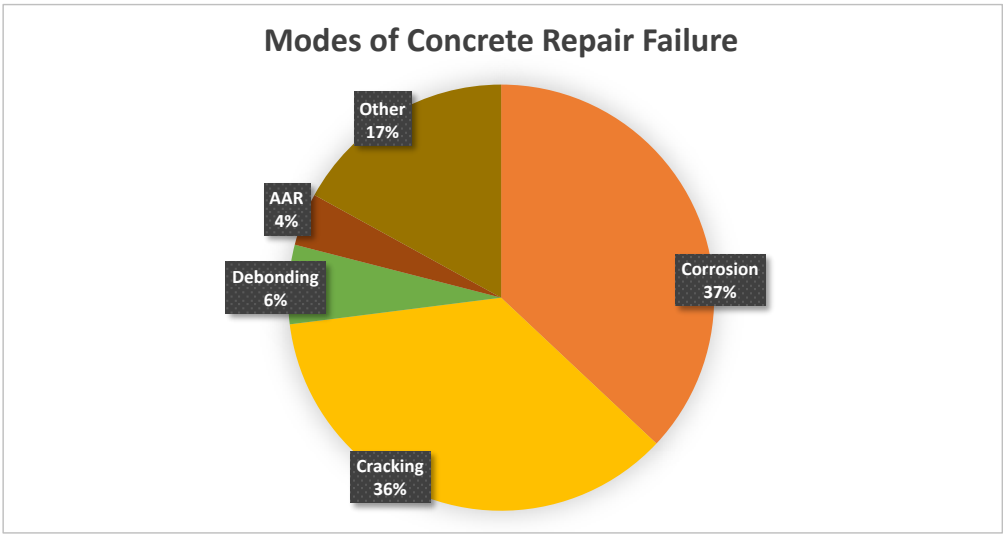

Figure 2-6: Modes of repair failure in concrete structures (Tilly & Jacobs, 2007)

In a more recent study, Sprinkel et al. (2019) investigates the premature failure of patch repairs of continuously-reinforced concrete pavements (CRCP) in several locations of 4 national and interstate state highways in the state of Virginia, USA. The patch repairs had all failed within 1 to 5 years after repair. The leading cause of failure in the concrete repairs was found to be due to incorrect choice of repair material. The use of high early strength repair materials with a high cement content was found to result in excessive shrinkage and thermal cracking of the repairs (Sprinkel, Hossain & Ozyildirim, 2019). Other significant causes of failure identified by the authors were incorrect repair intervention for initial deterioration and poor repair application methods.

2.2 Patch repairs and compatibility factors

Patch repair techniques are commonly used in repair of RC structures. The term “patch repair” is typically used to describe a bonded concrete overlay in any orientation, of relatively small surface area compared to the repaired concrete element’s surface area.

2.2.1 Composite repair system

Vaysburd & Emmons (2006) refer to repaired concrete structures as composite systems, which may be divided into three phases, the existing, repair and transition phase, represented in Figure 2-7. The materials in the composite system, mainly consist of the substrate concrete and repair material, as part of the existing phase and repair phase, respectively. The bond between the materials and the nature of their interaction is represented by the transition phase.

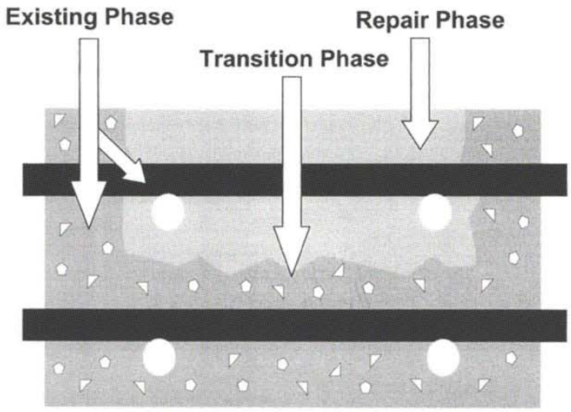

Figure 2-7: Composite repair system adopted from Vaysburd & Emmons (2006)

The substrate concrete and repair material are subjected to internal and external influences, as well as influences resulting form their interactions with each other. The respective materials and their properties interact with imposed loading and environmental conditions as well as each other inducing stresses and strains in the repaired concrete element. The performance of the concrete repair is determined by the ability of each material to withstand such stresses and avoid premature distress and/or deterioration (Emmons & Vaysburd, 1993).

2.2.2 Patch repair types

Concrete patch repairs are broadly categorised into structural and non-structural repairs. According to Plum (1991), stress-carrying is not a major consideration in non-structural or cosmetic repairs. However, in structural patch repairs, the patch repair is expected to enhance or contribute to the load carrying capability of the repaired element.

The durability function of patch repairs is primarily concerned with the protection of the reinforcing steel from corrosion. Carbon dioxide, chloride and other aggressive ions have an adverse effect on reinforcing steel, causing corrosion. In preventing the ingress of such aggressive ions, the prevention of crack development and propagation as well as the controlling the permeability of the material is of interest. Owing to the detrimental and potentially catastrophic failures in concrete structures due to reinforcing steel corrosion, the significance of durable concrete repairs has become the focus of research within the field of patch repairs and bonded overlays. See work by Beushausen & Alexander (2007) and Arito (2018) regarding the durability of patch repairs and their susceptibility to crack development and propagation. The factors affecting the durability of the repair are not the focus of this research and will thus not be elaborated further on unless applicable. This research will deal primarily with structural patch repairs.

According to the American concrete institute (ACI Committee 364, 2010), for the case of structural repairs, the load bearing capacity and stress distribution of the repaired concrete element must be considered where the replacement of load-bearing concrete is required. Depending on the structural function of the element, the concrete may be subjected to tensile,

compressive, and/or shear forces. Concrete plays an important structural role together with steel in resisting mainly flexural and compressive loads. The repair materials used to replace such concrete in a repaired element are expected to carry and distribute such loads.

2.2.3 Repair material types

There are several hundred commercial materials available for concrete patch repair, and more constantly being developed. Emberson & Mays (1990a) categorised these materials into nine generic types, which can be broadly categorised into three groups of materials shown in Table 2-4. The three groups of materials are namely: resinous materials; polymer modified cementitious materials and; cementitious materials.

Table 2-4: Categories of patch repair materials adopted from Emberson & Mays (1990a)

Resinous materials	Polymer modified cementitious materials	Cementitious materials
A: Epoxy mortar	D: SBR modified	G: OPC/sand mortar
B: Polyester mortar	E: Vinyl acetate modified	H: HAC mortar
C: Acrylic mortar	F: magnesium phosphate modified	I: Flowing concrete

2.2.4 Material compatibility

Concrete patch repairs involve the interaction or coming together of the patch repair material and the existing substrate concrete. Towards the end of the 20th century, researchers begun to emphasise the need for material compatibility between the repair material and the substate concrete to ensure durability of concrete repairs. Emmons et al. (1993) defines material compatibility between the repair material and substrate concrete as the balance of physical, chemical and electrochemical properties and dimensions, without causing damage and deterioration over a designated time period. Material compatibility may depend on various factors, including the cause of the initial deterioration to the structure, environmental conditions and imposed loading conditions. In assessing the effects of these various factors on the different aspects of material compatibility, Emmons et al. (1993) has divided material compatibility into chemical, electrochemical, permeability and dimensional compatibility. Figure 2-8 schematically represents the various aspects of material compatibility that affect the durability of concrete repairs.

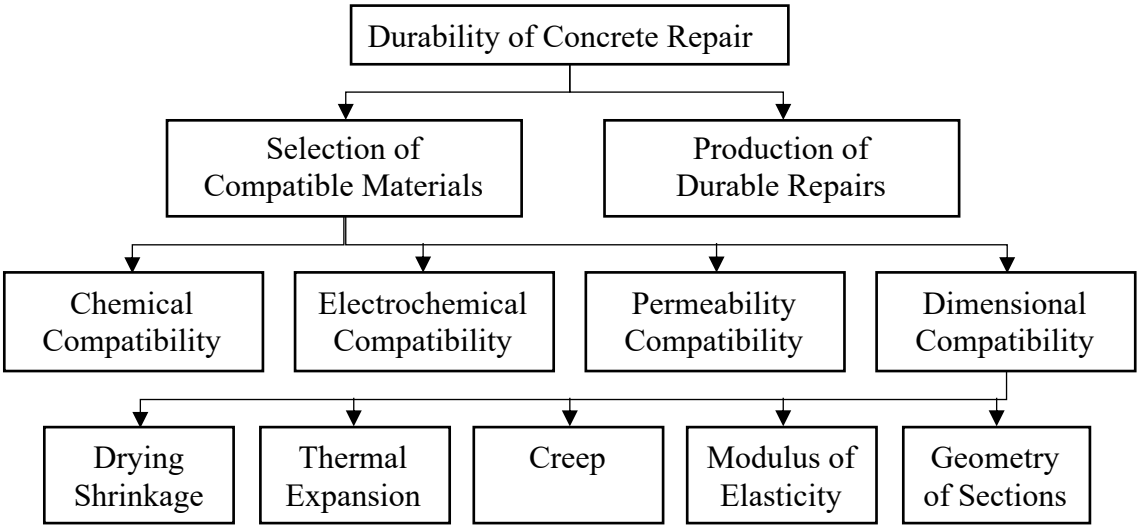

Figure 2-8: Aspects affecting durability of concrete repairs, adopted from Emmons et al. (1993)

2.2.4.1 Chemical compatibility

Chemical compatibility involves the selection of a repair material that through its interaction with the repaired components of the RC structure does have any adverse effects as a result of its chemical composition. A common example of a risk to achieving chemical compatibility, is if the repair material releases chloride ions through its chemical interaction with the repaired components, inhibiting steel reinforcement passivation in the RC structure and eventually resulting in corrosion occurring. Other examples of risks include the release of sodium or potassium ions which could promote alkali-aggregate reactivity (AAR) in the substrate concrete, should the substrate concrete contain aggregates susceptible to AAR (Morgan, 1996).

2.2.4.2 Electrochemical compatibility

The primary aim in achieving electrochemical compatibility is inhibiting steel reinforcement corrosion by avoiding the development of a corrosion cell within the repair area or surrounding unrepaired area in a RC structure. The above aim may be accomplished by meeting one or more of the following objectives in a repair of corrosion-induced damage: stopping the anodic process; stopping the cathodic process and/or; stopping the electrolytic conductivity of the patch repair (Vaysburd, Bissonnette & von Fay, 2014). The anodic process is linked to chemical compatibility as the de-passivation of reinforcement steel allowing for anodic reaction to take place is dependent on the pH and the availability of aggressive ions in the concrete and repair material. The cathodic process is more dependent on the availability of water and oxygen in encouraging cathodic reaction to take place. The permeability (discussed further below) and porosity of the repair material may aid both anodic and cathodic reactions by increasing the availability of aggressive ions and carbon dioxide, and water and oxygen at the anode and cathode respectively. The electrolytic conductivity may be affected by the environment, conductivity of repair material

and/or the presence of stray electrical currents, facilitating the movement of electrons from anode to cathode in the repaired RC structure.

2.2.4.3 Permeability compatibility

The permeability of the repair material relative to the substrate concrete is an important consideration when taking into account the effect it has on the electrochemical compatibility of repaired RC structure. Low permeability of the repair material is favourable as it inhibits the diffusion of chloride ions, carbon dioxide, water and oxygen which may promote the development of a corrosion cell (Cusson & Mailvaganam, 1996; Morgan, 1996; Cabrera & Al-Hasan, 1997; Decter & Keeley, 1997; Vaysburd, Bissonnette & von Fay, 2014). However, the use of low permeability repair materials is not necessarily always applicable in concrete repairs as some situations are more complex. Morgan (1996) cautions the use repair materials which are impermeable to moisture vapour in the repair of hydraulic structures, such as dams and reserves, as well as other structures where the concrete supports rising damp. In such situations, an impermeable patch repair may cause saturation of the substrate concrete behind the repair. In extremely cold climatic conditions this problem may be compounded by the frost penetration of the saturated substrate concrete, causing failure in the substrate concrete and eventual delamination of the repair.

2.2.4.4 Dimensional compatibility

The dimensional compatibility of the repair material and the substrate concrete is considered to be one of the most important requirements in meeting material compatibility in concrete repairs (Emmons, Vaysburd & McDonald, 1993; Morgan, 1996; Vaysburd, Bissonnette & von Fay, 2014). The most significant material properties and elements affecting dimensional compatibility between the repair material and the substrate concrete are:

- Differential shrinkage strains;
- Differential thermal expansion and contraction strains;
- Differential creep properties;
- Differences in modulus of elasticity properties, causing unequal stress and strain distribution.

The listed differences in material properties result in differential volume changes and stresses induced the repair material and substrate concrete and along their bonded interfaces. Differential stresses may result in failure of a particular material under stress, formation of cracks, or cause debonding at the repair interface, the occurrence of any of which may negatively impact the durability and/or load carrying capacity of the RC structure (Vaysburd, Bissonnette & von Fay, 2014).

2.2.5 Structural compatibility

For structural patch repairs, where the repair material is expected bear the load originally carried by the removed concrete, the structural compatibility of the repair material and substrate concrete needs to be considered. The considerations for structural repairs are more complex than those for non-structural repairs, depending on the type of loading the repair is subjected to. Emberson & Mays (1990a,b, 1996) have shown the significant adverse structural implications resulting from property mismatch between the repair material and substrate concrete. These implications include high stress concentrations in the repair material, substrate concrete or interface resulting in material failure or debonding of the repair. Emberson & Mays (1990a) recommended a set of general requirements for patch repair materials for structural compatibility, which are presented in Table 2-5.

Table 2-5: General requirements of patch repair materials for structural compatibility, adopted from Emberson & Mays (1990a)

Property	Relationship of repair material (R) to concrete substrate (C)
Strength in compression, tension and flexure	$R \geq C$
Modulus in compression, tension and flexure	$R \approx C$
Poisson's ratio	Dependant on modulus and type of repair
Coefficient of thermal expansion	$R \approx C$
Adhesion in tension and shear	$R \geq C$
Curing and long term shrinkage	$R \leq C$
Strain capacity	$R \geq C$
Creep	Dependent on whether creep causes desirable or undesirable effects
Fatigue performance	$R \geq C$

Structural patch repairs are expected to effectively and safely distribute stress and strain, avoiding the development of excessive stresses and/or deflections in the repaired structure. Depending on the type of loading the repair is subjected to, the first requirement is that the strength of the repair material exceeds that of the substrate concrete. Most repair materials generally meet this requirement (Emberson & Mays, 1990a; Morgan, 1996). Table 2-6 adopted from Mays & Wilkinson (1987), shows typical mechanical properties of resin mortars, polymer modified cementitious mortars and plain cementitious mortars. Beyond repair material strength, material properties affecting dimensional compatibility such as modulus of elasticity, shrinkage, creep and thermal expansion coefficients are concerns for structural compatibility. Resin based repair

materials generally have lower elastic of modulus and higher thermal expansive properties in comparison to cement based repair materials (Mays & Wilkinson, 1987; Emberson & Mays, 1990a; Morgan, 1996). The property mismatch between resin-based repair materials and the substrate concrete, generally favour the use of cement-based repair materials for structural applications. However resin-based materials, owing to their exceptional physical and chemical properties, are often used in structural repairs where low permeability, rapid setting time, high chemical resistance and/or thin layers of applications are a requirement (Morgan, 1996).

Table 2-6: Typical mechanical properties of repair materials adopted from Mays & Wilkinson (1987)

Property	Resin mortar	Polymer modified cementitious mortar	Plain cementitious mortar
Compressive strength, MPa	50-100	30-60	20-50
Tensile strength	10-15	5-10	2-5
Modulus of elasticity in compression, GPa	10-20	15-25	20-30
Coefficient of thermal expansion (per °C)	$25\text{-}30 \times 10^{-6}$	$10\text{-}20 \times 10^{-6}$	10×10^{-6}
Water absorption (% by mass)	1-2	0.1-0.5	5-15
Maximum service temperature (°C)	40-80	100-300	> 300

2.3 Repair material properties

Understanding the material properties of the substrate concrete and repair material are important in determining the stress and strain behaviour and thus effectiveness of the repair. The material properties of the substrate concrete are relatively stable compared to the developing properties of the new repair material.

A review of literature is conducted on repair material properties with respect to structural patch repair applications. Material properties required for structural compatibility as well as their various aspects and associated phenomena are discussed. Cement-based repair materials form the focus of the review, however, reference to other types of repair materials are made for comparative purposes. Aspects regarding the time dependent development of the material properties and how to estimate them are considered. Furthermore, where applicable, how the material properties affect stress and strain distribution in a patch repaired element are discussed.

2.3.1 Compressive strength

The compressive strength of a repair material is the measure its capacity to withstand compressive stresses. The compressive strength of a material is considered to be one of the most important physical properties (Oluokun, Burdette & Deatherage, 2010). For structural patch repairs, the compressive strength of the repair material at a specific age determines at what point a load may safely be applied on the repaired structure. It is a general requirement that the repair material must have a compressive strength equal or greater than the substrate concrete at loading. Research by Mays & Wilkinson (1987), Emberson & Mays (1990a), Mangat & Limbachiya (1994) and Cabrera & Al-Hasan (1997) have found that most repair material systems meet and surpass this requirement.

Proprietary cement-based repair materials continue to be developed with the ability to achieve high compressive strength properties at early ages, allowing repairs to be subjected to loading earlier than the 28 days required for normal concretes to achieve their optimum strength. Cabrera & Al-Hasan (1997) found that the compressive strength of proprietary cement based repair mortars tested achieved values of 50 MPa, equivalent of what plain ordinary Portland cement (OPC) concretes would achieve in a year. Oluokun et al. (2010) attributes the high early age strength of cement-based materials to the cement content of the mix. Mixes with higher cement content lead to increased rates of hydration in the material, leading to rapid development of physical properties at early ages.

2.3.2 Tensile strength

The tensile strength of the repair material is the measure its capacity to withstand tensile stresses. It is an important material property in resisting the tensile stresses induced in the repair material due to restrained volume change such as shrinkage, which may otherwise result in the formation of cracks in the repair material.

The tensile strength of cement based materials, develops at a similar rate to the compressive strength of the material. Tensile strength development may occur rapidly within the first 7 days. Yuan & Marosszeky (1994) found the 7 day tensile strength of three polymer modified cement concretes to be 67%, 70% and 86% of their respective 28 day strength values.

Vaysburd (2016) asserts that there is a common misconception that higher-strength cement-based repair materials provide enhanced durability in harsh environments. This misconception neglects the realisation that higher strength is often accompanied by higher stiffness in such materials, increasing its susceptibility to cracking. The elastic modulus is often directly proportional, where the tensile strength is proportional by ratios between 0.06 and 0.1 to the compressive strength of cement-based repair materials (Vaysburd, Bissonnette & von Fay, 2014). By the above ratios, an increase in tensile strength results in a disproportionately higher increase in compressive strength and elastic modulus properties in cement-based material. A stiffer material under restrained volume change will induce higher stresses in the material. High

early strength repair materials may also have the potential of higher shrinkage, as a result of higher rates of hydration. Higher restrained shrinkage, coupled with a stiffer repair material may result in disproportionately higher tensile stresses induced compared to the increase in tensile strength making the repair material more susceptible to cracking.

2.3.3 Modulus of elasticity

The modulus of elasticity properties of a repair material is a measure of the stiffness of the material. Within the linear stress-strain range of the material, it represents a constant proportion between the stress and strain in the material. A material with a higher modulus of elasticity is more rigid and will deform less under an applied stress, in comparison with a more flexible material with a lower modulus of elasticity. The modulus of elasticity of a material is different under compression, tension and flexural loading. Emberson & Mays (1990a) found that resin-based repair materials covered the lower spectrum of compression modulus ranging between 17 000 N/mm^2 and 25 000 N/mm^2, in comparison to cement-based repair materials covering the upper end of the range, with values as high as 50 000 N/mm^2. Values of tension modulus of the repair materials tested were found to cover a similar range to that of the compression modulus of various repair materials. The flexural modulus values of the repair materials were lower than both the compression and tension modulus, indicating that repair materials are generally more flexible under bending (Emberson & Mays, 1990a).

The modulus of elasticity of repair materials used in structural applications is required to be similar to the substrate concrete (Morgan, 1996). Morgan (1996) and Decter & Keeley (1997) report that cement-based repair materials are better suited for structural applications as their modulus of elasticity properties are similar to most substrate concretes in comparison to lower modulus resin based repair materials. In repaired members loaded axially, large stress concentrations may form at the interface of the repair material and substrate concrete, requiring high values of interfacial adhesion when the modulus of elasticity of the repair material and substrate concrete differ significantly (Emberson & Mays, 1990b). In flexural members, repair materials with low modulus values in comparison to the substrate concrete generate high stresses in the substrate accompanied by longitudinal interface shear stresses between the materials. Furthermore, repair materials with a modulus higher than the substrate concrete, attract more load to the repair material, imposing a greater structural demand on it (Emberson & Mays, 1996). The above mechanics are discussed in more detail applying to cement-based repair materials in structural patch repair applications.

2.3.3.1 Modulus of elasticity in patch repairs

The modulus of elasticity of the repair material and substrate concrete influence patch repaired elements differently, depending on the imposed conditions. We look at these influences from two scenarios, i.e. where there is no external imposed load and where an external load is imposed on the patch repaired element.

In a scenario where no external load is imposed on the patch repaired element, the modulus of elasticity of the repair material primarily affects the development of tensile stresses in the repair material. Tensile stresses develop in the repair material when the material is restrained from undergoing free shrinkage strain, discussed in Section 2.3.6.4. Higher tensile stresses develop in the repair material for higher values of modulus of elasticity.

When an external load is imposed on the repaired element, the modulus of elasticity of the repair material and substrate concrete distribute such load in the composite system. For structural patch repair applications, this may be when the propping or stress relieving mechanisms that were employed for the repair application are removed and the repaired element is subjected to and imposed load. The stiffer material, i.e. higher modulus of elasticity, will attract a greater proportion of the stress than the material with lower modulus of elasticity. According to ACI Committee 546 (2014), when a repair material is intended to share load in a repaired system, it will attract more of the applied load if it's modulus of elasticity is higher relative to the substrate concrete. A representation, adapted from Cusson & Mailvaganam (1996), on the effects of differential modulus of elasticity on the structural behaviour of a repair is shown in Figure 2-9. The representation shows composite repair elements loaded under compression. In Figure 2-9 (a), the external load is applied perpendicular to the interface of the materials, the stress in the materials will be the same with the material with low modulus deforming comparatively more than the high modulus material. In Figure 2-9 (b), the external load is applied parallel to the interface of the materials, the stress in the high modulus material will be greater than the low modulus material. This may cause high axial stress concentrations in the high modulus material, potentially leading to compressive failure in the material.

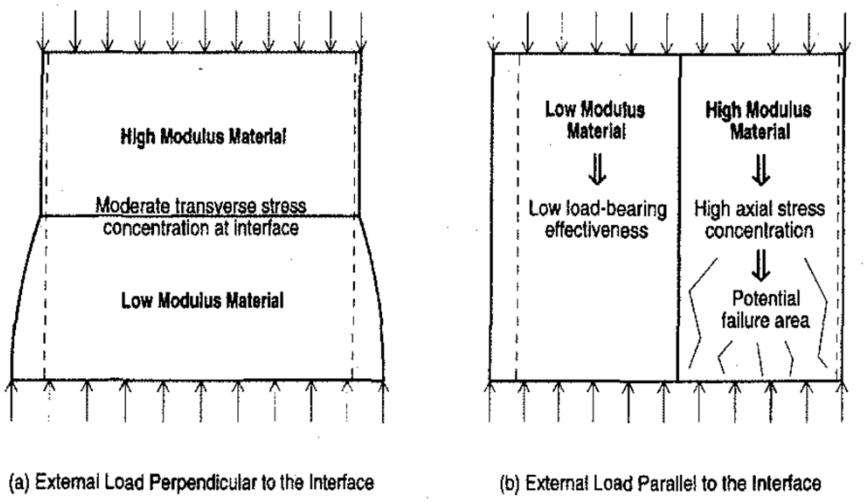

Figure 2-9: Structural behaviour of differential modulus of elasticity in concrete repairs adopted from Cusson & Mailvaganam (1996)

Experimental research on repaired concrete specimens loaded under axial tension, by Emberson & Mays (1990b, 1996), confirms that materials with low modulus values generate relatively high stresses in the substrate concrete whereas materials with high modulus values tend

to attract load into the repair material. Similar findings have been obtained by others, who have conducted experimental research on loaded concrete repairs (Mays & Barnes, 1995; Sharif et al., 2006; Da Porto, Stievanin & Pellegrino, 2012). Mangat & O'Flaherty (2000) found that repair materials with lower modulus of elasticity properties compared to the substrate concrete display no structural interaction. They recommend that the modulus of elasticity of the repair material always be higher than that of the substrate concrete, to ensure efficient interaction between the two materials. However, some research shows that a significantly higher modulus of elasticity properties of the repair material may not have favourable effects on the structural behaviour of the repaired system. Ortega et al. (2018b) and Ortega et al. (2018a) tested the compressive load capacity of repaired concrete elements repaired with Class R3 and Class R4 repair materials respectively, according to European Standard EN 1504. The Class R4 material possessed modulus of elasticity properties of 37 GPa, compared to 25 GPa for the Class R3 repair materials, both of which were higher than the substrate concrete (19 GPa). The columns repaired with the Class R3 repair material behaved structurally better than those repaired with the Class R4 materials, allowing for a more evenly distributed load, resulting in a higher ultimate compressive capacity. The authors attributed the better structural behaviour to the fact that the Class R3 properties were more similar to the substrate concrete. Emberson & Mays (1996) recommended that the modulus of elasticity of the repair material be within 10 GPa of the substrate concrete, which corresponds with the findings of Ortega et al. (2018b) and Ortega et al. (2018a).

2.3.3.2 Restrained elastic loading strain

Restrained action against differential strain between repair material and substrate concrete, typically takes place when there is a good bond between the materials. In repaired elements where the repair material is not actively participating in load sharing, elastic strain due to the imposed load is only experienced in the substrate concrete. This may occur when the repair material has little or no contact with the loading plane or when the repair material is applied to element in a loaded condition. For repaired elements under axial compression, the application of additional load will result in increased elastic strain only in the substrate concrete. Assuming a strong bond between the substrate concrete and repair material, both materials will experience similar compressive strain at their bond interface. A portion of the compressive strain is thus restrained and transferred from the substrate concrete to the repair material. This result was observed by Mangat & O'Flaherty (1999b), where patch repair materials were able to partake in load sharing in the long term (with the application of additional load) in the repaired element despite being applied to the element in a loaded condition.

2.3.3.3 Elastic modulus estimation

The most practical approach to predicting the elastic modulus of cement-based materials is through its relationship with compressive strength properties, despite the dissimilar factors affecting each property. Most structural design codes offer guidance on the prediction of elastic modulus as a function of compressive strength. The rate of elastic modulus development is

relatively faster at early ages, in comparison to the compressive and tensile strength development in cement-based materials, and relatively slower at later ages (Oluokun, Burdette & Deatherage, 2010). Figure 2-10 shows the time-dependent development of elastic modulus and compressive strength properties of PC-42,5 concretes within the first 28 days, adopted from Harrison (2003).

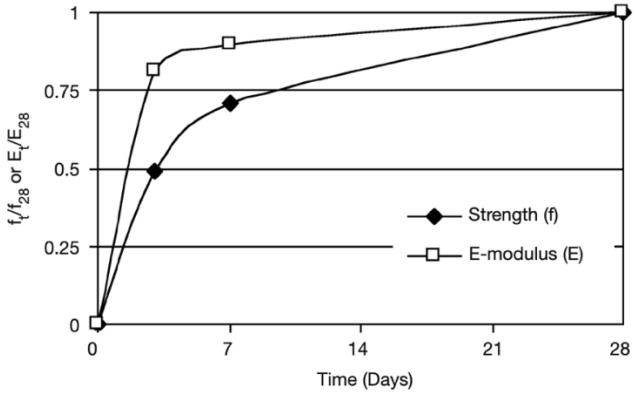

Figure 2-10: Time-dependent development of elastic modulus and compressive strength

2.3.4 Poisson's ratio

A material's Poisson's ratio is the ratio of lateral strain to longitudinal strain, where the longitudinal strains result from pure longitudinal applied stresses. Emberson & Mays (1990a) found that the Poisson's ratio of most of the available repair systems is similar to most substrate concretes, at 0.2, with the exception of high alumina cement mortars and flowing concretes which have values closer to 0.1.

The effect of the Poisson's ratio is closely linked to the elastic modulus properties of the materials. Differential elastic modulus and Poisson's ratio properties between the repair material and substrate concrete causes a concentration of stresses at the interface of the two materials. Emberson & Mays (1990b, 1996) report on the significance of the Poisson's ratio of repair materials in axial and flexural loaded applications. For axially loaded repaired members, the effects of the Poisson's ratio were found to be minimal for repair materials with low modulus of elasticity values. Where repair materials have higher modulus of elasticity than the substrate concrete, a mismatch of Poisson's ratio influences the development of concentrated stress zones on the surface adjacent to the transverse interface of the two materials. This influence was found to be greater in unreinforced patch repairs than in reinforced patch repairs, where the presence of reinforcement steel limits lateral strain in the materials and thus mitigates the development of stresses between the materials. In repaired reinforced concrete beams under flexural loading, the Poison's ratio of the repair material only has second-order effects on the distribution of stresses in the repaired member.

2.3.5 Coefficient of thermal expansion or contraction

The coefficient of thermal expansion/contraction (CTE) represents the change in unit length of a material per change in degree of temperature (Vaysburd, Bissonnette & von Fay, 2014). According to Morgan (1996), similar values of CTE for repair material and substrate concrete are essential for structural and mechanical compatibility in concrete repairs. Dissimilar CTE values between materials leads to differential volume change in the materials when the repaired system is subjected to a significant change in temperature. The restraint in either material to deformation, may cause the development of direct stresses, bending stresses and interface shear stresses in both materials. Development of such stresses may result in adhesion failure between the repair material and substrate concrete, at either the interface or one of the materials in the case where the materials are well-bonded.

Cement based repair materials generally have CTE values similar to most substrate concrete, which are significantly lower than CTE values of resin based repair materials (Emberson & Mays, 1990a; Emmons & Vaysburd, 1994; Morgan, 1996; Decter & Keeley, 1997; Vaysburd, Bissonnette & von Fay, 2014). Emmons & Vaysburd (1994) reports that resin based repair materials may exhibit CTE values up to eight times that of concrete. Morgan (1996) investigated a repair of a concrete base subjected to in service temperature fluctuations between -50ºC and +40ºC. The repair comprised of a 100mm thick layer of resin-based material bonded to the substrate concrete. The resin based repair material with CTE values much higher than the substrate concrete, undergoes differential restrained volume change inducing stresses close to the interface of the materials. The differential thermal stresses between the thick repair material layer and substrate concrete eventually led to the rapture of the substrate concrete 20mm beneath the bond line, owing to the high level of bond between the materials and lower capacity of stress of the substrate concrete.

2.3.6 Shrinkage

Shrinkage is the change in volume of a material associated to the movement of moisture in and out of the material. It may be divided into early-age shrinkage (or plastic shrinkage), which typically takes place within the first couple of hours when the material is in a plastic state, and long-term shrinkage, referring to the movement of moisture in and out of the material in the hardened state.

2.3.6.1 Mechanism of shrinkage

Drying shrinkage

Drying shrinkage is a result of the loss of moisture from hardened concrete to the environment. The total drying shrinkage of a material is influenced largely by the shape and dimensions of the material. Other influences include: content and quality of cement paste; characteristics and amount of admixtures; water content; temperature and relatively humidity of exposed

environment and; distribution of reinforcing steel. The moisture is lost commonly by evaporation to the atmosphere at the exposed surface of the repair material, however loss may also occur through suction of the underlying dry substrate concrete (Vaysburd, Bissonnette & von Fay, 2014).

The properties of cement-based repair materials affecting drying shrinkage the most, are the cement content and quality as well as the availability of water in the repair material mixture. The water held in the cement paste consists of interlayer, gel pore water and free capillary water. The free capillary water is typically lost to the environment at early ages, followed by the gel pore water, which is much more tightly held (Beushausen, 2005). An increase in porosity of the cement paste results in a more free movement of water and thus an increase in drying shrinkage in the material. The porosity of the cement paste increases with an increase in water to cement (w/c) ratio and decrease in the degree of hydration in the material. The largest source of shrinkage is typically apparent in concrete mixtures with a w/c ratio greater than 0.42 (Vaysburd, Bissonnette & von Fay, 2014). High strength/high performance cement-based repair materials typically possess w/c ratios less than 0.42, with high degrees of hydration, in order to facilitate high strength development at early ages. This tends to lead to low drying shrinkage values in such materials.

The environmental influences affecting drying shrinkage are the curing regime and the drying conditions, which include: temperature; relative humidity and; the wind conditions. Shrinkage strains in repair materials generally increase, with an increase in temperature, decrease of relative humidity and/or the presence of strong winds. Furthermore, drying shrinkage, is a function of the ratio of volume to surface area of the material, where an increase in material thickness will result in a decrease in total drying shrinkage. This presents inconsistencies with regard to reported measurements of drying shrinkage for materials. Prisms sizes used for measurement, vary in standards around the world, allowing for different drying shrinkage measurements made for the same materials (Decter & Keeley, 1997).

Carbonation shrinkage

Carbonation shrinkage results from reduction of volume in repair material due to the reaction between the carbon dioxide in the atmosphere and the hardened cement paste constituents. Carbonation shrinkage is a function of the relative humidity of the exposed environment and is largest at intermediate humility's and lower at both high and low relative humility's. The reaction between the carbon dioxide and cement paste constituents may occur over long periods and, in some case, the carbonation shrinkage may exceed the drying shrinkage in the material (Alexander & Beushausen, 2009).

Autogenous shrinkage

Autogenous shrinkage, or basic shrinkage, is the reduction in volume of cement-based materials as a result of the hydration of the cement and internal consumption of water. This mechanism of shrinkage is internal and does not involve the exchange of moisture between the concrete and

environment. The hydration products, i.e. cement-paste, formed have less volume in comparison to the water and cement constituents before the hydration process takes place. In normal strength concrete, autogenous shrinkage strain is typically less than that of drying and carbonation shrinkage respectively. However this does not necessarily apply to high strength concrete with low w/c ratios. Such materials have a higher consumption of mixing water in the hydration process thus comparatively higher autogenous shrinkage. Autogenous shrinkage is not affected by external curing and is thus unavoidable, even when good curing practices have been applied (Termkhajornkit et al., 2005). About 40% of the total autogenous shrinkage occurs in the first 24 hours after mixing (Alexander & Beushausen, 2009).

Autogenous shrinkage is larger than drying shrinkage in concrete mixtures with w/c ratios less than 0.42 (Vaysburd, Bissonnette & von Fay, 2014). High performance cement-based repair materials have comparatively lower w/c ratios and higher cement content than normal concrete, resulting in greater autogenous shrinkage values in such materials. Lee et al. (2003) investigated the effect of w/c ratio on autogenous shrinkage in high performance concretes. The autogenous shrinkage of an OPC mix with w/c ratio of 0.27 was about nine times greater than an OPC mix with a w/c ratio of 0.5. Pane & Hansen (2002) and Lee et al. (2003) investigated the effect of extenders on the development of autogenous shrinkage in high performance cement-based materials. Both found that the presence of fly ash (FA) in the mix had reduced the autogenous shrinkage at a given age when compared to a similar OPC mix. Pane & Hansen (2002) found that the same applies for the presence of ground granulated blast-furnace slag (GGBS); however, the presence of silica fumes (SF) resulted in an increase in autogenous shrinkage. Lee et al. (2003) found that the higher percentage of FA replacement in the mix, the lower the autogenous shrinkage at a given age. The reduction in autogenous shrinkage is attributed to the reduction in cement content, as it is replaced by FA. Although the replacement of OPC with FA or GGBS may be beneficial in decreasing autogenous shrinkage, the strength development in the repair material mix may be significantly delayed and should be considered in the context of the concrete repair application.

2.3.6.2 Typical shrinkage values in repair materials

The early age shrinkage properties of materials are typically measured within a 0-24 hours curing period. Emberson & Mays (1990a) measured early age shrinkage of 9 generic repair material systems and found the values ranging between +830 and –4680 micro strains, where the positive and negative values indicate expansion and shrinkage respectively. Resin-based materials generally had lower shrinkage values when compared to the cement-based material with the exception of the polyester mortar, having the highest early-age shrinkage. A polymer modified cement-based material containing magnesium phosphate was the only material found to have expanded at early ages. Yuan & Marosszeky (1994) obtained varying results when testing 4 polymer cement-based repair materials for early age shrinkage. Materials containing styrene butadiene rubber and styrene-acrylic were found to expand in the first 24 hours before shrinking. The acrylic-based material showed excess of 100 micro strains of early-age shrinkage while the

material containing vinyl acetate-ethylene copolymers showed stable to no shrinkage strain within the first 24 hours.

Shrinkage may continue for many years depending on the dimensions and properties of the material. Long-term shrinkage is typically measured from at age of the material 1 day, neglecting early-age shrinkage strain. Emberson & Mays (1990a) measured long-term shrinkage strain of nine generic repair materials, over a 16 month period. They found that resin-based repair materials generally have smaller and relatively stable shrinkage properties beyond the age of 1 month when compared to cement-based materials, which continued to undergo shrinkage strain over the entire 16-month testing period. It is reported (Emmons, McDonald & Vaysburd, 1983) that approximately 70% of the total shrinkage strain of concrete repair materials takes place within the first 30 days. The shrinkage strain of the cement-based repair materials measured within the first month by Emberson & Mays (1990a) ranged between 60-73% of the shrinkage strain at the end of the 16 month period. The shrinkage strain values after one month ranged between 440 and 700 micro strains for these materials. Measurement of shrinkage strain of cement-based repair materials by Mangat & Limbachiya (1994), Yuan & Marosseky (1994) and Shambira & Nounu (2000) confirmed a similar range of values after one month.

2.3.6.3 Shrinkage compensating materials and shrinkage classification

There has been an increasing drive to create repair materials that exhibit low shrinkage properties for the repair of concrete structures (Decter & Keeley, 1997). Some proprietary cement-based materials are labelled ‘shrinkage compensated’, in which they undergo expansion in wet conditions. Such materials may contain expansive cements or agents that result in the expansion of the materials in the first few days after casting. The initial expansion of the material is aimed at compensating or off-setting the net shrinkage in the material. Robery & Shaw (1997) showed the benefit of measuring and taking into consideration the early age expansion (within the first 24 hours) of shrinkage-compensating materials, as the true (net) shrinkage of a material may be decreased by 70% when compared to the measured shrinkage of the material after 24 hours. Morgan (1996) cautions the use of shrinkage compensated repair materials, noting that their continuous exposure to wet conditions may result in continuous expansion, the consequences of which, may be as severe as excessive shrinkage of a repair material in dry conditions.

Emmons & Vaysburd (1993) sought to investigate the benefit of proprietary repair materials, claiming to have non-shrink, expansive or shrinkage compensating properties. They presented a classification of repair materials based on their shrinkage properties, presented in Table 2-7.

Table 2-7: Classification of repair materials based on shrinkage properties at 28 days (Emmons & Vaysburd, 1993)

Classification	Range of free shrinkage strains at 28 days [10^{-6}]
Very low shrinkage	0 – 250
Low shrinkage	250 – 500
Moderate shrinkage	500 – 1000
High Shrinkage	> 1000

Of the products tested, half exhibited shrinkage strains twice or more that of plain concrete. Only 15% of 46 surface repair materials tested were considered low shrinkage, in spite of the manufacturers claims that they are non-shrinkage products. Beushausen (2005) conducted shrinkage measurements on four common South African concrete repair products, labelled as "non-shrink". He found that the shrinkage strains within the first 21 days were within the low shrinkage range, in agreement with the classification and findings of Emmons & Vaysburd (1993). The existence of such materials is remains questionable. In a technical note, the ACI Committee 364 (2018) warns against the use of repair materials labelled "shrinkage-compensating" or "non-shrink" without sufficient supporting time-dependent volume change data.

2.3.6.4 Shrinkage restraint

In patch repair applications, the comparatively newer repair material will experience larger shrinkage strains than the substrate concrete. Differential shrinkage is experienced through the depth of the repaired concrete element. A strong bond between repair material and substrate concrete will restrain the repair material from undergoing the extent of its free shrinkage strain, a phenomenon referred to as restrained shrinkage. The portion of free shrinkage in the repair material restrained results in the development of tensile stresses in the material. The tensile stress are a function of the restrained shrinkage strain and elastic modulus properties of the repair material. Tensile creep and relaxation in the repair material may act reduce the tensile stresses experienced. When such tensile stresses exceed the tensile strength of the repair material, cracking occurs, adversely affecting the repair.

Employing curing regimes to the repair material, preventing the rapid loss of water to the atmosphere, may result in lower drying shrinkage strains. However, low shrinkage strain do not necessarily decrease the possibility of crack development in the repair material under restrained conditions. Curing controls may be used to control shrinkage strain and develop tensile strength at early ages, which assist to prevent cracking in cement-based repair materials. Beushausen (2005) notes, however, that extensive curing results in comparatively higher elastic modulus and

lower creep factors at the initiation of shrinkage strain at early ages, which may have an unfavourable effect on crack behaviour. High performance repair materials have comparatively high elastic modulus and low creep factors, which, at the onset of comparatively less shrinkage strain, may still result in the development of high tensile stresses in the material. In such cases the net effect of material property development needs to be considered when determining crack behaviour.

2.3.6.5 Shrinkage in patch repairs

The effects of shrinkage in the repair material on the repair system may be viewed from two stand points, the presence and absence of externally applied load.

In the absence of an externally applied load, restrained shrinkage resulting in tensile stress development in the repair material will occur. Often only a portion of the shrinkage is restrained in the repair material. Assuming a full bond between substrate concrete and repair material, the substrate concrete will undergo the same deformation at their interface inducing localised compressive stresses in the substrate concrete (Beushausen & Alexander, 2006). Mangat & O'Flaherty (1999b) found that repair materials with comparatively higher modulus of elasticity than substrate concrete are able to effectively transfer a portion of the shrinkage strain to the substrate concrete. In addition, the bond experiences shear forces due to the differential stresses generated in the repair material (tensile) and substrate concrete (compressive) close to their interface. A combination of various components affects the total stresses in a repaired system under restrained shrinkage, the most important being the elastic strains in the materials, substrate creep and repair material tensile relaxation.

In the presence of an externally applied compressive load on the repaired element, differential shrinkage strain leads to stress distribution from repair material to the substrate concrete over time. The theory of load being shed from the repair material to the substrate concrete is a generally accepted theory, however there is very few empirical studies that test for it. Among the few studies done, Shambira & Nounu (2000) investigated the effect of time-dependent deformations, such as shrinkage and creep, on the structural function of patch repaired short columns. Shambira & Nounu (2000) repaired reinforced columns in a laboratory conditions with two different cement-based repair materials, a commercially available polymeric repair mortar (comparatively low shrinkage) and a polymer-modified concrete (comparatively high shrinkage). Figure 2-11 shows the strain distribution over a 44 day period in the cross-section of a column repaired with a polymer-modified repair concrete to a repair depth of 100mm (from right edge). The increased strain experienced in the substrate concrete, left edge of the figure, is attributed to the transfer of compressive stresses from the repair material to the substrate concrete.

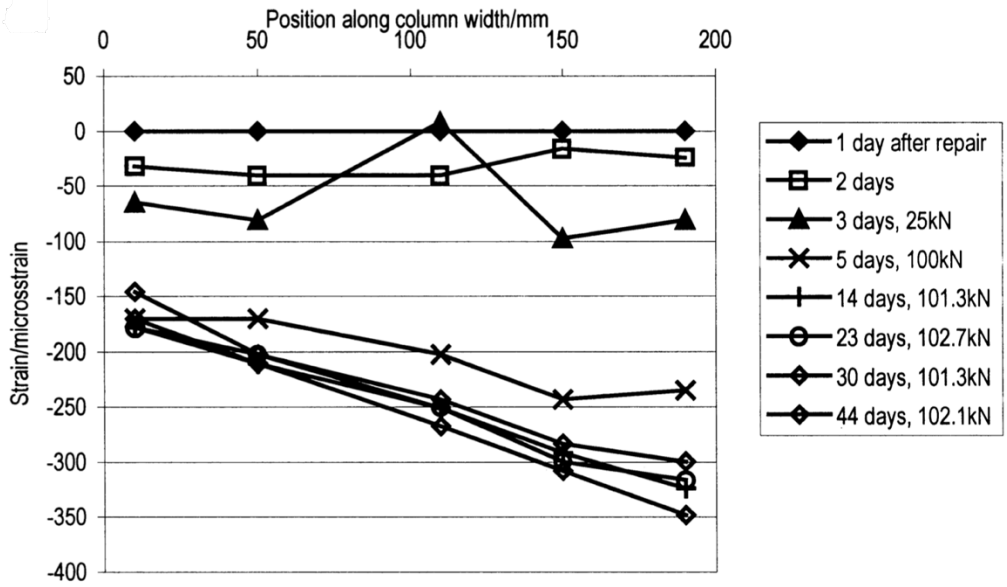

Figure 2-11: Redistribution of stress to substrate concrete due to differential volume change in cross-section of repaired column adopted from Shambira & Nounu (2000)

Mangat & O'Flaherty (1999a) conducted a field investigation into the stress and strain distribution of structural patch repairs on existing bridge abutments over a 60 week period. The bridge abutments were repaired in a propped and unpropped state with four flowing cement-based repair materials, with modulus of elasticity ranging between 24-32 GPa and free shrinkage strains ranging between 388-791 micro strains. For patch repaired abutments in a propped state the authors found similar results to Shambira & Nounu (2000). Compressive stresses are transferred to the substrate concrete as the repair material undergoes shrinkage strain. Figure 2-12 shows the strain-time of the various components of the patch repaired abutment.

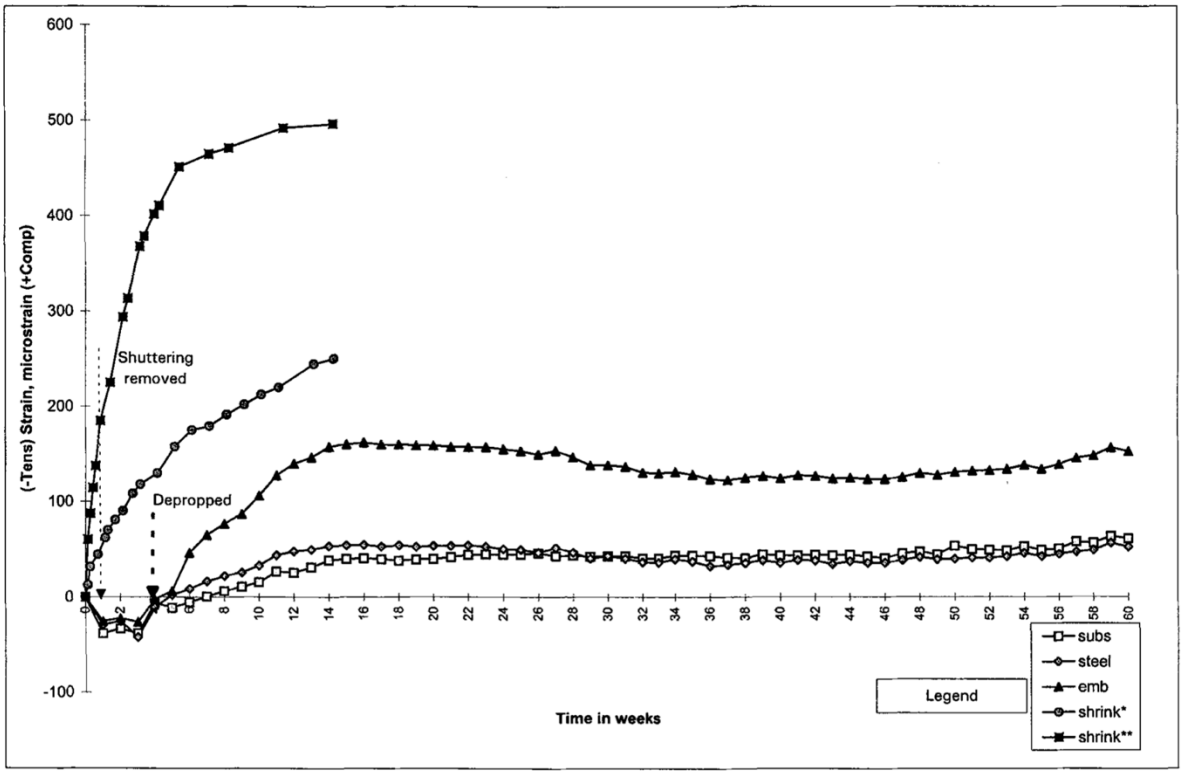

Fig. 6 – Strain-time relationships for the repair patch of flowing material S1 on the propped column of Sutherland Street bridge. $E_{rm} > E_{sub}$. (* free shrinkage after 28 day curing in water, ** free shrinkage after 24h).

Figure 2-12: Strain-time measurement of structural patch repair undergoing shrinkage adopted from Mangat & O'Flaherty (1999a)

2.3.6.6 Shrinkage estimation

Most structural design codes provide means to estimate linear shrinkage in concretes, which are dependent on mix proportions, in-service environmental conditions and element size. The sum of variables affecting shrinkage is large, making such predictions often less than perfect. Most of the estimation methods in the codes are based on normal strength concretes, which may not apply to high strength repair materials. According to Dilger et al. (1996), the shrinkage and creep behaviour of high strength concretes is significantly different from normal strength concretes. As a result several current estimation methods in the respective codes underestimate early age shrinkage (<24 hours) and overestimate long term shrinkage in high performance concretes (Alexander & Beushausen, 2009). Dilger et al. (1997) have proposed estimation methods for shrinkage of high strength concretes.

2.3.7 Creep

Creep is defined as a time-dependent increase in the material's strain due to sustained stress. It may also present itself as a relaxation of stress in a material under a constant strain. Creep has a reservable component and irreversible, plastic component. The former may be considered as a delayed-elastic strain.

The parameter used to describe the creep properties of a material is called specific creep C_c, which is defined as creep strain ε_c per unit stress. This parameter may be used to describe and compare the creep properties of different materials. Creep may also be expressed in the form of a creep coefficient ψ, which is defined as creep strain ε_c divided by the initial elastic strain ε_0 at the time of initial loading. Expressions for specific creep C_c and the creep coefficient ψ are represented in equation 2.1 and 2.2 respectively.

$$C_c = \varepsilon_c/\sigma \qquad \textbf{[2.1]}$$

$$\psi = \varepsilon_c/\varepsilon_0 \qquad \textbf{[2.2]}$$

The creep strains of concrete are measured on specimens loaded below 40% of the strength of the material at the age of loading. The reason for this, is that the concrete is in its linear elastic state at this level of loading, for which the creep is proportional to the stress (Kristiawan, 2006). Most testing standards specify that concrete specimens used for creep testing be loaded at a concrete age of 28 days, allowing for sufficient compressive strength development and decreasing the influence of drying shrinkage on creep strain values. A higher compressive strength allows for higher applied testing loads, resulting in less sensitive creep measurements to the small fluctuations in stress throughout the testing period. In practice, repair materials are often subjecting to loading at early ages when the material may not have obtained its 28-day strength. At times, these stresses may be above 40% of its respective strength. This creates a challenge in determining creep behaviour in repair materials.

2.3.7.1 Typical creep characteristics in repair materials

Creep strains may be tensile or compressive, depending on the stress induced in the material. Majority of experimental work on the creep characteristics of materials have been conducted under compression. Emberson & Mays (1990a) found that resin-based repair materials generally had higher creep strain values over 15 month loading period in comparison to cement-based repair materials. Among the cement-based materials, the authors found the polymer modified vinyl acetate material to exhibit the largest creep strains. Similarly, Mangat & Limbachiya (1994) found the significantly higher creep strains for a single component polymer modified repair mortar when comparing it to a mineral-based concrete with no additives or aggregate, and a high performance concrete with a blend of Portland cement and aggregate. According to Pan & Meng (2016) the creep characteristics of high performance concretes are different to those of normal concretes, owing to their low permeability, low w/c ratio and dense microstructure. High performance concretes and other cement based materials with high cement content generally show slow development of creep coefficients with lower ultimate creep values (Manita & Triantafillou, 2011; Vaysburd, 2016). A high quantity of pozzolan content, i.e. fly-ash, ground granulated blast furnace slag and silica fume, was found to result in significantly higher creep coefficients, reported by Pane & Hansen (2002) and Manita & Triantafillou (2011). Water content also plays a significant role in creep. According to Acker & Ulm (2001), cement-based materials are subjected to little to no creep where the evaporable water has completely dried up.

For cement-based materials, the shorter the age at which the material is loaded, the larger the creep coefficient of the material (Pan & Meng, 2016). The creep coefficient of a material decreases with an increase in curing age and tends to be less sensitive to age of loading beyond a curing age of 21 days. Yuan & Marosszeky (1994) measured the creep coefficient of four polymer modified cement based repair materials at loading ages of 2, 4, 7, 14 and 28 days after casting. From Figure 2-13, the creep coefficient of the styrene butadiene rubber (SBR) repair concrete when loaded 2 days after casting is almost two and half times higher, in a two week measurement period, than the same material loaded at 28 days.

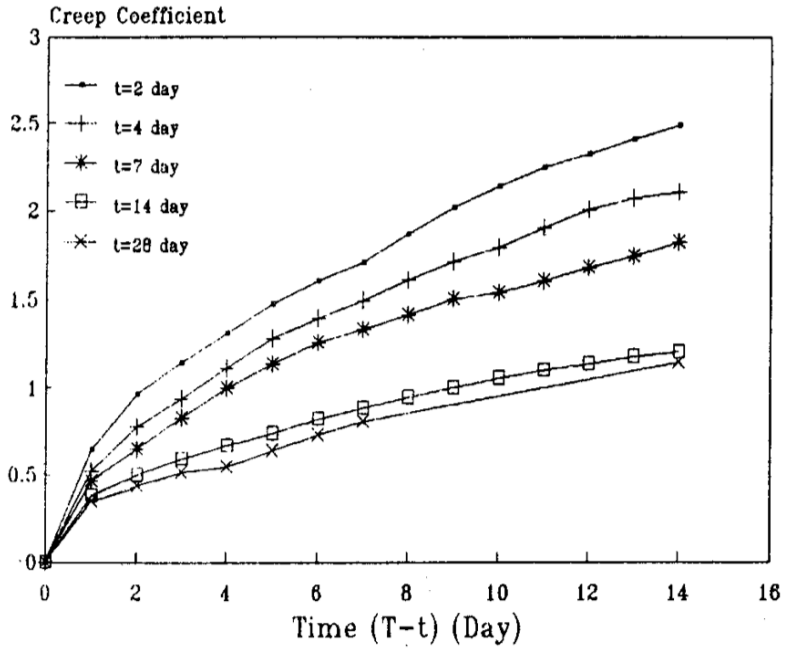

Figure 2-13: Creep coefficient of styrene butadiene rubber (SBR) cement based repair concrete for loading at different concrete ages adopted from Yuan & Marosszeky (1994)

Pan & Meng (2016) found similar results of increasing creep coefficient as the age of loading was decreased when concrete samples were loaded at age 7 and 14 days, respectively. The creep measurements were taken over a 19 month period. They further found that the rate of development of the creep coefficient beyond 30 days of loading, is unaffected by the age of loading. Implying that rate of development of the creep coefficient prior to 30 days of loading is comparatively higher for materials loaded at younger ages.

Pan & Meng (2016) conducted an investigation on the effect of sample size and magnitude of load on the creep coefficients of plain concrete loaded at age of 14 days. They found that the larger the sample size, the lower the creep coefficient for samples loaded at the 40% of the compressive strength of the material at time of loading. This was attributed to the close relationship between creep and the migration of moisture and drying of the concrete, both being slower in larger sample sizes. Pan & Meng (2016) also measured creep strains on samples loaded to 20% and 40% of the compressive strength of the concrete at 14 days of age. The level of applied stress in both cases falls within the linear elastic range of concrete, however the concrete

samples loaded to 40% of the compressive strength exhibited slightly higher creep coefficients than those loaded to 20% of the compressive strength. It was concluded that the high compressive stresses may result in the closure of drying microcracks in the material, increasing the compressive deformation in the concrete.

2.3.7.2 Creep in patch repairs

The creep characteristics of the repair material may render desirable or undesirable effects, depending on imposed conditions and type of repair (Emberson & Mays, 1990a). The imposed conditions on patch repair may be viewed from two stand points, one with the presence of an externally imposed compressive stress in the repair and one without.

In patch repairs where there is no externally imposed stress on the repair, the onset of restrained shrinkage action, induces tensile stresses in the repair material. Under such stress the repair material undergoes tensile creep strain, resulting in the relaxation of a portion of the induced tensile stress in the material. This phenomenon, known as tensile relaxation, is beneficial in reducing the likelihood of crack development in the repair material. Beushausen & Alexander (2006) found tensile relaxation to be crucial for the serviceability of bonded concrete overlays, releasing approximately 40-50% of overlay tensile stresses. Similar results were obtained by Altoubat & Lange (2001) in a study on normal and high strength concretes. There is limited research on direct measurements of tensile relaxation and its link to tensile creep characteristics in concrete repairs, due to complexities in quantifying tensile relaxion behaviour (Beushausen, 2005).

In patch repairs subjected to external imposed loading, creep may have undesirable effects with respect to the distribution of load in the repaired member. The creep coefficient of cement-based materials develops at a decreasing rate. Hence, substrate concretes may undergo little to no creep deformation in comparison to fresh repair materials. In repaired concrete elements subjected to compressive stresses, differential creep strain in the repair material results in the redistribution of stress from the repair material to the substrate concrete. This may render the load sharing capacity of the repair material less active with time (Mangat & Limbachiya, 1994). The mechanism of load transfer to the substrate concrete under differential creep strain is similar to that of differential shrinkage discussed earlier. This often makes it difficult to experimentally differentiate their independent contributions to load transfer, as both phenomena often occur concurrently in repair applications. There is a limited amount of empirical research measuring the effect of creep on load transfer in repair systems. Experimental research by Shambira & Nounu (2000) and Mangat & O'Flaherty (1999a) identify the mechanism transfer of load transfer to the substrate concrete, however, their conclusions attribute these effects to the influences of shrinkage strain. It is reasonable to assume that under a period of sustained loading in both these works, the repair systems may be susceptible to differential creep, contributing to the load transfer mechanisms. It is important to note that the transfer of load to the substrate concrete, effectively decreases the load sustained by the repair material over time. This will result in comparatively less ultimate creep strain than if the full load was sustained on the material.

2.3.7.3 Creep under varying load

Determining the creep strain in a material that is subjected to varying stresses may be conducted using the Boltzman superposition principle, owing to the linear relationship between creep and stress (Alexander & Beushausen, 2009). The principle states that the total creep strain $\varepsilon_c(t)$ at time *t* may be determined by adding the creep strains from separate stress increments, applied at different ages of the material's loading history. Applying the Boltzman principle, Trost (1967) developed a simplistic equation to determine creep due to incremental loading.

$$C_c = \varepsilon_{creep}(t) = \frac{\sigma_0}{E} \cdot \varphi(t, t_0) + \frac{\sigma_t - \sigma_0}{E} \cdot \rho\varphi(t, t_0) \qquad \textbf{[2.3]}$$

where ρ is an aging coefficient which considers the incremental effect of applied stress $(\sigma_t - \sigma_0)$ over period $(t - t_0)$.

Simplified linear creep laws, based on the principle of superposition have been developed to offer approximate solutions for creep strain analysis of structures under varying stresses. Among the oldest are methods consisting of a single elastic solution, which are based on the effective modulus of the material and tend to overestimate creep strains, according to Bažant (1975). Bažant (1975) believes that the rate-of-flow method offers creep predictions closer to the exact solution. The method separates the development of creep strain into a recoverable and irrecoverable creep component, both of which are proportional to the applied stress. The recoverable component is estimated to be equivalent to 40% of the elastic strain of the material at 28 days. This component is considered to be affected negligibly by loading and environmental conditions. The irrecoverable creep or flow component is calculated for each stress increment.

2.3.7.4 Creep recovery

The SANS 10100-1:2000 code, corresponding to the BS 8110, provides a measure of the final creep recovery, which is equivalent to 30% of the elastic recovery of the material on unloading over a period of one year. Alexander & Beushausen (2009) represent the recoverable and irrecoverable components of creep strain graphically in Figure 2-14, indicating the increase of irrecoverable creep over time.

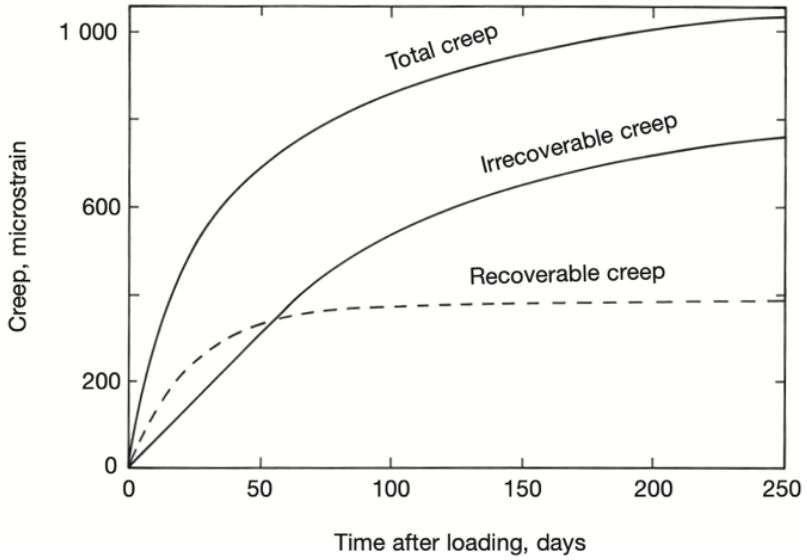

Figure 2-14: Creep and creep recovery over time adopted from Alexander & Beushausen (2009)

2.3.7.5 Creep estimation

Empirical methods for the prediction of creep are available in most structural design codes. The factors influencing creep are however complex, preventing the adoption of an agreeable approach that is universally applicable (Alexander & Beushausen, 2009). For this reason, as with shrinkage prediction, the estimations for creep are imperfect at best. The choice of prediction method usually depends on the level of accuracy desired, as well as the quality of information available. The South African National Standards code (SANS 10100-1:2000), adopted from the British Standard BS 8110, estimates a single creep strain value for the material after 30 years as a function of the elastic strain at the time of loading and a creep factor. The creep factor is read off a graph as a function of concrete member dimension, age at the time of loading and relative humidity According to the code, the creep development over time may be assumed to be 40%, 60% and 80% of the final creep strain after one, 6 months and 30 months, respectively. The CEB-FIP and RILEM Model B3 documents make provision for higher levels of estimation of creep at specific times. However, these models require substantially more information. Dilger et al. (1996) found that the creep behaviour of high strength concretes, which may be more applicable to high strength cement based repair materials, was significantly different from normal strength concretes. Dilger et al. (1997) have proposed new creep models applicable for high strength concretes.

An alternative method of estimating creep strains in concretes at a specific time is through forecasting creep strains, based on the measure creep strain in the material at 28 days. Brooks & Neville (1978) suggested an expression relating to long-term creep, with respect to 28-day values, obtaining a 95% confidence limit for 5-year creep deformations of various concretes. The expression determines the specific creep ($C_{c,t}$) at any time (t) after the application of the load on

the material, using the specific creep after 28 days of loading. The expressions for basic creep and total creep are found below.

$$basic\ creep \quad C_{c,t} = C_{c,28} \times 0{,}5t^{0{,}21} \qquad \textbf{[2.4]}$$

$$total\ creep \quad C_{c,t} = C_{c,28} \times [-6{,}19 + 2{,}15 \log_e t]^{0{,}38} \qquad \textbf{[2.5]}$$

where $C_{c,t}$ is the basic or total creep at time t, $C_{c,28}$ is the basic or total creep at 28 days and t is point in time where the creep is desired to be measured.

2.4 Other influences on stress and strain distribution in repairs

The stress and strain distribution in patch repairs is affected by various factors. The effects due to material properties of the substrate concrete and repair material have been discussed in earlier sections. The sections to follow describe some of the key influences with reference interaction between substrate concrete and repair material, additional material components, as well as the significant environmental and imposed conditions which repairs may be subjected to.

2.4.1 Interface bond

A long-lasting bond at the interface of the substrate concrete and the repair material is the primary performance criteria for successful concrete repairs (Vaysburd, Bissonnette & von Fay, 2014). The performance problems that arise from bond failure are cracking and delamination between the substrate concrete and repair material. Bond failure may impede the transfer of stresses in the repaired member, lead to ingress of water, and expose the various components (e.g. reinforcement steel) of the repaired structure to aggressive ions and environments, which may lead to deterioration. The interface bond line in concrete repairs is often subjected to stresses due to loading and differential volume changes between the substrate concrete and the repair material. When such stresses exceed the adhesion capacity of the bond between the two materials, cracking and delamination occurs.

Adhesion or bond may be characterised from two viewpoints: (1) the conditions and kinetics of joining the materials and; (2) the stress/energy that is required to separate the two materials. The latter is easier to measure and may be readily represented in a quantitative form, making it easier to compare different materials. Thus a large amount of available bond strength data is represented as the stress/energy required to separate two materials. Common test methods used to measure bond strength include interface shear, torsion and tensile testing. Relating the results from these various tests is difficult as they possess distinctly different bond mechanism characteristics. Emberson & Mays (1990a) conducted tensile pull-off tests on nine generic repair materials. The possible locations of failure in pull-off tests may be in the substrate concrete, repair material or at the bond line between the two materials, depending on which of the three has the lowest tensile stress capacity. Pull-off tests conducted on resin based repair materials resulted in tensile failure in the substrate concrete, indicating sufficient tensile strength in the repair material and similarly sufficient adhesion strength of the bond. In contrast, most of the

cement-based repair materials had failure planes along the interface, with tensile adhesion strengths ranging from 0.71MPa to 1.56MPa. Flowing concrete, however, was found to have sufficient tensile adhesion to cause failure in the substrate concrete, even surpassing strengths of most of the resin based materials.

There are a number of factors that affect the bond strength in concrete repairs. The process of preparation of the substrate surface before repair is considered to be crucial in obtaining a strong bond in concrete repairs. Yuan & Marosszeky (1994) tested the bond strength of four polymer modified repair concretes, under varying levels of surface roughness. They found that the rougher the surface, the closer the adhesion strength was to the tensile strength of the repair material. Other factors that affect the bond strength in concrete repairs are divided into those pertaining to the properties of the substrate concrete and repair material. The temperature at time of repair, moisture conditions and carbonation of the substrate concrete, as well as the repair material's workability, curing and tensile strength all contribute to the strength and durability of the bond. These factors are discussed in further detail by Beushausen (2005) and Vaysburd, Bissonette & von Fay (2014). The use of bonding agents to increase bond strength has been researched, with varying results. Bonding agents are helpful in small patch repair applications. Lower mechanical bond strengths are generated when stiff repair materials are applied on relatively small surface areas. For larger surface areas, Ortega et al. (2018a) found no appreciable effect on the bond or behaviour of columns when bonding agents were used in the repair application.

Remedying high bond interface stresses with high bond adhesion strength is not always the most favourable approach, as it may lead to failure of the bond regardless of the increase in strength. The ACI Committee 364 (2010) notes that, although a good bond strength is critical to the success of the repair, increasing the bond strength of the repair material is often accompanied with an increase in elastic modulus properties of the repair material. Under restrained shrinkage conditions, discussed in Section 2.3.6.4, an increase in elastic modulus may lead to a decrease in tensile strain capacity of the material and potential cracking. Decreasing bond interface stress in concrete repairs puts less strain on the bond, decreasing the probability of cracking and debonding. Emberson & Mays (1996) found that similar values for elastic modulus of the substrate concrete and repair material avoids the development of stress concentrations close to the bond interface in structurally loaded repairs.

2.4.2 Loading influences

2.4.2.1 Propped and unpropped

The primary performance requirement of structural patch repairs is to carry a portion of the load in the repaired concrete element. This may be achieved by recreating the original distribution of load in element. To achieve this, according to Emmons and Vaysburd (1994), full load is required to be relieved during the repair process and only reapplied once the repair material has achieved its specified strength. Loads on a element may be relieved by propping the element, which

primarily serve to either relieve load from the element or change the load path of the load (Cairns, 1993). Propping structural elements during the repair process is often quite costly and may not be possible in some instances, prompting research into the behaviour of concrete repaired during propped and unpropped implementations.

Cairns (1993) found that the flexural strength of repaired concrete beams were unaffected by the absence of propping. Mays & Barnes (1995) found similar results when load testing H-frames. The beams and H-frames tested by Cairns (1993) and Mays & Barnes (1995), respectively, were repaired in the tensile zone of the beams, which has less influence in the distribution of load and strength capacity. According to Emmons and Vaysburd (1994), in structural applications, it is most desirable to replace concrete in the compressive state, where the repair material will bear compressive stresses. Sharif et al. (2006) recommends that all loads are relieved during the repair on columns under axial compression. They found that columns repaired in an unloaded state were structurally effective compared to repairs conducted in a loaded state, which failed to participate in load sharing in the repaired column. In contrast, Mangat & O'Flaherty (1999b) found that repairs conducted on unpropped highway columns with repair materials with higher modulus of elasticity than the substrate concrete, are successful in attracting long terms external load. The stance held by the ACI Committee 346 (2010) on this particular finding is that "even with equivalent or higher modulus repair material, permanent loads will not be shared unless the existing member is unloaded prior to repair".

2.4.2.2 Formwork pressure

The use of formwork in repair application of flowing cement-based repair materials may result in the build-up of formwork pressure. When flowing repair materials are applied at a fast enough rate such that their internal structure is not built up to withstand the load from the materials cast above it, this results in lateral stresses being applied on the formwork (Kovler & Roussel, 2011). Once the formwork is removed tensile stresses are induce in the repair material causing tensile strains to form, corresponding to findings by Mangat & O'Flaherty (1999a) on flowing concrete repairs used for large patch repair applications. In smaller patch repairs the effect of formwork pressure may be insignificant due to small amount of materials used in the application.

2.4.3 Environmental and other influences

2.4.3.1 Environmental influences

The external environmental conditions play a significant role in the structural behaviour and durability of the repair system. Concrete repairs can be subjected to various temperatures, relative humidity, mechanical loads and/or chemically aggressive environments, which may affect the stress and strain experienced in the system. Direct stresses may be induced in the structure by means of mechanical loads such as wind or snow loads. Indirect stresses are induced as a result of differential volume change in the repair system, due to the interaction between the environment and the material properties of the repair material and substrate concrete. The

mechanism of stress and strain behaviour due to volume change are discussed elsewhere. Shrinkage strain is sensitive to temperature and relative humidity (Pan & Meng, 2016). Mangat & Limbachiya (1994) found that shrinkage strain in polymer-modified and high performance cement-based repair materials was more sensitive to change in relative humidity in comparison to plain concrete. Materials allowed to cure in 30% relative humidity were found be more susceptible to shrinkage at early ages than those at 50% relative humidity. Robery & Shaw (1997) note that at elevated temperatures, the creep of repair materials may be significantly higher than that of structural concrete.

2.4.3.2 Steel reinforcement

Corrosion of reinforcing steel is the leading cause of deterioration in RC structures. Patch repair application of these structures will result in the interaction between the repair material and the reinforcing steel in the repaired concrete system. Mangat & O'Flaherty (1999b) found that efficient composite action between the repair material and substrate concrete is created when the steel reinforcement is continuous through the two materials. According to Pellegrino et al. (2009; 2011), 50mm thick patch repairs that include steel reinforcement behave structurally better than 15-20mm repaired that don't. Pellegrino et al. (2009; 2011) tested concrete repairs in axially loaded columns, as well as beams under four point bending loads. The repair materials that included reinforcing steel were able to share load in the structure, resulting in higher levels of ultimate strength for the repaired members. Repairs without reinforcement showed signs of premature debonding when subjected to loads.

Steel reinforcement may also play a role in time-dependent volume changes, like creep and shrinkage in the repair material. According to Pan & Meng (2016), the presence of reinforcing steel imposes considerable restraint action on the development of shrinkage and creep strains in high performance concretes. This effect increases at high ratios of steel reinforcement. Mangat & O'Flaherty (1999b) found similar restraining action of reinforcement steel in field repair applications.

2.4.3.3 Crack formation

Cracking is detrimental to the performance and durability of the concrete repair for several reason, irrespective of the cause of cracking. From a durability point of view, cracks enable the ingress of water and aggressive ions into the repair. The formation of cracks in repair materials may have a detrimental effect on its ability to carry load (ACI Committee 364, 2003). Cracks in the repair material and the bond line of the repair cause discontinuities, preventing the transfer of stress in the repair material.

2.4.3.4 Coarse aggregates

The addition of course aggregates to repair materials may affect the structural behaviour of the repaired concrete system. It primarily affects the physical properties of the repair material. It has been reported (Emmons & Vaysburd, 1994; Mangat & Limbachiya, 1994) that the addition of

course aggregate in repair materials creates dimensional stability, decreasing the strain due to shrinkage, creep and thermal expansion/contraction while increasing the modulus of elasticity of the material. The combination of these effects may prevent the distribution of load from the repair material to the substrate concrete in the long term, increasing the load sharing capacity of the repair material. Coarse aggregate usually also has economic advantages, replacing volume of often expensive commercial repair products. The use of course aggregate is not always possible in patch repair applications where a limit on particle size exists. Some aggregates may also have adverse effects on the chemical composition of the repair, leading to an increase in porosity or reduction in strength of the repair material (Emmons & Vaysburd, 1994).

2.5 Repair performance

The performance of structural patch repairs may be viewed from two stand points, the performance of the repaired element as a whole or the performance of the repair material within the repaired element. These may be respectively considered as the “macro” or “micro” view of the repair performance. The sections below primarily review the methodology and results obtained from empirical research for both these views of repair performance, with reference to the short- and long-term effects where applicable.

2.5.1 Repair material performance

Emberson & Mays (1990b) examined the stress and strain distribution in patch repaired RC beams under axial tensile load. The load was transferred through 4 bars that ran through the length of the beams. Repairs were conducted on opposite sides of the beams at mid span at depths covering the steel bars, with 9 generic repair materials previously characterised by the authors (1990a). Repair materials with higher tensile modulus in comparison to the substrate concrete attracted more load, while lower modulus repair materials attracted more load to the substrate concrete. Two of the repair materials failed to participate in load sharing in the repaired beam, as bond failure occurred at the interface of the repair prior to loading due to restrained shrinkage stresses.

Emberson & Mays (1996) conducted three types of tests on repaired RC beams: four-point bending static test; long term creep test and; dynamic fatigue test. The repairs were conducted with 6 different repair materials, in either the tension or compression zone of the beams at varying lengths. The authors found a correlation between the creep material properties of the repair material and behaviour in the repaired system, under the long-term creep test. Resin-based materials performed the best in dynamic tests due to high resistance to cracking and relatively low deflections under cyclic loading.

Shambira & Nounu (2000) conducted time dependent experiments over a 44 day period to measure the distribution of strain in patch repaired RC columns under loaded (under axial compression) and non-loaded conditions. The experiments were conducted on one-side of the columns and varied by the use of one resin-based and one cement-based repair material. The

resin-based and cement-based repair materials, a comparatively lower shrinkage polymetric material (PM) and comparatively higher shrinkage polymer modified material (PMM) respectively. The cavity depth of the repairs was modified between tests. Prior to repair, the concrete columns were allowed to cure for two years, to ensure negligible shrinkage strain in comparison to the repair materials. Load was applied to the columns two days after the repair, for the experiments in the loaded case. In the short term, both materials attracted load but was shed to the substrate concrete over time, due to differential shrinkage and creep in the repair material. The redistributive effects were less in the case of the low shrinkage PM, resulting in larger load sharing capacity over time compared to the PMM. For the non-loaded specimens, the shrinkage strain in the repair materials induced bending in the column, resulting in lengthening in the substrate measured on the face opposite to the repair face. This was more pronounced in the high shrinkage PMM. The lengthening of the substrate increased with the increase in repair cavity depth. Observed bending action in this study, generally indicates satisfactory bonding between substrate concrete and repair material and thus good composite action in the column repaired with the PMM. The research provides meaningful results with respect to the influence of shrinkage and creep on load sharing and distribution in the repaired column over time. However, the elastic modulus of the repair materials was not reported and, thus, their influence on load sharing and distribution in the column not considered.

Sharif et al. (2006) investigated the structural effectiveness of patch repairs on RC columns under axial compression using two materials with high and low modulus of elasticity respectively. The experimental work includes repairing the columns in an unloaded and loaded state. In the unloaded state, when repaired using the high modulus of elasticity repair material, the stress distribution in the repair material and the substrate concrete are similar showing good structural effectiveness. The low modulus of elasticity repair material in contrast, attracts substantially lower levels of stress. Both repair materials, fail to attract any loaded in the loaded scenario. However, in the case where additional incremental load is added to the column repaired in the loaded repair state, the repair materials are active in sharing a portion of the additional load. Similar to the unloaded scenario, the higher modulus of elasticity repair material was more effective in attracting the portion of the load.

2.5.2 Repaired member performance

Emberson & Mays (1996) conducted four-point bending static tests on repaired RC beams as part of the research previously mentioned. They found the repaired beams to retain 78% to 98% of the ultimate strength of the unrepaired control beam. All the beams failed under ductile flexural with yielding in the tensile reinforcement. Some beam failures were accompanied by bond failure. Beams repaired with comparatively low elastic modulus materials failed at comparatively lower stresses compared to the other beams, which the authors attribute to a shift in neutral axis of the beams allowing the reinforcement to yield at lower stresses.

Mays & Barnes (1995) loaded repaired RC H-frames to failure to determine the ultimate strength of the repaired member. The H-frames were repaired in the tension and compression

zones of the beams and opposite sides of the columns, with two cement-based repair materials. The repairs were conducted under three different loading scenarios: no loads; only dead loads and; dead and live loads. The loading scenario during the repair had an insignificant effect on the final load carrying capacity of the H-frames which was similar to the unrepaired control samples tested. The H-frames failed due to primary tensile failure in the beams, i.e. yielding in the tensile reinforcement, similar to results obtained by Emberson & Mays (1996). Other studies (Río et al., 2005; Pellegrino, Da Porto & Modena, 2011) show similar failure modes, recommending high bond strength of the repairs to avoid accompanying bond failures. These results indicate the less significant role of the repair material in resisting which lead to tensile failure in repaired beam elements. In such applications, greater significance is put on bond strength in prevention of debonding in the during the failure process.

Pellegrino et al. (2009) tested the ultimate axial compressive strength of repaired RC columns, repaired on one side with a polymer-modified cementitious repair mortar. The repairs were conducted in two thicknesses, 50 mm and 15 mm, which included and excluded the longitudinal reinforcing steel, respectively. The repair material experienced low shrinkage and had mechanical properties the similar to the substrate concrete. The authors found that the repaired column was unable to reinstate the original ultimate strength of the column. The thicker, 50mm, repair that included reinforcing steel showed better structural action, in comparison to the 15mm thick repair. It obtained 91% of the control column's ultimate strength and avoided premature debonding, which was apparent in most of the 15mm thick repairs.. In a follow up study, Da Porto et al. (2012) tested the load carrying capacity of RC columns repaired on all four sides at 50mm thickness, with three different polymer-modified repair mortars, having different modulus of elasticity properties. The materials were unable to restore the original ultimate strength of the columns, however the material with the highest modulus of elasticity of 29 GPa (compared to 25 GPa and 28 GPa) was able to restore 95% (compared to 85% and 86%) of the original strength.

Ortega et al. (2018c,a,b) conducted experimental work on the ultimate strength of RC columns, repaired on one and all four sides. The materials used in the experimental work included R3 and R4, in accordance with the European Standard EN 1504. The repair material was applied, with and without bonding agents. In both repair cases, one sided and four-sided repairs, the relatively lower modulus of elasticity R3 material performed better than the R4 material, retaining 97% and 84% compared to 65% and 64% of the original ultimate strength, respectively. The use of a bonding agent made no tangible improvement to the load carrying capacity of the repaired columns. The lower modulus R3 material had similar mechanical properties to the substrate concrete, compared to the stiffer R4 material, to which, the authors attributed the improved performance of the material.

Kristiawan et al. (2019) conducted experiments on patch repaired RC columns under an eccentric compressive load. The columns were repaired with a low modulus repair materiel, 9-10 GPa. The eccentric force was applied off-centre of the column, with the repairs was conducted

in three configurations, as shown in Figure 2-15. The load was applied above the repaired side in each configuration. The repaired columns failed in compression resulting in spalling of the concrete cover at the top of the column in the region below the concentrated load. The undamaged column failed in a similar mode, additionally experiencing failure at the base of the column. The patch repaired columns showed high stress concentrations in the reinforcement steel and undamaged concrete zone of the column, indicating the ability of the repair material in distributing the stresses from an eccentric force to other components of the repaired member. The repaired columns were, however, unsuccessful in retaining the original ultimate strength of the column, obtaining between 71%-92% of the original strength.

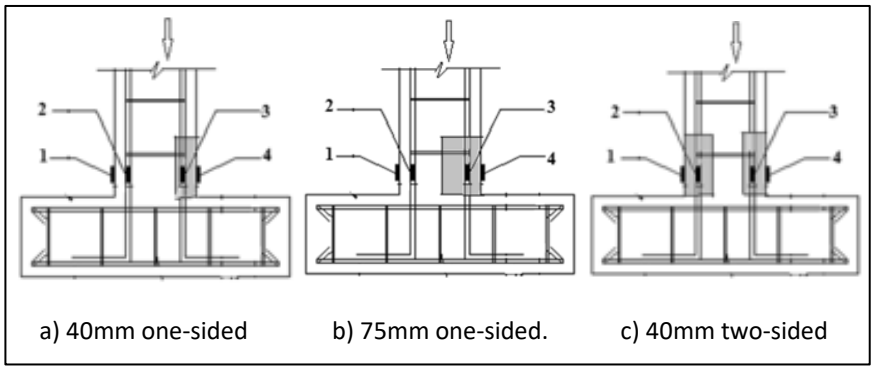

Figure 2-15: Force and repair configurations adapted from Kristiawan et al. (2019)

2.6 Repair models and repair material models

2.6.1 Introduction

The use of models assists us to understand past behaviours but, more importantly, are able to predict future behaviours. The challenge with concrete repairs is the non-uniformity in cause of damage, type of structure, type of repair, material properties and environmental and imposed conditions, which has proven to be difficult in implementing wide reaching codes of practice let alone developing universally applicable models.

Models used to analyse the stress and strain behaviour of structural patch repairs may be divided into analytical and numerical techniques. Numerical models are typically based on specific solutions for unique repair problems or scenarios, whereas analytical models are focussed on sets of formulas used to describe the general behaviour of a repair. For structural patch repair applications, numerical models have been developed mostly using finite element methods. However, there is a dearth of empirical research on analytical models for such repairs. Numerous analytical models for non-structural patch repairs have been proposed by researchers, based on differential shrinkage between substrate concrete and repair material. Some of these models are discussed below.

2.6.2 Numerical repair models

Emberson & Mays (1990b, 1996) used experimental data to validate a linear finite element (FE) numerical model used to determine the stress and strain distribution in patch repaired concrete columns and beams. The adjustable material parameters governing the structural behaviour in the models were the modulus of elasticity and Poisson's ratio of the repair material. Based on the FE model for a repaired column under uniaxial tensile load, for significantly different modulus of elasticity properties between the repair material and substrate concrete, localised stress concentrations developed close to the interface of the materials, requiring high values of adhesion. Differential Poisson's ratios between the materials result in stress zones on the surface adjacent to the transverse interface in unreinforced columns, which was less apparent in reinforced columns. Repair materials with a tensile modulus higher than the substrate concrete attract more stress to the repair. The converse was true for repair materials with low modulus properties, attracting stress to the substrate concrete. The same holds true, based on the FE model under flexural loading, with respect to the distribution of stresses in repair materials for higher and lower modulus of elasticity properties, for repairs conducted in the compression and tensile zones of beams. Similar to the column, significant differential modulus of elasticity properties between the repair material and substrate concrete, resulted in stress concentrations at the interface of the repair.

Pellegrino et al. (2009) developed a three-dimensional non-linear FE model to simulate results obtained from experiments (previously discussed in Section 2.5.1) on repaired RC columns under axial compression. In addition to showing good correlation with the experimental results of the column's ultimate strength, the model was able to show debonding failure between the materials with sudden discontinuities at the upper bound of the stress ranges.

Shambira & Nounu (2001) conducted a non-linear FE simulation for the behaviour of moderately loaded patch repaired RC columns, under the time-dependent influence of shrinkage and creep in the patch repair material. In the short term, patch repair materials participate in load sharing in the column. Over time, as differential shrinkage and creep strain in the repair material develops, load is shed from the repair to the substrate concrete creating a bending effect in the column. The deeper the cavity depth, the higher the bending effect. The simulations showed qualitative agreement with experimental work conducted by the authors (2000); however, significant quantitative deviation was observed in the results. Possible shortcomings in the model may include to neglecting the effects of creep strain in the substrate and assuming a complete bond at the interface of the materials (i.e. no debonding). Regarding the former, in the experimental work by the authors (2000), the columns were allowed to air-dry for two years in an unloaded condition allowing for negligible shrinkage strain in the substrate concrete once repaired. This condition, however, does not allow the substrate concrete to undergo any of its potential creep strain, which may manifest once the columns are repaired and subjected to load.

2.6.3 Analytical repair models

The lack of research available on analytical models for structural concrete patch repairs may be attributed to the large variability in factors and conditions affecting the stress and strain distribution in such repairs. This is further made complex by the difficulty to accurately quantify the contribution of each of these factors and conditions. Repair designers are often left to make decisions on material choice and the long-term structural effectiveness of the repair based on basic engineering principals and experience.

A number of analytical models have been developed over the years to represent the stress and strain distribution in concrete overlays subjected to restrained shrinkage. The primary purpose of these models is predicting crack initiation and propagation in overlays. Most of the models developed to date are based on a theory first introduced by Birkeland (1960), considering the relative dimensions of the overlay and substrate in estimating the partial restraint of overlay shrinkage. The expression for restrained shrinkage strain by Birkeland (1960) is shown below.

$$\varepsilon_{direct} = \frac{\varepsilon_{FSS}}{1 + \frac{E_s \cdot A_s}{E_o \cdot A_o}} \qquad \textbf{[2.6]}$$

wherein ε_{FSS} is the free shrinkage strain of the overlay material, E_s & E_o and A_s & A_o are the elastic modulus and cross-sectional area properties of the substrate concrete and overlay material respectively.

This expression is based on simple beam theory and largely follows three basic assumptions, regarding the composite behaviour of the system:

- Bernoulli's principle – plane sections remain plane after being stressed;
- the overlay shrinkage is completely restrained and;
- shear stress at interface only develop at ends.

In a model developed by Beushausen (2005), he considers the localised strain conditions at the interface of repairs subjected to restrained shrinkage. In predicting total overlay strain, the model considers elastic strains, substrate creep strain and the effects of overlay relaxation in strain redistribution. The model for localised strain the in the overlay is represented below.

$$\varepsilon_{shrink}(t) = \varepsilon_{FSS} \cdot \frac{1}{1 + \frac{E_s}{E_o} \cdot C_\varepsilon} \qquad \textbf{[2.7]}$$

where parameter C_ε denotes the net effects of member dimensions and strain patterns in the substrate concrete and repair material. Experimental research (Beushausen, 2005) shows the model can reasonably predict overlay stress development.

Despite not being able to precisely determine overlay stresses and strains by reason of the multiple visco-elastic influences and time-dependent material factors, analytical models may still provide reasonable approximations fit for application.

2.7 Literature review summary

The leading cause of premature deterioration in RC structures is corrosion of reinforcing steel. In remedying the above, structural concrete patch repair interventions are often implemented to maintain the service life of the structure and/or prevent further deterioration. Research has shown, however, that the majority of concrete repairs fail within the first 5 years of the repair. These failures have largely been attributed to inappropriate repair design and inappropriate repair material choice.

The existing codes of practice and guidelines for concrete repairs provide a framework for concrete repair design, implementation and management. These frameworks are sufficient to guide concrete repairs conceptually at a high level, however, limited in providing measurable guidance on repair material selection to designers and applicators.

None of the reviewed repair codes or guidelines contain a justifiable, i.e. either scientific or engineering-based, guidance on selection of structural repair mortars. Some of the repair codes make reference to guidance on material selection based on concrete design codes intended for new structures, which are not representative for concrete repairs. There is a need to develop appropriate tools and guidelines for structural repair mortar selection.

Research has helped identify various components of structural patch repairs and what affects their performance. The substrate concrete and repair material properties interact with imposed loading and environmental conditions inducing stresses and strains in the repaired concrete element. The performance of the concrete repair is determined by the combined ability of the materials to withstand such stresses and avoid premature distress and/or deterioration.

The repair material properties found to most significantly influence the performance of structural patch repairs are the elastic modulus, shrinkage and creep properties of the material. Other material properties such as material compressive and tensile strengths, Poisson's ratio and coefficient of thermal expansion or contraction have secondary effects on the performance of such repairs. Numerous proprietary repair materials and systems have been developed and continue to be developed for structural patch repair applications, with the above material properties in mind. Among such material, cement-based repair mortars are often preferred in structural patch repair applications based on their reported material properties. However, the reported repair material properties are insufficient to determine the performance of the repair mortar in structural applications over time.

Some empirical studies have been conducted to determine the performance of structural patch repairs using cement-based repair mortars. The performance of the structural patch repairs may be viewed from two stand points: performance of the repair material and; performance of

the repaired concrete element as a whole. The studies regarding latter are largely concerned with the ultimate load carrying capacity of the repaired element. These studies do not consider the performance of the repaired element under normal service conditions. On the other hand, studies on repair material performance consider the effects of individual material properties, on the distribution of stresses in the repaired element. However, there is dearth of research that considers the performance of the repair material due to the varying effects of multiple repair material properties. There is also very little evidence in literature that cement-based repair mortars actually structurally contribute to the performance of the repaired element under service conditions.

Currently, there exists no analytical model or tool used to determine the stress and strain behaviour and thus performance of structural patch repairs. Furthermore, very few numerical models have been developed to describe the stress and strain behaviour and performance of the structural concrete repairs, most of which have been developed to validate prior conducted empirical studies on the performance of the concrete repairs.

This research seeks to contribute towards the gaps in the research on structural patch repairs, leading to an understanding of the effectiveness of structural patch repairs in concrete structures. In doing so, an analytical model is developed in the following sections, aimed at determining the distribution of structural stresses in patch repaired elements under axial compression. The model considers the varying influences of multiple repair material properties on stress distribution in the repaired element, thus informing appropriate repair material selection.

The model is applied, in this research, to determine the stress distribution in repaired concrete elements repaired with commonly used cement-based repair mortars and concretes. This is done to determine the efficacy of such material in contributing towards load sharing in repaired concrete elements over time. The repair material properties required as input in the model are not readily available on proprietary data sheet and, thus, require specific material property testing. The material property tests are conducted in conditions which best represent the conditions of structural patch repairs. The experimental testing methodology and results, the analytical model, validation and simulation results are presented in the Chapters 3 to 7 in this dissertation.

3. Experimental Methodology

3.1 Introduction

Differential creep and shrinkage strains between the substrate concrete and repair material, together with the respective materials' elastic modulus properties, have the most significant effect on the distribution of load-induced stresses between structural patch repairs and the repaired member. Currently, no analytical model or tool exists, which is able to approximate or predict the stress distribution behaviour in such repair applications, i.e. the literature contains insufficient information on the actual structural contribution of "structural" patch repairs.

The analytical model developed in Chapter 5 seeks to predict the stress distribution behaviour in structural patch repairs conducted on concrete members under axial compression. Properties of the repair material are required as inputs into the model, which is the basis for the experimental work described here. Four types of high strength cement-based repair materials were tested for their material properties and later used in the development and application of the model.

Based on empirical research and literature, the significant repair material properties, for repair material classification and stress distribution in structural patch repair applications, were identified for testing. The repair materials were tested for the following properties:

- Compressive strength;
- Tensile strength;
- Static elastic modulus;
- Shrinkage, and;
- Compressive creep.

The compressive and tensile strength of the materials were used to classify the repair materials according to existing repair codes and guidelines. Strength properties are, furthermore, important in determining the repair material's capacity to withstand induced stresses in the material. These may either be imposed compressive stresses or tensile stresses resulting from restrained shrinkage.

The static elastic modulus, shrinkage and compressive creep properties of the repair material are important in determining the stress distribution in the repaired concrete member. These properties form integral inputs in the model developed in Chapter 5.

The materials property tests were conducted according to the South African National Standard (SANS) at the civil engineering laboratories at the University of Cape Town. For cases where no testing standard provision is made in SANS, the relevant British Standard (BS) or International Organisation for Standardization (ISO) testing standard was used. Furthermore,

modifications were applied to the standard test methods in order to obtain repair material properties which are more representative of the repair conditions. The standard material testing methods and modifications are detailed in the sections below.

3.2 Test specimens

3.2.1 Repair materials

Cement-based repair materials were selected for testing and as inputs for the repair model in Chapter 5, due to their suitability for in structural patch applications. In recommendations, first proposed by Emberson & Mays (1990a), for structural compatibility, the elastic modulus of the repair material should be similar to that of the substrate concrete. Using estimation methods proposed by codes of practice, a good quality substrate concrete of 50 MPa compressive strength, would have an elastic modulus of the order of 30 GPa. Cement-based repair materials typically obtain such values at early ages making them suitable for structural repair applications, whereas most resin-based repair materials cover the lower spectrum of elastic modulus properties, i.e. 17-25 GPa (Emberson & Mays, 1990a; Morgan, 1996; Decter & Keeley, 1997).

The repair materials selected for this experimental research were proprietary high strength cement-based repair materials. The repair materials are sourced from Sika South Africa, a commercial chemical company specialising in building supplies. Three structural repair materials were selected, based on their high early age strength and stiffness properties. A brief description of each material is provided below, followed by their reported strength and stiffness properties in Table 3-1. The full data sheet of each selected repair material can be found in Appendix A.

- Sika MonoTop-615: a high-build cementitious, polymer modified, low permeability, repair mortar.
- SikaGrout-212: high strength shrinkage compensated cementitious grout
- SikaGrout-295ZA: fatigue tested, ultra-high strength cementitious grout

Table 3-1: Reported strength and stiffness properties for repair selected repair materials

Material Property	Sika MonoTop-615	SikaGrout-212	SikaGrout-295
Compressive Strength			
- 1 day	~ 18 MPa	~ 31 MPa	~ 35 MPa
- 7 days	~ 38 MPa	~ 80 MPa	~ 80 MPa
- 28 days	~ 46 MPa	~ 95 MPa	~ 95 MPa
Elastic Modulus			
- 28 days	~ 22 GPa	n.a.	~ 30 GPa

From the three materials selected above the Sika MonoTop-615 possesses the lowest 28 day compressive strength. Both the SikaGrout-212 and SikaGrout-295ZA have similar compressive strength, although the SikaGrout-295ZA is indicated to have a higher stiffness.

High strength repair mortars have been specially developed for structural concrete repair and strengthening applications, whereas, high strength repair grouts are recommended for the repair of machine and base plates, doweling and general purpose grouting. However, in South Africa, high strength repair grouts are often used in structural repair applications due to their high early-age strength, high flowability and strong bond to concrete characteristics. These repair grout characteristics are interpreted as suitable for structural repair applications. It is within this context that the above materials were selected in this dissertation, for which their efficacy in structural patch repair applications is investigated.

The commercial repair materials were mixed to produce two repair grouts and one mortar. In addition, SikaGrout 212 was bulked up with 9.5mm Greywacke coarse aggregates to produce one self-levelling repair concrete for investigation. The mix proportions are guided by the supplier's recommendations and can be found in Table 3-2.

Table 3-2: Repair material mix proportions

		Material 1	Material 2	Material 3	Material 4
Designation*		HS grout	HS concrete	UHS grout	PMRM
Dry-mix type		SikaGrout-212	SikaGrout-212	SikaGrout-295	Sika MonoTop-615
Dry-mix content	kg/m^3	2000	1645	2049	2083
Water content	kg/m^3	280	230	246	333
9.5mm Greywacke	kg/m^3	-	461	-	-
Water to dry-mix ratio		0.14	0.14	0.12	0.16

**For this research the following designations were given to Materials 1-4 for ease of reference:

Material 1: HS grout = High Strength repair grout

Material 2: HS concrete = High Strength repair concrete (bulked with aggregate)

Material 3: UHS grout = Ultra High Strength repair grout

Material 4: PMRM = Polymer Modified repair mortar

3.2.2 Curing conditions

All test specimens were subjected to identical curing conditions. These curing conditions were applied to simulate typical site conditions of repaired concrete elements in practice. The

specimens were in cast in plastic or steel moulds. They were demoulded 20 h to 24 h after casting and wrapped in cling wrap. The specimens were allowed to cure in a drying room with a relative humidity of 55±5% and temperature of 22±2°C, until just prior to testing. These curing conditions were consistent for all the material tests conducted below.

3.2.3 Loading scenarios

The model in Chapter 5 considers that the loads on the concrete member are completely relieved for the duration of the repair and reapplied when the repair is complete. Two scenarios are considered regarding the reapplication of the load to the repaired concrete member, the reapplication of the loads after 1 day and after 7 days respectively. These two scenarios were chosen as reasonably short durations to relieve stresses on the repaired element, given the often large costs associated with relieving loads on concrete elements in service. Both scenarios further offer a significant difference in repair material properties at ages 1 day and 7 days respectively, offering a spread of inputs in the modelling and analysis of the behaviour of repaired concrete members. The interval of testing conducted on the specimens is done with the above in consideration.

3.3 Material testing

Not all repair material property data, required as input for the model in Chapter 5, is made readily available by material manufacturers, and thus, require specific testing to be obtained. Furthermore, for material property data which is made available, there is a lack of standardised testing methods as well as tests which are being conducted in conditions which are not representative of typical repair conditions. This often results in inaccurately quoted material property data (ACI Committee 546, 2014).

The repair materials in Section 3.2.1 were initially tested for, and characterised by, their strength properties, both in compression and tension. Thereafter, the materials where tested for their elastic modulus, shrinkage and compressive creep properties, required as inputs for the model in Chapter 5. The PMRM (Polymer Modified Repair Mortar), i.e. Material 4, was not tested for elastic modulus, shrinkage and compressive creep. The compressive and tensile strength properties of the PMRM were significantly lower than the other three materials, and thus set aside, with the research focus on the comparatively high strength repair materials.

3.3.1 Compressive strength

Compressive strength is important in characterising the repair material, as in EN 1504, as well as determining its load carrying capacity in compression. It represents the maximum possible uniaxial load the material can carry in compression across its cross-section. In addition, the compressive strength results of the repair materials are required as an input to conduct various other material tests, such as the elastic modulus and compressive creep tests.

The compressive strength of all four repair materials was tested in accordance to SANS 5863:2006 on 100 mm cubes. The materials were tested at ages 1 day, 7 days and 28 days, using an Amsler hydraulic compression testing machine. Three cube specimens were tested for each material for a given age, with the mean compressive strength result recorded.

3.3.2 Tensile splitting strength

The tensile strength of the repair material is important in determining its capacity to resist tensile stresses and thus cracking, arising from restrained shrinkage conditions. The tensile strength is also important for the structure to resist cracking due to an applied external load, i.e. tension zone during bending. The tensile splitting tests represents one of the indirect methods to measure the tensile strength of the material, where more direct methods are impractical owing to the difficulty of applying a truly axial tensile load on concrete specimens. Indirect tensile strength testing methods are found to overestimate strength of materials at early ages when compared to direct tensile test methods. The strength results in this research are only used as a means to compare the tensile capacity of the repair materials. The approximation of tensile stress behaviour and the respective materials' resistance to cracking, involves the consideration of a larger number of variables which are not included in the scope of this research. See work by Beushausen (2005) for more information on tensile stress and cracking behaviour in bonded overlays.

The tensile strength of all four repair materials was tested in accordance to SANS 6253:2006 on 100 mm cubes. The materials were tested at ages 1 day, 7 days and 28 days, using an Amsler hydraulic compression testing machine. Three cube specimens were tested for each material for a given age, with the mean tensile splitting strength result recorded. The tensile strength of the material was determined by the compressive load, applied on the loading pieces, required to split the cube. The set-up of apparatus used for the test is found below in Figure 3-1.

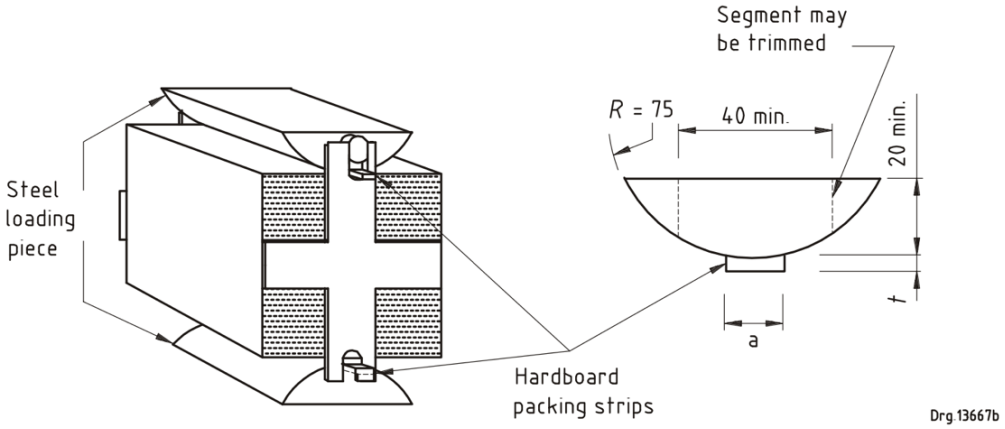

Figure 3-1: Set-up apparatus for tensile splitting test adopted from SANS 6253 (2006)

3.3.3 Elastic modulus

The elastic modulus properties of the repair materials are important in approximating the stress distribution in a repaired concrete element, and is required for the model in Chapter 5. The model represents a repaired element under axial compression, thus only the compressive elastic modulus of the material was considered in testing.

The HS (High Strength) grout, HS concrete and UHS (Ultra-High Strength) grout, Materials 1, 2 and 3 respectively, were tested for their compressive static modulus of elasticity in accordance with BS1881: Part 121:1983. Cylinders of 100 mm in diameter and 200 mm in height were tested at 1 day, 7 days and 28 days material age, using the Amsler hydraulic compression testing machine. The displacement measurements, for the conducted test, were taken as specimens and were loaded and unloaded between 0.5 MPa and one third of their compressive strength at their respective material ages. The displacement measurements were taken using a strain gauge extensometer on targets attached to the sides of the cylinders, from which elastic modulus values computed. Three cylinder specimens were tested for each material for a given age, with the mean compressive static modulus of elasticity result recorded. The set-up of the equipment used for the test is shown in Figure 3-2.

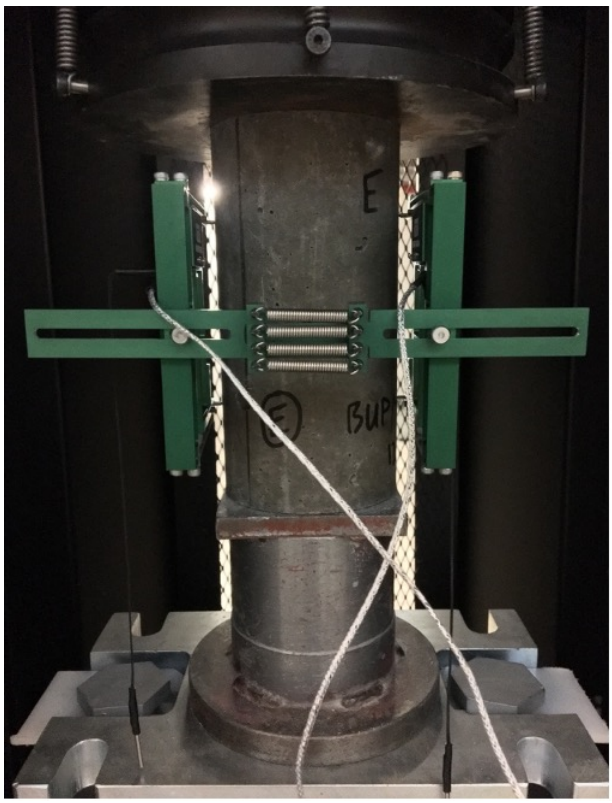

Figure 3-2: Set-up apparatus for static elastic modulus test

3.3.4 Shrinkage

The shrinkage strains of the repair materials are important in approximating the stress distribution in a repaired concrete element, and is required for the model in Chapter 5. The shrinkage measured in the experimental work is considered to be the sum of the various mechanisms of shrinkage, i.e. drying shrinkage, autogenous shrinkage and carbonation shrinkage. The shrinkage strains are further used as input for compressive creep testing of the repair material in Section 3.3.5.

The HS grout, HS concrete and UHS grout, Materials 1, 2 and 3 respectively, were tested for their shrinkage properties in accordance with ISO 1920-8:2009. Cylinders of 100 mm in diameter and 300 mm in height are used to measure shrinkage for the repair materials over a period of 0-90 days after casting of the specimens. The shrinkage was measured from the time of demoulding, i.e. 24 h after casting. The displacement strains were measured on three specimens for each of the repair materials, for which the average strain measurements of all three samples were recorded and shrinkage strain computed. The displacement measurements were taken using a strain gauge extensometer on targets attached to the sides of the cylinders.

3.3.5 Compressive creep

Repair material creep strains are important in approximating the distribution of stresses in repaired concrete element. The repaired concrete element modelled in Chapter 5 is subjected to an axial compressive load, thus only the compressive creep strain of the repair materials was measured in this research.

Compressive creep strains are highly influenced by the imposed loading conditions. This research considers two scenarios where load is reapplied to the repaired element as detailed in Section 3.2.3. The repair materials were thus tested for compressive creep for specimen load applications at material ages 1 day and 7 days respectively.

The HS grout, HS concrete and ULS grout, Materials 1, 2 and 3 respectively, were tested for compressive creep in accordance with ISO 1920-9:2009. Cylinders of 100 mm in diameter and 300 mm in height are used to measure compressive creep for the repair materials over a loading period of 0-90 days for two loading scenarios. Two cylinders were used for each material for each respective loading scenario. The specimens were loaded to stresses of 11.0 MPa and 19.8 MPa for the age of loading 1 day and 7 days respectively. The stresses were equivalent to one third of the lowest compressive strength of the three materials at the respective age of loading. The displacement measurements were taken using a strain gauge extensometer on targets attached to the sides of the cylinders, from which compressive creep strains computed. The strain gauge extensometer and set-up used for the test is shown in Figure 3-3 and Figure 3-4, respectively.

Figure 3-3: Reference bar (left) and strain gauge extensometer (right)

Figure 3-4: Set-up apparatus for compressive creep test

3.3.6 Material testing summary

A summary of the material properties tested, test method used and testing interval for the respective repair materials are summarised in Table 3-3 below.

Table 3-3: Summary of experimental tests and testing intervals

Material Property	Test Method	Test Intervals	Repair Materials
Compressive Strength	100 mm cubes SANS5863:2006	1-d, 7-d & 28-d	1, 2, 3 & 4
Tensile Splitting Strength	100 mm cubes SANS6253:2006	1-d, 7-d & 28-d	1, 2, 3 & 4
Static Elastic Modulus	200 x 100 mm ϕ cylinders BS1881: Part 121:1983	1-d, 7-d & 28-d	1, 2 & 3
Shrinkage	300 x 100 mm ϕ cylinders ISO1920-8:2009	1-90 days	1, 2 & 3
Compressive Creep	300 x 100 mm ϕ cylinders ISO1920-9:2009	1-90 days (1-d & 7-d loading)	1, 2 & 3

Material 1: HS grout = High Strength Repair Grout

Material 2: HS concrete = High Strength Repair Concrete (bulked with aggregate)

Material 3: UHS grout = Ultra High Strength Repair Grout

Material 4: PMRM = Polymer Modified Repair Mortar

4. Experimental Results

4.1 Introduction

Results, analysis and discussion from the experimental research component are contained in this chapter. The material property tests were conducted on high-strength cement based repair materials, with results presented and analysed in the form of graphs and tables.

4.2 Compressive strength

All four repair materials were tested for compressive strength. The cube specimens tested all failed under a satisfactory failure mode, in accordance with SANS 5863 (2006). The failure mode for the PMRM tested at 1 day is shown in Figure 4-1.

Figure 4-1: Failure mode for PMRM specimen tested for compressive strength at 1 day

A summary of the compressive strength results for the four repair materials tested at their respective ages is presented in Figure 4-2, with the detailed results found in Appendix B.

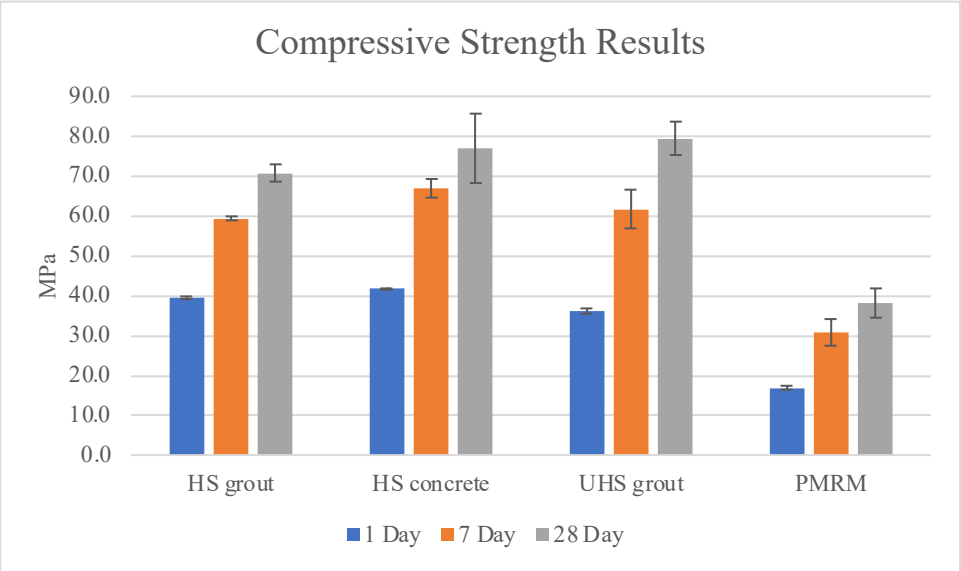

Figure 4-2: Compressive strength results for the repair materials

The PMRM, achieves the lowest compressive strength values of the materials tested, with 16.9 MPa, 30.9 MPa and 38.2 MPa at material ages 1, 7 and 28 day respectively. The HS grout, HS concrete and UHS grout, all primarily composed of high strength cementitious grouts, show similar compressive strength properties at their respective ages, approximately double that of the PMRM. These materials may thus be able to withstand higher stresses than the PMRM, making them appealing to structural applications where significant load is applied to the repair at early ages. Furthermore, these three materials, achieve 1 day compressive strength values of 39.4 MPa, 41.7 MPa and 36.3 MPa, which are significantly higher than the strength of the PMRM tested after 7 days. When comparing the HS grout and HS concrete, both containing the same cementitious grout, the aggregate bulked HS concrete achieves consistently higher strength values at all respective ages tested. The inclusion of aggregate, is found to improve the mechanical and dimensional stability properties of repair materials (Mangat & Limbachiya, 1994; Vaysburd, Bissonnette & von Fay, 2014).

When comparing the results obtained to those given in the material data sheet, it can be seen that for material age 1 day, the reported compressive strengths are similar to those obtained in testing for the HS grout, UHS grout and PMRM. However, at 7 and 28 days, the values provided on the material data sheets overestimate the compressive strengths for all three materials. The compressive strength is not an intrinsic property of cementitious materials, highly dependent on the method of testing. The difference between the test results and reported values of the parameter may be attributed to the water content in the experimental mixes as well as the curing conditions employed during the experimental testing in this research. The recommended water content for the cementitious grouts and mortars ranges between 3,0 – 4,0 litres of water per 25 kg bag (refer to material datasheets in Appendix A). The water content for the HS grout and PMRM, under the experimental testing, was 3,5 litres and 4,0 litres per bag, respectively. The material manufacturer may have used a water content closer to 3,0 litres per bag, likely

resulting in higher reported strength results for the respective materials tested. With respect to curing conditions, the material manufacture is likely to have allowed the test specimens to cure in water after demoulding, which affects the specimens strengths tested at 7 and 28 days. Furthermore, the material manufactures may have used different specimen types when testing for compressive strength. The reported compressive strength, by the material manufacturer, for the UHS grout was determined using 40 × 40 × 160 mm prismatic specimens as opposed to cube specimens (refer to SikaGrout-295ZA in Appendix A). The practice of using prismatic specimens to test for compressive strengths is common for grouts and mortars. The comparison between material testing results and those provided in the material data sheets are represented in Figure 4-3.

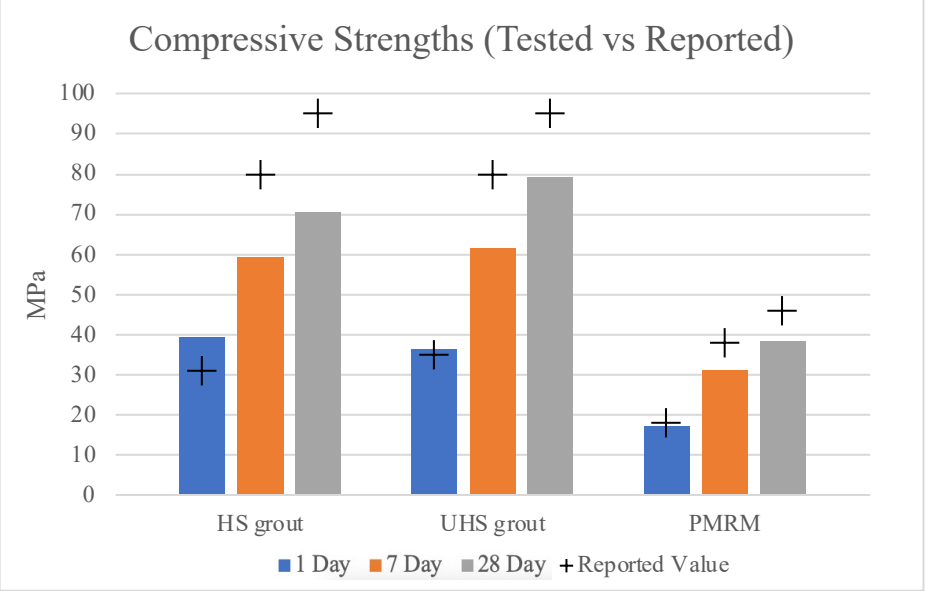

Figure 4-3: Compressive strengths, tested vs reported (data sheet)

The compressive strength development of each of the materials, relative to its 28 day strength, is shown in Figure 4-4. All the repair materials showed similar rates of development in compressive strength over 28 days, with the materials achieving around 50% and above 75% of their 28 day strength after 1 and 7 days, respectively. Harrison (2003) found that normal concretes obtain about 50% of their 28 day strength at 3 days vs 1 day achieved by the repair material, while obtaining 70% of their 28 day strength at 7 days. This shows significant faster rate of compressive strength development in the repair materials when compared to normal concretes, which is attributed to the powder formation, admixtures used and higher rates of hydration in such repair materials at early ages.

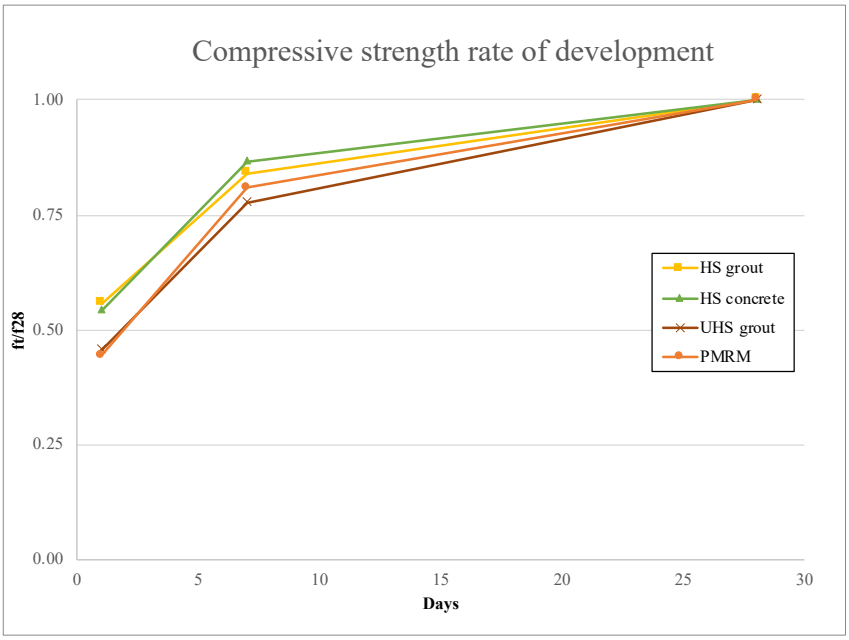

Figure 4-4: Compressive strength development relative to 28 day strength

4.3 Tensile splitting strength

The tensile splitting strength of all four repair materials was tested. Figure 4-5 shows the split plane of a cube specimen tested.

Figure 4-5: Split specimen of HS concrete tested for tensile splitting strength at 1 day

The tensile splitting strength of the repair materials in Figure 4-6 follow a similar trend to the compressive strength, where the values obtained for the HS grout, HS concrete and ULS grout are comparatively higher than for the PMRM. The full tensile splitting strength results may be found in Appendix B.

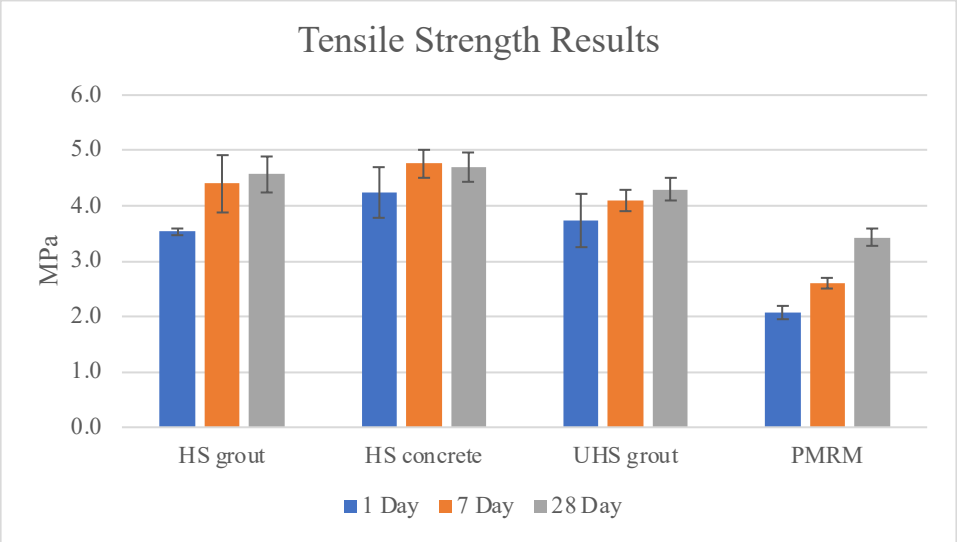

Figure 4-6: Tensile strength results for repair materials

The rate of development of tensile strength in the repair materials is more rapid at early ages when compared to the compressive strength development, in agreement with the findings by Yuan & Marosszeky (1994) who conducted similar tests on cement-based repair materials. The ratio of tensile strength to compressive strength of the repair materials at 28 days range between 0.05 and 0.07, which is in good agreement to with the ratio range of 0.06 to 0.1 for repair materials, noted by Vaysburd et al. (2014).

4.4 Elastic modulus

The HS grout, HS concrete and UHS grout were tested for their static elastic modulus in compression. The results are found in Figure 4-7 below. The rate of elastic modulus development in the HS concrete and UHS grout, between 1 and 7 days, were significantly higher than in the HS grout over the same period. In the case of the HS concrete, this may be attributed to the stability offered by the presence of aggregate in the mix. Based on proportion of aggregate in the mix, the aggregate properties are highly influential in the properties of the repair material (Emmons & Vaysburd, 1994). The elastic modulus of most aggregates are inherently higher than the respective cement pastes in material mixes at earlier ages, thus having a greater influence on the repair materials with and without aggregate tested at 1 and 7 days. The HS grout has a higher elastic modulus value at 28 days in comparison to the HS concrete containing coarse aggregates. This result was not expected, as the material containing aggregate is expected to have a higher elastic modulus than the one without.

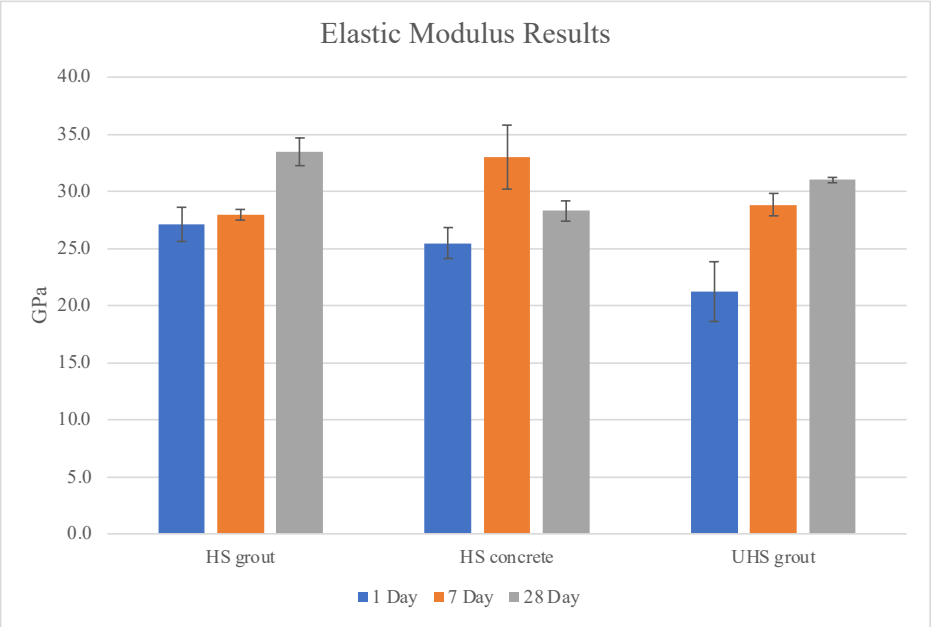

Figure 4-7: Elastic modulus results for repair materials

The UHS grout was the only material for which elastic modulus data has been provided in its respective data sheet. The manufacturer has quoted a value of ~30 GPa after 28 days which is in good agreement with the 31 GPa obtained in testing.

4.5 Shrinkage

The total shrinkage strains of the HS grout, HS concrete and UHS grout are represented in Figure 4-8. The shrinkage strains for all three materials develop rapidly in the first 14 days, achieving between 84% and 90% of the total 90-day strains. The shrinkage strain develops faster in the aggregate-bulked HS concrete in comparison to un-bulked HS and UHS grouts. This result is unexpected as research (Emmons & Vaysburd, 1994; Mangat & Limbachiya, 1994) reports that the presence of coarse aggregate in repair materials results in the decrease of total shrinkage strain. This result may be attributed to the aggregate properties. Aggregate grading and moisture content are two possible factors that may affect the shrinkage strain. Poorly graded aggregate creates larger gaps in the pore structure of the material allowing for freer movement of moisture out of the material. Further analysis on the aggregate properties, not conducted in this research, is required to sufficiently explain this result.

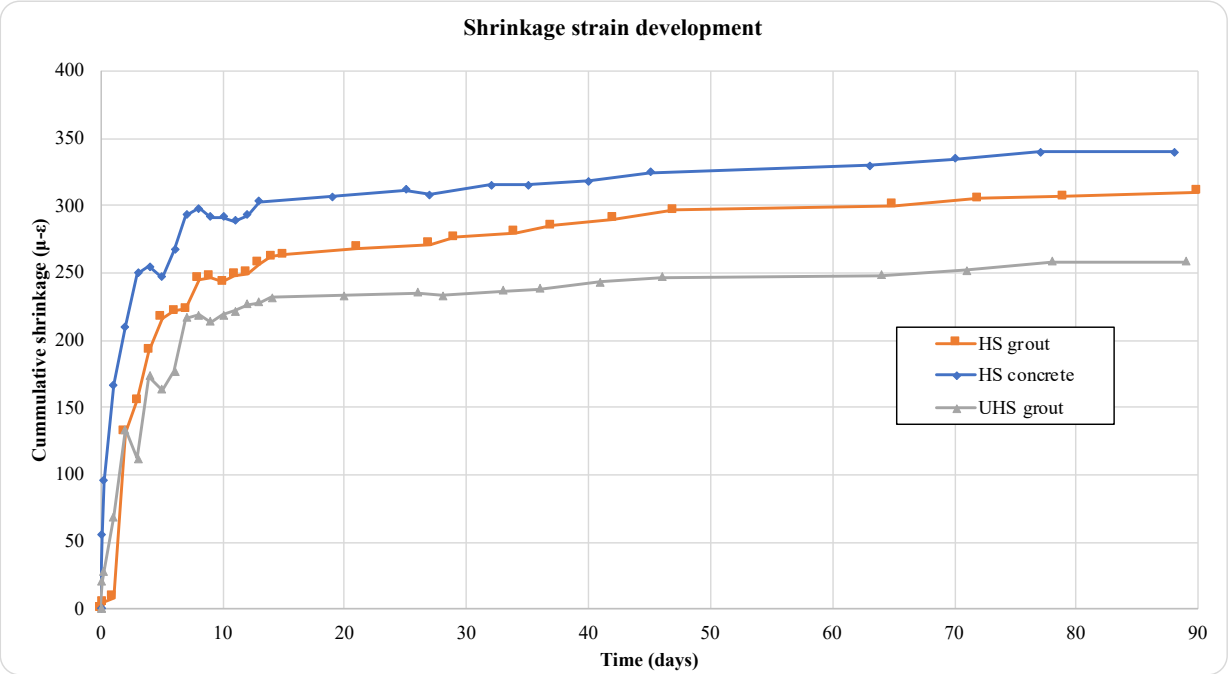

Figure 4-8: Repair material total shrinkage strain over a 90-day period

Generally, the shrinkage strain experienced by all three materials is considered to be within the very low to low shrinkage range within the first 28 days, between 200.10^{-6} and 350.10^{-6}. These results are unexpected, as results by Chilwesa (2012) when measuring shrinkage for similar commercial repair mortars, yield strains between 500.10^{-6} and 1000.10^{-6} at 28 days.

The high-strength cementitious grout used for both the HS grout and HS concrete is labelled as a "shrinkage compensating" material. The 28-day shrinkage strains of the HS grout and HS concrete were 273.10^{-6} and 310.10^{-6} respectively, categorising these materials as low shrinkage materials according to Emmons & Vaysburd (1993). Similar results were obtained by Beushausen (2005) when testing common South African concrete repair products, labelled as "non-shrink".

4.6 Compressive creep

Compressive creep tests were conducted on specimens of the HS grout, HS concrete and UHS grout for the two loading scenarios.

4.6.1 Cumulative strains

The cumulative strains, including elastic, shrinkage and creep strains, were measured and are presented in Figure 4-9 and Figure 4-10 for the 1-day and 7-day loading scenarios respectively.

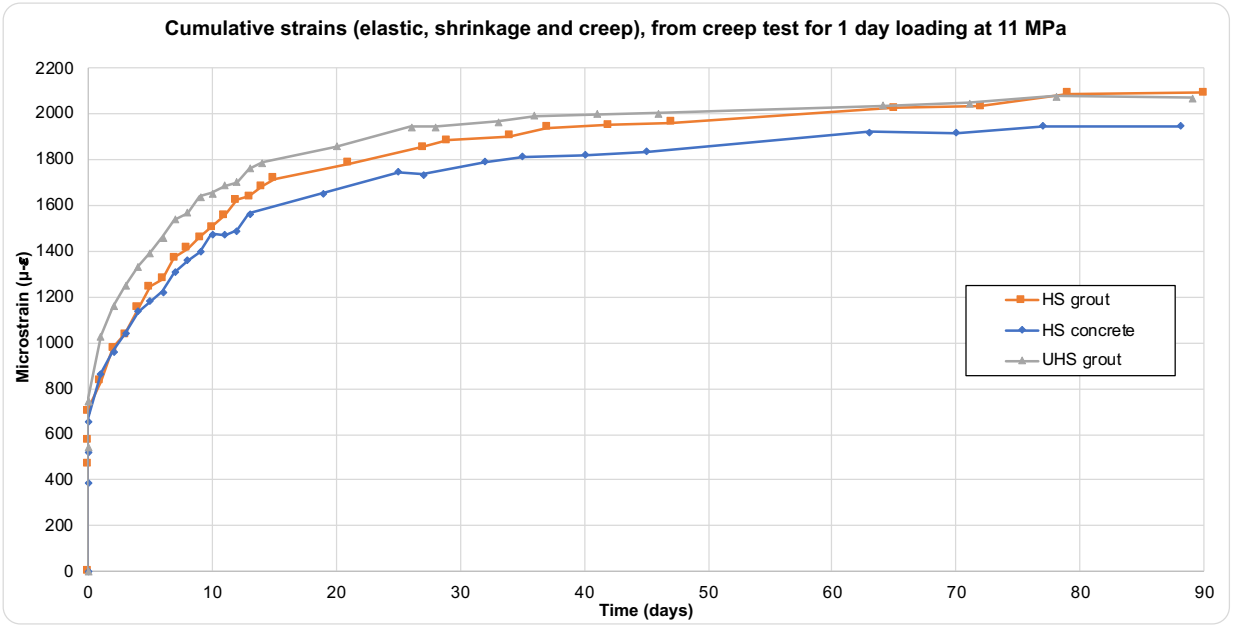

Figure 4-9: Cumulative strains (elastic, shrinkage and creep), from creep test for 1 day loading at 11 MPa

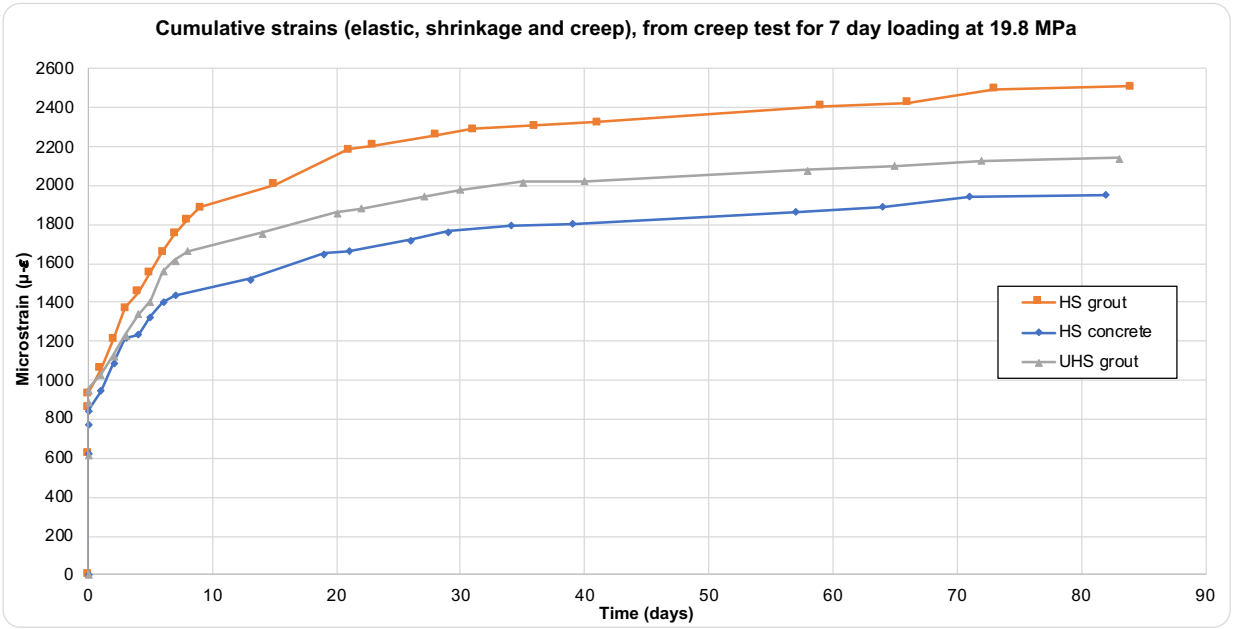

Figure 4-10: Cumulative strains (elastic, shrinkage and creep), from creep test for 7 day loading at 19.8 MPa

The measured elastic, shrinkage and creep strain for each loading scenario are found in Table 4-1 and Table 4-2. The aggregate-bulked HS concrete has the least net creep strain of the three materials for both loading scenarios, with 1220 μ-ϵ and 1260 μ-ϵ respectively. This result is in agreement with Emmons & Vaysburd (1994) and Mangat & Limbachiya (1994) who report that the presence of aggregate in the repair mixture results in a decrease of total creep strains

experienced by the material. The HS grout has the highest net creep strains in both scenarios, 1310 μ-ϵ and 1800 μ-ϵ, comparatively higher than both the HS concrete and UHS grout.

Table 4-1: Elastic, shrinkage and creep strains (μ-ϵ) - 1 day loading @ 11 MPa

	Total Strain	Elastic	Shrinkage	Net Creep
Material	24h to 12weeks	at loading	24h to 12weeks	24h to 12weeks
HS grout	2090	470	310	1310
HS concrete	1950	390	340	1220
UHS grout	2070	550	260	1260

Table 4-2: Elastic, shrinkage and creep strains (μ-ϵ) - 7 day loading @ 19.8 MPa

	Total Strain	Elastic	Shrinkage	Net Creep
Material	24h to 12weeks	at loading	24h to 12weeks	24h to 12weeks
HS grout	2510	620	90	1800
HS concrete	1960	630	70	1260
UHS grout	2140	620	80	1440

4.6.2 Creep rig elastic modulus

The elastic modulus properties of the materials may be inferred from the elastic strain readings at the time of loading. These properties are compared with previously obtained elastic modulus properties from experimental tests, discussed in Section 4.4. A comparison of the properties at material ages 24 hours and 7 days are found in Figure 4-11.

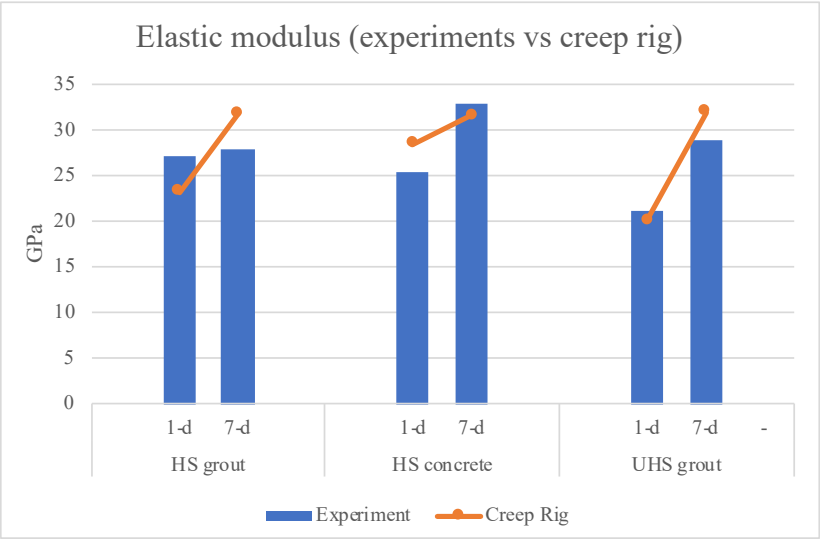

Figure 4-11: Elastic modulus values (experiments vs creep rig measurements)

The elastic modulus results from the experimental tests and the creep rig measurements, for the all three repair materials, are similar. This result highlights that both methods yield reliable elastic modulus measurements.

4.6.3 Specific creep

The specific creep development over time of the materials for loading at 1 and 7 days age are found in Figure 4-12 and Figure 4-13, respectively.

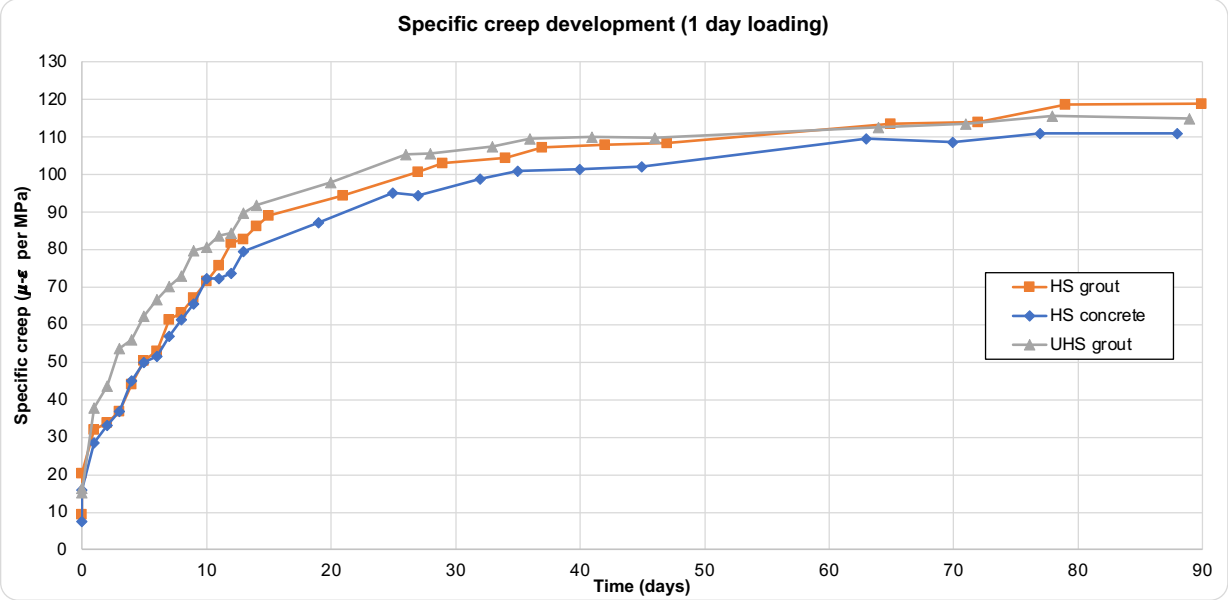

Figure 4-12: Specific creep development (1 day loading)

The development of specific creep properties of the materials were similar when the materials are loaded 1 day of age, with values after 12 weeks ranging between 110 and 120 μ-ϵ/MPa.

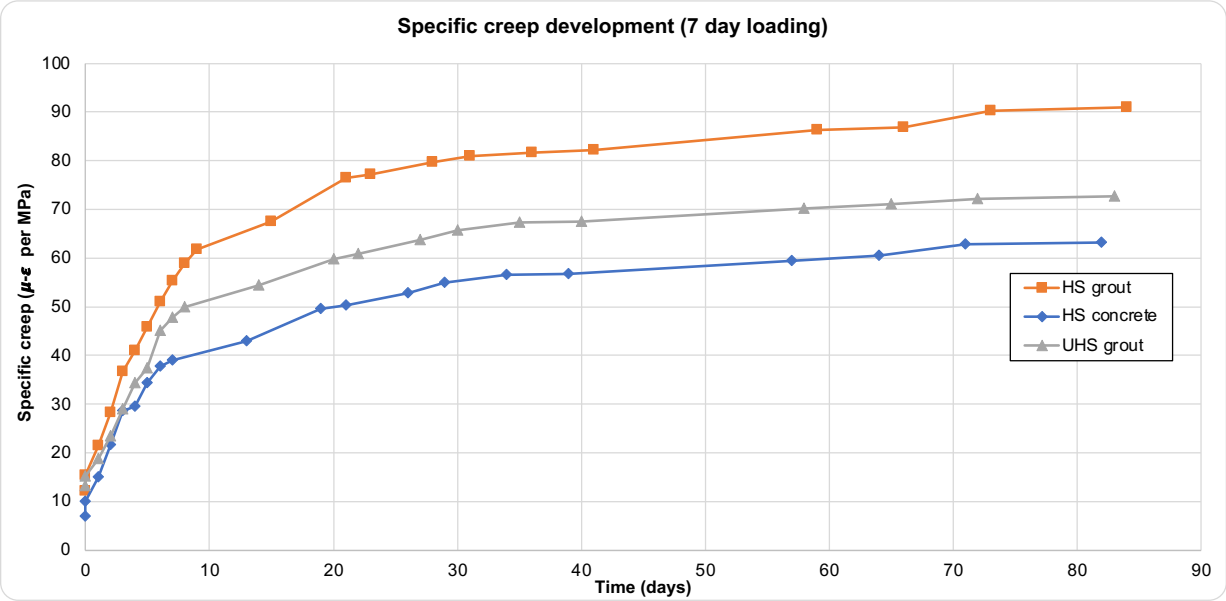

Figure 4-13: Specific creep development (7 day loading)

For the materials loaded at 7 days of age, the specific creep development for all the materials became similar after 20 days of loading. However, at earlier ages, the specific creep develops at a faster rate for the HS grout than both the HS concrete and UHS grout. The HS concrete has the slowest development of specific creep of the three materials at early ages. This phenomena may be attributed to the presence of aggregate in the material, in agreement with past studies (Emmons & Vaysburd, 1994; Mangat & Limbachiya, 1994), attributing to the decrease in creep strain with the presence of aggregate. Comparing Figure 4-12 and Figure 4-13, it may be seen that the effects due to the presence of aggregate are more pronounced at 7 days of loading than 1 day.

The specific creep development at different ages of loading (i.e. 1 day and 7 day) was compared for each material in Figure 4-14 to Figure 4-16. The trends regarding the rate of specific creep development were similar for all three materials. The specific creep develops in each material at a similar rate after 30 days of loading, before which time the rate of development in specimens loaded at age of loading 1 day develop at a significantly faster rate than the specimens loaded at 7 day age of loading. These results are consistent with the studies by Yuan & Marosszeky (1994) and Pan & Meng (2016), where the creep strain properties were found to increase for a material loaded at earlier ages. Furthermore, Yuan & Marosszeky (1994) found that concretes loaded at ages beyond 21 days were less affected by these effects. When comparing Figure 4-14 with Figure 4-15 and Figure 4-16, it may be observed that the decrease in rate of creep development in materials loaded at older ages is more sensitive in the aggregate-bulked HS concrete and UHS grout materials.

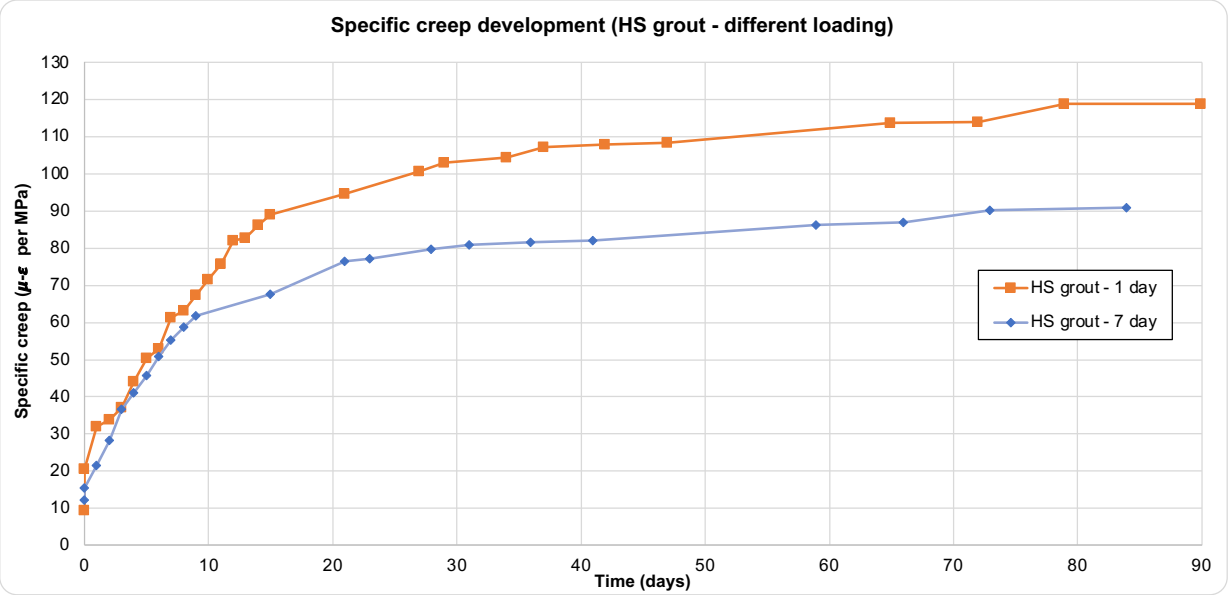

Figure 4-14: Specific creep development of HS grout for varying age at time of loading

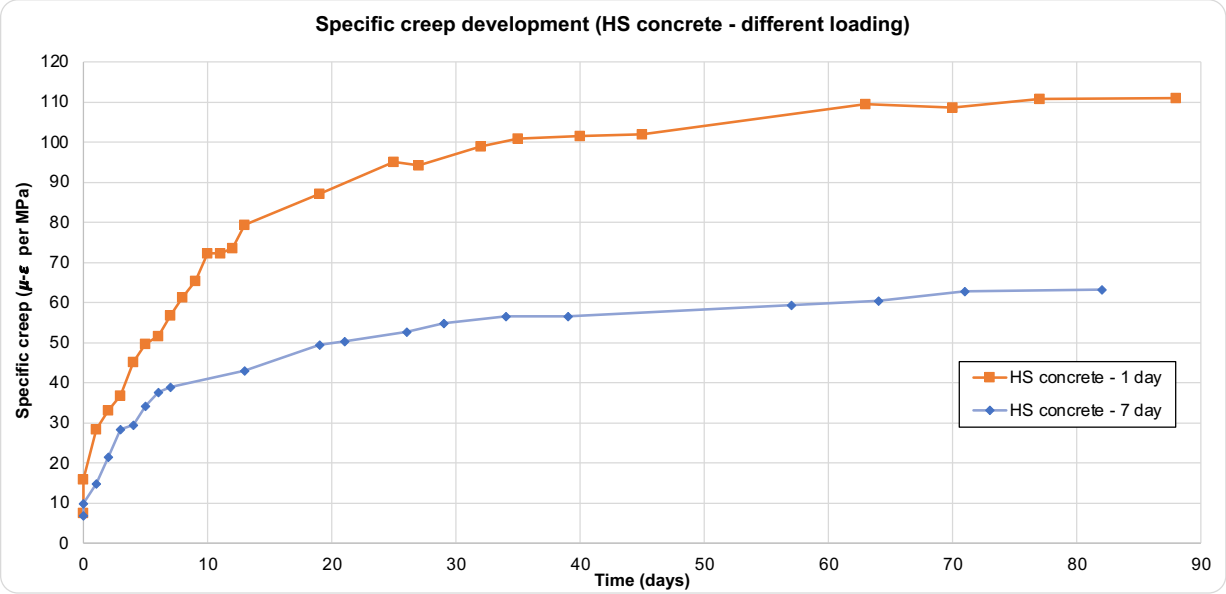

Figure 4-15: Specific creep development of HS concrete for varying age at time of loading

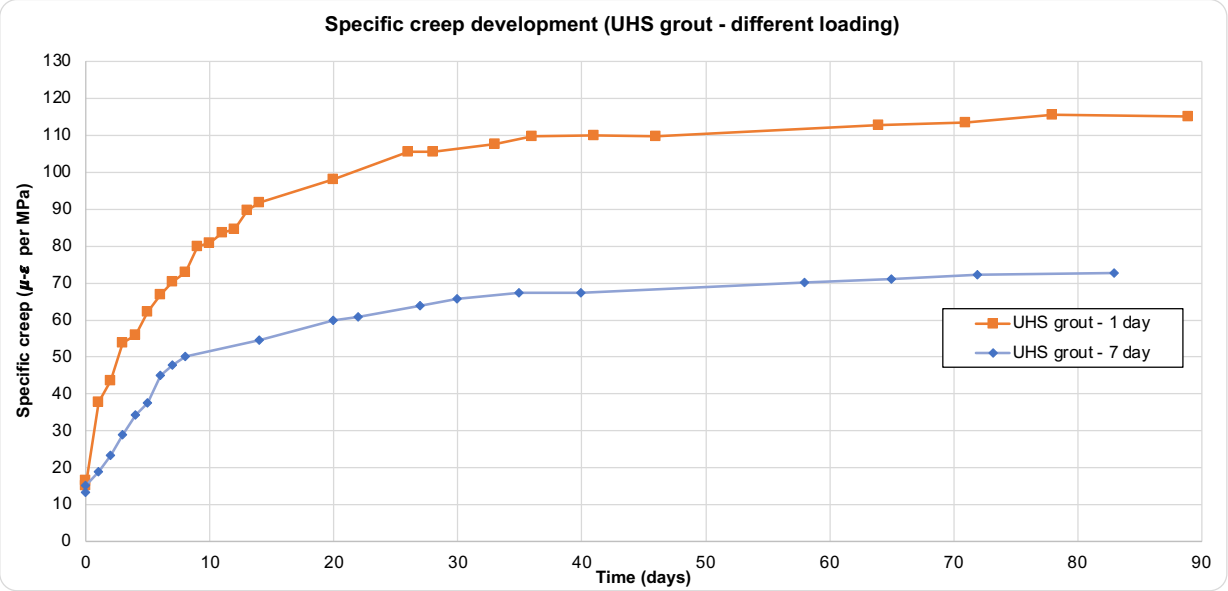

Figure 4-16: Specific creep development of UHS grout for varying age at time of loading

5. Model Development

5.1 Introduction

This chapter presents the development of an analytical model used to approximate the stress and strain behaviour over time in a repaired concrete element under axial compression. The model represents a first order analysis of the stresses and strains in the repaired element, i.e. within the linear elastic range of the substrate concrete and repair material, respectively. The primary purpose of the model is to establish to what extent do repair materials structurally contribute in patch repair applications.

The stress and strain distribution in the repaired element is influenced by the material properties of the substrate concrete and repair material, and their interaction with the environment and imposed loading conditions. The model was thus developed by quantifying the effects of these various influences and using key material property information as inputs. Figure 5-1 represents a schematic of the development of the analytical model.

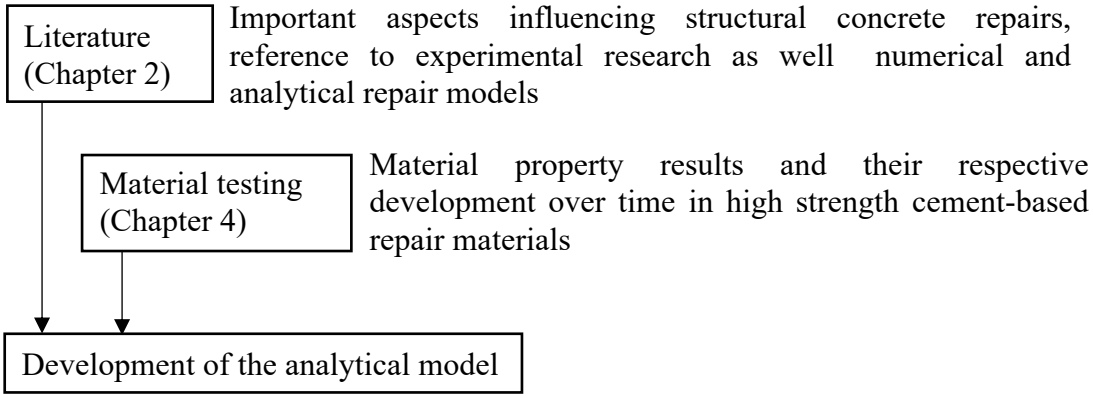

Figure 5-1: Schematic of the development of an analytical model, based on literature and repair material property testing

The material property information typically provided on repair material data sheets is insufficient to use in such modelling. The material property results from the experimental tests in Chapter 4 were, thus, used as inputs to the model. These results pertain to the elastic modulus, shrinkage and creep properties of the repair materials, which are identified as the key material properties of the stress and strain distribution in repaired concrete elements.

The layout and development of the proceeding chapter is briefly described herein. The stress and strain mechanisms resulting from the development of the key material properties in the repair material and substrate concrete, form the building blocks of the repair model. The initial sections, discuss and define these mechanisms, applicable to the repair material properties, making reference to literature and experimental data from this research. Thereafter, the model and material property assumptions taken in this research are stated and discussed. Finally, model

implementation is conducted, based on the model assumptions and material property mechanisms defined previously.

5.2 Material property development

The formulae to approximate material property development described below are based on literature and experimental data obtained in this research from Chapter 4. The formulae are applicable to cement-based materials adapted to the repair materials tested under this research. They primarily describe the material property behaviour of the repair material in a patch repaired concrete member, and not the substrate concrete. The assumptions taken, in the development of the model, for substrate concrete and repair material properties are defined later in Sections 5.3.4 and 5.3.5 respectively.

5.2.1 Elastic modulus

The modulus of elasticity of the repair material is assumed to develop within the first 28 days, and remain constant thereafter. The development of the repair materials' elastic modulus is based on the experimental values, measured at 1 , 7 and 28 days of age (see Chapter 4). The early-age development of elastic modulus in concrete, inferred from literature (Harrison, 2003; Kocab et al., 2017), follows a logarithmic function. However, results obtained during repair material testing in Chapter 4, are insufficient to establish such a relationship. The elastic modulus development of the repair materials between 1 and 28 days is thus, for simplicity, assumed to follow a linear function between known values. Equation [5.1] represents the general equation for the elastic modulus of the repair material used in the model.

$$E_r(t) = \begin{cases} E_{r,1} + (t-1) \cdot \dfrac{\left(E_{r,7} - E_{r,1}\right)}{6} & for \quad 1 \le t < 7 \\ E_{r,7} + (t-7) \cdot \dfrac{\left(E_{r,28} - E_{r,7}\right)}{21} & for \quad 7 \le t < 28 \\ E_{r,28} & for \quad 28 \le t \end{cases} \qquad \textbf{[5.1]}$$

where, $E_{r,1}$, $E_{r,7}$ *and* $E_{r,28}$ are the elastic modulus properties of the repair material at ages 1, 7 and 28 days respectively and *t* represents the age of the material in days with $t = 1,2,3 \ldots, n$

5.2.2 Shrinkage

The repair material shrinkage strain development is determined as a function of the measured free shrinkage, for ages 1-90 days, from experimental test results in Chapter 4. The modelled repair material shrinkage strain, in the patch repaired concrete element, takes into account the restraining effects of the substrate concrete, detailed further in Section 5.2.2.1 below.

In the analytical model, the strain due to shrinkage is modelled as one-dimensional, with the shrinkage strain direction being parallel to the axial loading. Although shrinkage is a three-dimensional phenomenon, in the case of an axially loaded element, the shrinkage in the two

directions perpendicular to axial loading have negligible bearing on the structural mechanism of the element. Furthermore, the shrinkage strain experienced in the repair material is assumed to be constant throughout the depth of the repair material, i.e. the shrinkage strains experienced at the repair interface and free surface are equal.

Early-age shrinkage or expansion, i.e. for repair material ages less than 1 day, was not measured during the experiment tests. The effects of early-age shrinkage or expansion were not considered in the model due to the difficulty associated with the prediction of their behaviour in repair applications, as the repair material properties are rapidly changing in ages less than 1 day (Beushausen, 2005).

5.2.2.1 Restrained shrinkage strain

A perfect bond is assumed between the substrate concrete and repair material, thus creating restraint to free shrinkage strains in the repair material. Equation [5.2], adopted from Beushausen (2005), is used to model the occurring strain due to shrinkage in the repair material at time *t.* This is a function of the elastic modulus of the substrate concrete and repair material as well as the free shrinkage strain in the repair material at time *t*.

$$\varepsilon_{shrink,r}(t) = \varepsilon_{FSS,t} \cdot \frac{1}{1 + \frac{E_s}{E_{r,t}} \cdot C_\varepsilon} \quad , \qquad \textbf{[5.2]}$$

where E_s and E_r represent the elastic modulus of the substrate concrete and the repair material at time *t* respectively. $\varepsilon_{FSS,t}$ represents the free shrinkage strain of the material at time *t* and the parameter C_ε denotes the net effects of member dimensions and strain patterns in the substrate concrete and repair material, which is determined empirically for different systems for practical application of the prediction model.

According to Beushausen (2005), the parameter C_ε can be assumed to take a value of 1 unless contradictory information is available, under the assumptions that the relative repair material and substrate concrete dimensions have no practical influence on interfacial strains. Equation [5.2] is thus re-written as

$$\varepsilon_{shrink,r}(t) = \varepsilon_{FSS,t} \cdot \frac{1}{1 + \frac{E_s}{E_{r,t}}} \quad . \qquad \textbf{[5.3]}$$

5.2.3 Creep

5.2.3.1 Specific creep

The creep strain in the repair material is determined as a function of the specific creep property of the repair material in compression, C_c. The specific creep of the repair material was tested for a period of 90 days and presented in Chapter 4. Specific creep values were not determined every

day within the testing period. Thus, for duration of loading *t* where no experimental data is available, the specific creep was estimated for application in the model.

Brooks & Neville (1978) proposed a model to estimate creep characteristics of concrete, presented in equation [5.4].

$$C_{c,t} = C_{c,28} \times 0{,}5t^{0{,}21} \quad \textbf{[5.4]}$$

where, $C_{c,t}$ is the specific creep at duration of loading time *t* and $C_{c,28}$ is the measured specific creep of the material at duration of loading 28 days.

The model proposed by Brooks & Neville (1978) in Equation [5.4] was found to generally overestimate specific creep properties of the repair materials found in Chapter 4. A comparison between the specific creep values obtained through experimental tests and those estimated by the model proposed by Brooks & Neville (1978) may be found in Appendix C.

Through numerical trials, a fifth order polynomial of the general form in Equation [5.5] was found to sufficiently represent the specific creep properties of the tested repair material over the 90 day testing period. The time-development creep expressed by this polynomial, fits the measured data (Chapter 4), and is used in the model. However, it does not necessarily represent the long term creep behaviour of the repair material beyond 90 days.

$$C_{c,t} = b_5 t^5 + b_4 t^4 + b_3 t^3 + b_2 t^2 + b_1 t + a \quad \textbf{[5.5]}$$

where coefficients b_1, b_2, b_3, b_4, b_5, b_6 and a were numerically solved from known experimentally measured specific creep values.

The fifth order polynomial in Equation [5.5] was used to estimate the specific creep properties of the repair materials in the model over the first 90 days. A representation of specific creep estimated by polynomial best-fit curve vs the model by Brooks and Neville (1978) in Figure 5-2, for the HS grout loaded at age of loading 1 day, shows the suitability of this choice.

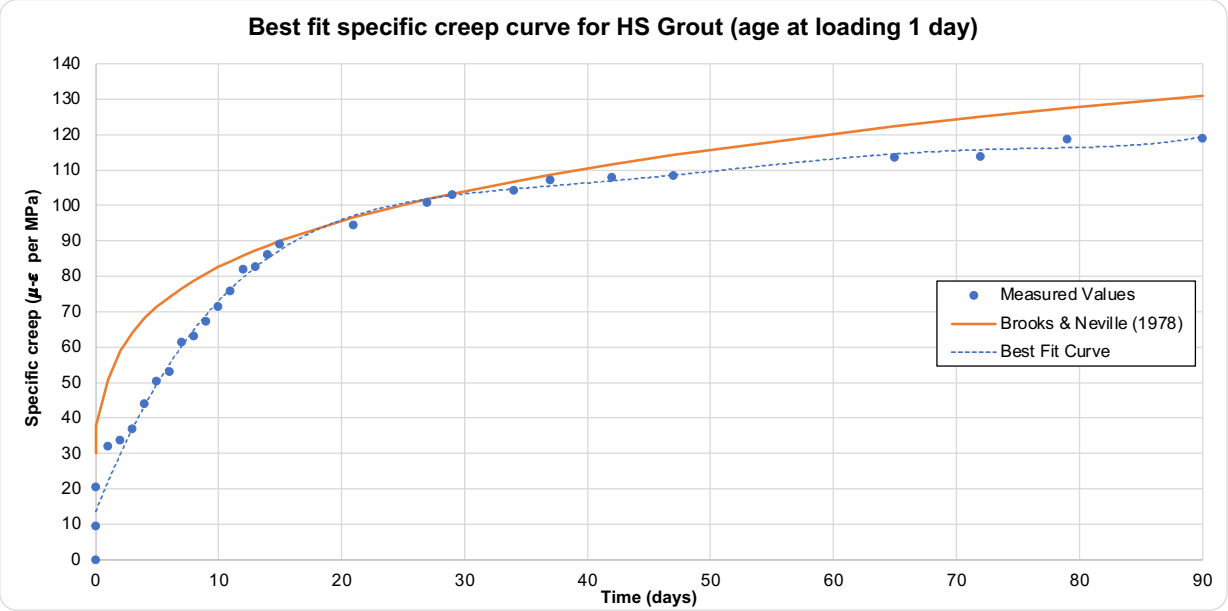

Figure 5-2: Polynomial best-fit curve of measured specific creep vs Brooks & Neville (1978) for HS grout, at age of loading 1 day

5.3 Model assumptions

5.3.1 Engineering principles

Two main principles were applied in the development of the model, namely Hooke's law and Euler-Bernoulli beam theory. Hooke's law, governs the distribution of the imposed axial stress in the repaired concrete element. The Euler-Bernoulli theory accounts for strain compatibility in the model. There are two popular beam theories, i.e. the Euler-Bernoulli and Timoshenko–Ehrenfest beam theory. The strain deformations in the modelled repaired element follow the two main assumptions made in the Euler-Bernoulli beam theory for simplification, i.e. plane sections remain plane under stress and deformation angles in the beam are small. The Timoshenko–Ehrenfest beam theory takes account for shear deformations and bending affects, which are assumed to have a negligible affect for the purpose of the model.

5.3.2 Applied stresses

The modelled repaired concrete element is subjected to axial compressive stresses. The loads are applied instantaneously and are assumed to act uniformly, i.e. no eccentricities in loading application are assumed. No curvature in the column as a resulting of loading is assumed, thus neglecting the effects of bending in the modelling of stresses and strains in the element. Note that loading concentricity as assumed above, does not guarantee uniform deformation or strain in these cases. Material stiffness differentials may introduce eccentricities and thus curvature even

under concentric loads assumed above. The results of the simplified model are accepted as a first approximation only.

5.3.3 Time-stepping

Material property development and stress distribution or redistribution in a repaired concrete element are continuous phenomena. In the development of the model, these phenomena were discretised. The time step increments for material property development and approximation of stress distribution in the repaired concrete member was taken to be 1 day.

5.3.4 Substrate concrete material property assumptions

The substrate concrete material properties are modelled based on an aged concrete. The elastic modulus of substrate concrete is assumed to be constant . The creep and shrinkage deformations of concrete, under stress, are generally expected to reach their final values after about 30 years, beyond which such deformations may be considered negligible (Brooks, 2005). The model, thus, assumes that the substrate concrete is beyond such age and the concrete no longer undergoes measurable creep and shrinkage deformations.

It may be argued that the substrate undergoes a change in creep strain due to the unloading and loading as a result of the repair process (i.e. recoverable creep) as well as creep strain due to the incremental shedding of load from the repair material to substrate concrete after the repair is completed and load reinstated. These mechanisms are considered negligible in the modelling, owing to the short duration of the repair where the substrate is unloaded, i.e. very little creep recovery, and age of the substrate concrete at reloading, i.e. minimal creep strain in the aged substrate concrete. Furthermore, this was done to avoid making the model too complex.

5.3.5 Repair material property assumptions

The assumptions made in the model with reference to the repair material properties were based on the repair materials tested under the experimental component of this dissertation. The elastic moduli of the repair materials were modelled to develop fully within the first 28 days, beyond which they were assumed to be constant. The free shrinkage strain was measured over the first 90 days period, beyond which, additional shrinkage was not considered. The creep characteristics of the repair materials were measured over a 90 day period. A time-development estimate of the creep characteristics for each material was developed over the first 90 days, which fits the measured data for each repair material, as discussed in Section 5.2.3.1. This time-development measure was used to determine the creep characteristics in each repair material in the model. This measure is however not necessarily representative of the long-term creep characteristics of the materials, i.e. beyond 90 days.

Complete bond is assumed at both the transverse and longitudinal interface of the substrate concrete and repair material. At the transverse interface, this facilitates the complete transfer of axial stresses through the materials, at the point of contact. Strains in both the substrate and repair

material are assumed equal, along the longitudinal interface, thus, offering restraint to deformations in each material, e.g. restrained shrinkage in the repair material discussed in Section 5.2.2.1.

5.3.6 Effect of steel reinforcement

The effects of any available steel reinforcement are not considered in the modelled patch repair. Steel reinforcement, bonded in the composite repaired concrete element, contributes towards the distribution of stress in the element as well as offering restraint to deformations such as shrinkage and creep in the repair material. Such effects require to be quantified through empirical research and/or more complex modelling of reinforced concrete elements, which falls outside the scope of this dissertation.

5.3.7 Compatibility and equilibrium principles

Two key principles govern the development of the model, namely, strain compatibility and force equilibrium. The two principles facilitate the estimation of stress in the repaired element. The equations for both strain compatibility and force equalibrium with reference to the materials in the repaired element are given in Equation [5.6] and Equation [5.7] below, respectively.

$$\varepsilon_{substate} = \varepsilon_{repair} \qquad \textbf{[5.6]}$$

Under strain compatibility, Equation [5.6], the strain deformations across the cross-section of the repaired concrete element are assumed to be constant. This implies that the strain in the substrate concrete is equal to the strain experienced by the repair material. This is only applicable to the load-induced strain in the substrate concrete.

$$F_{total} = F_{subtrate} + F_{repair} \qquad \textbf{[5.7]}$$

The principle of force equilibrium, Equation [5.7], refers to the equilibrium of forces through the cross-section of the repaired element, i.e. the total force through the element is equal to the sum of the forces through the substrate concrete and repair material, respectively.

5.4 Level of analysis

In the analytical model, the mechanisms and influences affecting the internal stress and strain distribution in the repaired concrete element were modelled through externally applied forces at the member ends. This is often described as a global level of analysis, where the repaired element is viewed as a whole. A representation of how stresses are modelled under this level of analysis is shown in Figure 5-3.

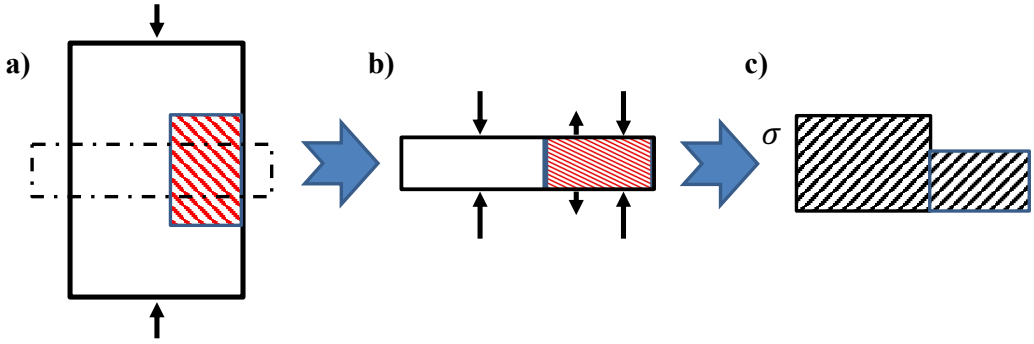

a) External applied forces, applied on the whole element at a global scale
b) Internal forces through material sections, due to applied force and material influences
c) Internal stresses in the materials, resultant internal forces over material cross-sectional area

Figure 5-3: Modelling stresses in repaired concrete element using a global scale

The repaired element under axial compression is considered as a whole in Figure 5-3 a), where the applied forces act at the element ends. In Figure 5-3 b), the internal forces through a section of the substrate concrete and repair material are shown. The internal forces are as a result of the external applied force and various internal material influences, assumed to be constant throughout the depth of the material acting at the material ends. The internal compressive forces in the repair material are due to the applied external load on the material, where the internal tensile forces represent a release of stress due to the effects of creep and shrinkage strain in the repair material. The internal compressive forces in the substrate concrete are attributed to the applied external load as well as stress transfer from the repair material to substrate concrete as a result of creep and shrinkage strain in the repair material. Finally, Figure 5-3 c), represents the internal stresses in the respective materials computed from the resultant internal forces over the respective material cross-sectional areas.

The global level of analysis described above considers that the internal forces and thus internal stresses, due to imposed load and material influences in the respective materials, are initiated at the material ends and constant through the depth of the material. In reality, the stress initiation due to the various load and material influences takes place at a local and micro level. An example of a phenomenon of a local level of stress initiation is restrained shrinkage, which is initiated at the repair interface. Stresses due to shrinkage and creep in the substrate concrete and repair material are examples where stress is initiated at a microscopic molecular level in the materials, i.e. at a micro level.

The local and micro level of analysis are important in accurately describing the actual stress and strain distribution in the repaired concrete element, however, these were not considered in the development of the analytical model under this dissertation. The analytical model is intended to be used as an indicative tool and at best an approximation of the stress and strain behaviour in the repaired concrete element. For this purpose, the global level of analysis is sufficient. Further experimental testing and material information, outside the scope of this work, is required to inform the development of an analytical model considering the local and micro levels of analysis.

5.5 Model implementation

The following section outlines the foundation on which the model estimates stress and strain in the repaired concrete element over time, based on the various model theory and components outlined in the preceding sections. The section initially defines how creep is modelled in this research followed by the basis for stress and strain distribution in the repaired concrete element.

5.5.1 Creep modelling

In the model, the repair material is assumed to be subjected to stress which, due to redistribution of stresses in the substrate/repair material system, incrementally decreases over time. The phenomenon of creep recovery and incremental loading, discussed below, are considered in the modelling of creep strain in the repair material.

The considerations of creep recovery and incremental loading increase the complexity of the model, without necessarily adding increased accuracy to the model. This is attributed to the general uncertainties associated with creep modelling and estimation. The considerations are, nonetheless, taken into account in the model for the sake of presenting a formally complete approach to the distribution of stress and strain in the repaired concrete element.

5.5.1.1 Creep recovery

The phenomenon of creep recovery is typically relevant if a load is removed from a member. Empirical research (Mangat & O'Flaherty, 1999a; Shambira & Nounu, 2000) suggests that stress is shed from the repair material to the substrate concrete in structural repair applications, thus resulting in an incremental decrease of stress in the repair material over time. The incremental decrease of stress in the repair material may be considered as an incremental unloading of the material and therefore resulting in the repair material experiencing incremental creep recovery.

Compressive creep strain is composed of a recoverable and irrecoverable component. When sustained stress is released from a material, only the recoverable component of the strain is restored over time, while the irrecoverable component results in permanent deformation. The irrecoverable creep strain at time t_i of the released stress between time t_{i-1} and time t_i may be simplistically represented in Equation [5.8].

$$\varepsilon_{plastic}(t_i) = XC_{c,t_{i-1}}(\sigma_{r,t_{i-1}} - \sigma_{r,t_i}) \qquad \textbf{[5.8]}$$

where, $(\sigma_{r,t_{i-1}} - \sigma_{r,t_i})$, represents the release in stress between time t_{i-1} and time t_i and , $C_{c,t_{i-1}}$ the specific creep of the material at the previous time step. The parameter X represents the percentage of irrecoverable creep strain of the material.

According to SANS 10100-1:2000 (2000), the recoverable creep strain after 1 year, for a structure which has been unloaded, is 30% of the total creep strain. Leading from the above, the irrecoverable strain component in the model is assumed to be 70% of the total creep strain

resulting from the released incremental stress. Thus, parameter *X* in Equation [5.8] takes the value of 0.7.

5.5.1.2 Creep due to incremental loading

The repair material is assumed to be subjected to an incremental decrease in stress over time in the repaired concrete element, thus affecting its total creep strain over time.

Most empirical research on the creep characteristics of a material have been conducted under constant stress, which is not necessarily applicable to the incrementally varying stress in the composite modelled repaired element. The Boltzman principle of superposition may be applied for incremental loading at low stress levels where the relationship between creep strain and stress is linear. There are no existing applications of the above principle which consider the creep strain in a material due to the incremental decrease in stress. However, Trost (1967) developed a simplistic equation for the determination of creep strain under incremental increase in stress over time.

$$\varepsilon_{creep}(t) = \frac{\sigma_0}{E} \cdot \varphi(t, t_0) + \frac{\sigma_t - \sigma_0}{E} \cdot \rho\varphi(t, t_0) \qquad \textbf{[5.9]}$$

where ρ is an aging coefficient that considers the incremental application of stress ($\sigma_t - \sigma_0$) over time ($t - t_0$), $\sigma_t - \sigma_0$ represents the incremental increase in stress from time *0* to time *t* and $\varphi(t, t_0)$ is the creep factor for the material.

Equation [5.9] estimates the total creep strain in the material at time *t* by adding two terms together. The first term represents the creep strain, over time *t*, due to a constant stress (i.e. initial stress σ_0). The second term accounts for the creep strain due to the incremental increase in stress ($\sigma_t - \sigma_0$) over the time period, where $\sigma_t > \sigma_0$. When Equation [5.9] is applied to the case of a decreasing incremental stress, i.e. where $\sigma_t < \sigma_0$, it results in an overestimate of the total creep strain at time *t*, as it does not consider the recoverable creep strain component due to the decrease of stress within the time period *t*. Equation [5.9] may, thus, be modified and rearranged to estimate the total creep strain in the material at time *t* due to an incremental decrease in stress, where $\sigma_t < \sigma_0$, by summing the following two terms:

- creep strain due to the constant stress σ_t over time period *t*, and;
- irrecoverable component of creep strain due to incremental decrease in stress ($\sigma_0 - \sigma_t$) over time period *t*.

The modified Equation [5.9] for total creep strain at time *t* due to the incremental decrease of stress over time period ($t - t_0$) is presented as:

$$\varepsilon_{creep}(t) = \frac{\sigma_t}{E} \cdot \varphi(t, t_0) + \frac{\sigma_0 - \sigma_t}{E} \cdot \rho_t\varphi(t, t_0) \qquad \textbf{[5.10]}$$

where

$$\rho_t = X \cdot \rho \quad \textbf{[5.11]}$$

where, ρ_t is the aging coefficient ρ in [5.9] multiplied by *X*, which represents the percentage of irrecoverable creep strain over time period $(t - t_0)$.

Equation [5.10] may be written in terms of specific creep, $C_{c,t}$, to obtain Equation [5.12].

$$\varepsilon_{creep}(t) = C_{c,t}\sigma_t + \rho_t C_{c,t}(\sigma_0 - \sigma_t) \quad \textbf{[5.12]}$$

where

$$C_{c,t} = \frac{\varphi(t, t_0)}{E} \quad \textbf{[5.13]}$$

Equation [5.12], as with Equation [5.9] developed by Trost (1967), estimates the total creep strain at time *t* due to an incremental decrease or increase in stress from the point of initial loading. In the case of an incremental decrease of stress, the total creep strain at time *t* must include the irrecoverable component of the creep strain due to the difference in stress prior to the point where the stress starts to decrease. Equation [5.8] may be added to Equation [5.12] to form Equation [5.14], which is the total creep strain at time *t* for a material for a reduction in stress at time *n,* where $0 < n < t$.

$$\varepsilon_{creep}(t) = C_{c,t}\sigma_t + \rho_t C_{c,t}(\sigma_0 - \sigma_t) + XC_{c,n}(\sigma_0 - \sigma_t) \quad \textbf{[5.14]}$$

where, $C_{c,t}$ and $C_{c,n}$ are the specific creep values for the material at time *t* and *n* respectively, σ_0 is the initial stress that remains constant from time *0* to *n*, σ_t is the stress at time *t*, ρ_t is the aging coefficient that takes into consideration irrecoverable creep and *X* represents the percentage of irrecoverable creep strain over time period $(n - t_0)$.

Equation [5.14] is used as a basis to develop a general formula for the total creep strain in the repair material over time due to decrease in stress over discrete time steps. The total creep in the repair material at time t_0, t_1, t_2 and t_3 based on Equation [5.14] are calculated below.

For $t = t_0$

$$\varepsilon_{creep,r}(t_0) = 0 \quad \textbf{[5.15]}$$

For $t = t_1$

$$\varepsilon_{creep,r}(t_1) = C_{c,t_1}\sigma_{r,t_1} + \rho_1 C_{c,t_1}(\sigma_{r,t_0} - \sigma_{r,t_1}) \quad \textbf{[5.16]}$$

For $t = t_2$

$$\varepsilon_{creep,r}(t_2) = C_{c,t_2}\sigma_{r,t_2} + \rho_2 C_{c,t_2}(\sigma_{r,t_1} - \sigma_{r,t_2}) + XC_{c,t_1}(\sigma_{r,t_1} - \sigma_{r,t_2}) + \rho_1 C_{c,t_1}(\sigma_{r,t_0} - \sigma_{r,t_1}) \quad \textbf{[5.17]}$$

For $t = t_3$

$$\varepsilon_{creep,r}(t_3) = C_{c,t_3}\sigma_{r,t_3} + \rho_3 C_{c,t_3}(\sigma_{r,t_2} - \sigma_{r,t_3}) + XC_{c,t_2}(\sigma_{r,t_2} - \sigma_{r,t_3}) + \rho_2 C_{c,t_2}(\sigma_{r,t_1} - \sigma_{r,t_2}) + XC_{c,t_1}(\sigma_{r,t_1} - \sigma_{r,t_2}) + \rho_1 C_{c,t_1}(\sigma_{r,t_0} - \sigma_{r,t_1}) \quad \textbf{[5.18]}$$

From Equations [5.15], [5.16], [5.17] and [5.18], the general equation for the total creep in the repair material at time t_i may be represented in compact form in Equation [5.19]

$$\varepsilon_{creep,r}(t_i) = C_{c,t_i}\sigma_{r,t_i} + \sum_{n=1}^{i} \rho_n C_{c,t_n}(\sigma_{r,t_{n-1}} - \sigma_{r,t_n}) + \sum_{n=1}^{i-1} XC_{c,t_n}(\sigma_{r,t_n} - \sigma_{r,t_{n+1}}) \quad \textbf{[5.19]}$$

where, term

$$C_{c,t_i}\sigma_{r,t_i} \quad \textbf{[5.20]}$$

represents the creep strain due to the residual stress, term

$$\sum_{n=1}^{i} \rho_n C_{c,t_n}(\sigma_{r,t_{n-1}} - \sigma_{r,t_n}) \quad \textbf{[5.21]}$$

represents the irrecoverable creep strain between time steps after a decrease in stress and term

$$\sum_{n=1}^{i-1} XC_{c,t_n}(\sigma_{r,t_n} - \sigma_{r,t_{n+1}}) \quad \textbf{[5.22]}$$

represents the irrecoverable creep strain from the previous time steps after the stress has been relieved.

5.5.2 Model stress and strain estimation

The stress and strain in the substrate concrete and the repair material over time is estimated at each time step increment. Applying the strain compatibility principle, the strain along the cross-section of the repaired element is assumed to be uniform,

$$\varepsilon_{substate} = \varepsilon_{repair} \quad \textbf{[5.23]}$$

Equation [5.23] is applied to each time step increment, where the total strain in the substrate concrete is equal to the total strain in the repair material at time t_i.

$$\varepsilon_{total,s}(t_i) = \varepsilon_{total,r}(t_i) \quad \textbf{[5.24]}$$

The shrinkage and creep strain in the substrate concrete is assumed to be negligible, as discussed in Section 5.3.4. Thus the total strain in the substrate concrete at time t_i is the function of the elastic strain due to the applied stress in the material from imposed loading.

$$\varepsilon_{total,s}(t_i) = \frac{\sigma_{s,t_i}}{E_s} \quad \textbf{[5.25]}$$

The total strain in the repair material is the sum of the strain due to imposed loading, shrinkage and creep,

$$\varepsilon_{total,r}(t_i) = \frac{\sigma_{r,t_i}}{E_{r,t_i}} + \varepsilon_{creep,r}(t_i) + \varepsilon_{shrink,r}(t_i) \quad \textbf{[5.26]}$$

Substituting Equations [5.2] and [5.19] into Equation [5.26] we obtain,

$$\varepsilon_{total,r}(t_i) = \frac{\sigma_{r,t_i}}{E_{r,t_i}} + C_{c,t_i}\sigma_{r,t_i} + \sum_{n=1}^{i} \rho_n C_{c,t_n}(\sigma_{r,t_{n-1}} - \sigma_{r,t_n}) + \sum_{n=1}^{i-1} X_n C_{c,t_n}(\sigma_{r,t_n} - \sigma_{r,t_{n+1}}) + \varepsilon_{FSS,t_i} \cdot \frac{1}{1 + \frac{E_s}{E_{r,t_i}} \cdot C_\varepsilon} \quad \textbf{[5.27]}$$

Equation [5.25] and [5.27] may be substituted into Equation [5.24],

$$\frac{\sigma_{s,t_i}}{E_s} = \frac{\sigma_{r,t_i}}{E_{r,t_i}} + C_{c,t_i}\sigma_{r,t_i} + \sum_{n=1}^{i} \rho_n C_{c,t_n}(\sigma_{r,t_{n-1}} - \sigma_{r,t_n}) + \sum_{n=1}^{i-1} X_n C_{c,t_n}(\sigma_{r,t_n} - \sigma_{r,t_{n+1}}) + \varepsilon_{FSS,t_i} \cdot \frac{1}{1 + \frac{E_s}{E_{r,t_i}} \cdot C_\varepsilon} \quad \textbf{[5.28]}$$

Equation [5.28] is rearranged to obtain the stress in the substrate concrete at time t_i,

$$\sigma_{s,t_i} = E_s \left[\frac{\sigma_{r,t_i}}{E_{r,t_i}} + C_{c,t_i}\sigma_{r,t_i} + \sum_{n=1}^{i} \rho_n C_{c,t_n}(\sigma_{r,t_{n-1}} - \sigma_{r,t_n}) + \sum_{n=1}^{i-1} X_n C_{c,t_n}(\sigma_{r,t_n} - \sigma_{r,t_{n+1}}) + \varepsilon_{FSS,t_i} \cdot \frac{1}{1 + \frac{E_s}{E_{r,t_i}} \cdot C_\varepsilon} \right] \quad \textbf{[5.29]}$$

Using force compatibility along a cross-section of the modelled repaired element, the total force in the cross-section is equal to the sum of the forces in the substrate concrete and the repair material.

$$F_{total} = F_{subtrate} + F_{repair} \quad \textbf{[5.30]}$$

$$A\sigma = A_s\sigma_s + A_r\sigma_r \quad \textbf{[5.31]}$$

where σ, σ_s and σ_r, and A, A_s and A_r are the stresses and cross-sectional areas of the repaired element, substate concrete and repair material, respectively. Equation [5.31] may be rewritten to represent the equilibrium of forces in the cross-section of the repaired element at each time step increment t_i,

$$A\sigma_{t_i} = A_s\sigma_{s,t_i} + A_r\sigma_{r,t_i}. \quad \textbf{[5.32]}$$

Equation [5.29] may be substituted in equation [5.32]

$$A\sigma = A_sE_s\left[\frac{\sigma_{r,t_i}}{E_{r,t_i}} + C_{c,t_i}\sigma_{r,t_i} + \sum_{n=1}^{i}\rho_nC_{c,t_n}(\sigma_{r,t_{n-1}} - \sigma_{r,t_n}) + \sum_{n=1}^{i-1}X_nC_{c,t_n}(\sigma_{r,t_n} - \sigma_{r,t_{n+1}}) + \varepsilon_{FSS,t_i}\cdot\frac{1}{1+\frac{E_s}{E_{r,t_i}}\cdot C_\varepsilon}\right] + A_r\sigma_{r,t_i} \quad \textbf{[5.33]}$$

By decoupling the two summation terms for σ_{r,t_i} yields

$$\begin{aligned} A\sigma = {} & \frac{A\ E_s\sigma_{r,t_i}}{E_{r,t_i}} + A_sE_sC_{c,t_i}\sigma_{r,t_i} - A_sE_s\rho_nC_{c,t_i}\sigma_{r,t_i} - A_sE_sX_{i-1}C_{c,t_{i-1}}\sigma_{r,t_i} \\ & + A_r\sigma_{r,t_i} \\ & + A_sE_s\left[\rho_iC_{c,t_i}\sigma_{r,t_{i-1}} + \sum_{n=1}^{i-1}\rho_nC_{c,t_n}(\sigma_{r,t_{n-1}} - \sigma_{r,t_n})\right. \\ & \left. + X_{i-1}C_{c,t_{i-1}}\sigma_{r,t_{i-1}} + \sum_{n=1}^{i-2}X_nC_{c,t_n}(\sigma_{r,t_n} - \sigma_{r,t_{n+1}}) + \varepsilon_{FSS,t_i}\right. \\ & \left.\cdot\frac{1}{1+\frac{E_s}{E_{r,t_i}}\cdot C_\varepsilon}\right] \end{aligned} \quad \textbf{[5.34]}$$

Rearranging the above and factorising σ_{r,t_i}, the following relation is obtained:

$$\sigma_{r,t_i}\left[\frac{A_sE_s}{E_{r,t_i}} + A_sE_sC_{c,t_i} - A_sE_s\rho_iC_{c,t_i} - A_sE_sX_{i-1}C_{c,t_{i-1}} + A_r\right] = A\sigma - A_sE_s\left[\rho_iC_{c,t_i}\sigma_{r,t_{i-1}} + X_{i-1}C_{c,t_{i-1}}\sigma_{r,t_{i-1}} + \sum_{n=1}^{i-1}\rho_nC_{c,t_n}(\sigma_{r,t_{n-1}} - \sigma_{r,t_n}) + \sum_{n=1}^{i-2}X_nC_{c,t_n}(\sigma_{r,t_n} - \sigma_{r,t_{n+1}}) + \varepsilon_{FSS,t_i}\cdot\frac{1}{1+\frac{E_s}{E_{r,t_i}}\cdot C_\varepsilon}\right], \quad \textbf{[5.35]}$$

allowing one to obtain an equation for the stress in the repair material at time t_i

$$\sigma_{r,t_i} = \left[A\sigma - A_sE_s\left(\rho_iC_{c,t_i}\sigma_{r,t_{i-1}} + X_{i-1}C_{c,t_{i-1}}\sigma_{r,t_{i-1}} + \sum_{n=1}^{i-1}\rho_nC_{c,t_n}(\sigma_{r,t_{n-1}} - \sigma_{r,t_n}) + \sum_{n=1}^{i-2}X_nC_{c,t_n}(\sigma_{r,t_n} - \sigma_{r,t_{n+1}}) + \varepsilon_{FSS,t_i}\cdot\frac{1}{1+\frac{E_s}{E_{r,t_i}}\cdot C_\varepsilon}\right)\right] / \left[\frac{A_sE_s}{E_{r,t_i}} + A_sE_sC_{c,t_i} - A_sE_s\rho_iC_{c,t_i} - A_sE_sX_{i-1}C_{c,t_{i-1}} + A_r\right]. \quad \textbf{[5.36]}$$

Equation [5.36] forms the basis for which the model estimates stress at a particular point in time t_i in the cross-section of the repaired element. The stress in the repair material at time t_i is calculated from Equation [5.36] as a function of the cross-sectional geometry and material properties of the substrate concrete and repair material at time t_i, as well as the stress in repair material from previous time steps. The stress in the repair material at time t_i is then used to calculate the stress in the substrate concrete at time t_i using Equation [5.32]. Note that the stress in the repair material in Equation [5.36] is a function of the stress in the repair material from

previous time steps, thus the stress in the repaired element cannot be determined for a particular point in time without calculating the stress in the preceding time steps first.

5.5.3 Summary of model inputs

The model was programmed in Microsoft Excel. With reference to Sections 5.2 and 5.5.2, the required model input parameters are listed in Table 5-1.

Table 5-1: Required model input parameters

Input parameters	Description
Cross-sectional dimension	Cross-sectional dimensions of the column, including substrate concrete and repair area
F/σ	Total axial compressive force/stress in through element
E_s	Compressive elastic modulus of substrate concrete
$E_{r,t}$	Compressive elastic modulus of repair material for $t = 1, 7^{**}$ & $28\ day$
$\varepsilon_{FSS,t}$	Free shrinkage strain of repair material for $t = 1, 2, \dots, n$ days
$C_{c,t}$	Specific creep of repair material for $t = 1, 2, \dots, n\ day$,
X_n	Irrecoverable creep factor
ρ	Coefficient of aging load

**not required

6. Model Benchmarking

6.1 Introduction

The analytical model in Chapter 5 represents a formally complete approach with respect to the significant influences on the distribution of stress and strain in a repaired concrete element under axial compression. The disadvantage, however, in following a complete approach, is the resultant increase in the model complexity. A model benchmarking exercise was conducted under this section using alternative, simpler, assumptions in the application of the model. The simpler model contains less variables, thus making it easier to track for coherence. This was done to ensure that the model yields expected results.

6.2 Simplified repair material creep strain assumptions

The complexities of the model are largely contained in how the model accounts for creep strain in the repair material and thus its influence in the distribution of stress in the repaired element over time. The model considers creep recovery, where the recoverable component of the creep strain from previous time increments is recovered as stress is relieved in the repair material. The model further considers creep strain in the repair material due to an incremental decrease in stress in the repair material over time.

The model benchmarking exercise, in determining the stress distribution in the repaired element, considers the estimation of creep in the repair material from two extreme stand points: fully plastic (i.e., permanent) creep strains and; fully recoverable (i.e., temporary) creep strains. Fully plastic creep strains assume that the creep strains experienced by the repair material in previous time increments result in permanent deformation, i.e. no creep recovery. Fully recoverable creep strains assume that the creep strains experienced by the repair material in previous time increments are fully reversed on the release of the stresses. Considering the above assumptions, Equation [5.26] from Section 5.5.2 may be expanded to form Equation [6.1] and Equation [6.2] representing the strain in the repair material over time under fully plastic and fully recoverable creep strains, respectively,

$$\varepsilon_{total,r}(t_i) = \frac{\sigma_{r,t_i}}{E_{r,t_i}} + C_{c,t_i}\sigma_{r,t_i} + \sum_{n=1}^{i-1} C_{c,t_n}(\sigma_{r,t_{n-1}} - \sigma_{r,t_n}) + \varepsilon_{FSS,t_i} \cdot \frac{1}{1 + \frac{E_s}{E_{r,t_i}} \cdot C_\varepsilon} \qquad \textbf{[6.1]}$$

$$\varepsilon_{total,r}(t_i) = \frac{\sigma_{r,t_i}}{E_{r,t_i}} + C_{c,t_i}\sigma_{r,t_i} + \varepsilon_{FSS,t_i} \cdot \frac{1}{1 + \frac{E_s}{E_{r,t_i}} \cdot C_\varepsilon} \qquad \textbf{[6.2]}$$

where σ_{r,t_i} and E_{r,t_i} are the stresses in and elastic modulus of, the repair material at time t_i, respectively. C_{c,t_i} and ε_{FSS,t_i} represent the specific creep and free shrinkage strain of the repair material at the time t_i.

Similar to the model, Equations [6.1] and [6.2] were substituted into Equation [5.24] and solved simultaneously with Equation [5.31] to obtain σ_{s,t_i} and σ_{r,t_i}, the stresses in the substrate concrete and repair material over time, respectively, for the two creep strain assumptions. The expected stress in the repair material using the model, considering partial creep strain recovery in the repair material, should fall between those derived using the two estimates above.

6.3 Benchmarking of model

The model benchmarking was conducted based on the numerical example for a given element geometry, loading conditions and respective material property inputs. The properties of the HS grout, loaded at age of material 1 day, from Chapter 4 were used as the repair material property inputs for the model. A summary of the element geometry, loading conditions and substrate concrete material property inputs are found in Table 6-1 below.

Table 6-1: Model inputs (element geometry, loading conditions and substrate concrete material properties)

Model Inputs		
Cross-sectional areas		
Repaired element	A	0.250 m^2
Substrate concrete	A_s	0.200 m^2
Repair material	A_r	0.050 m^2
Loading conditions		
Applied stress	σ	50 MPa
Age of repair material at loading	-	1 day
Substrate concrete properties		
Compressive strength	-	80 MPa
Elastic modulus	E_s	40 GPa

Figure 6-1 plots the stress according to the model [5.36] in comparison to the two approximate estimates used to approximate the stress in the HS grout over time.

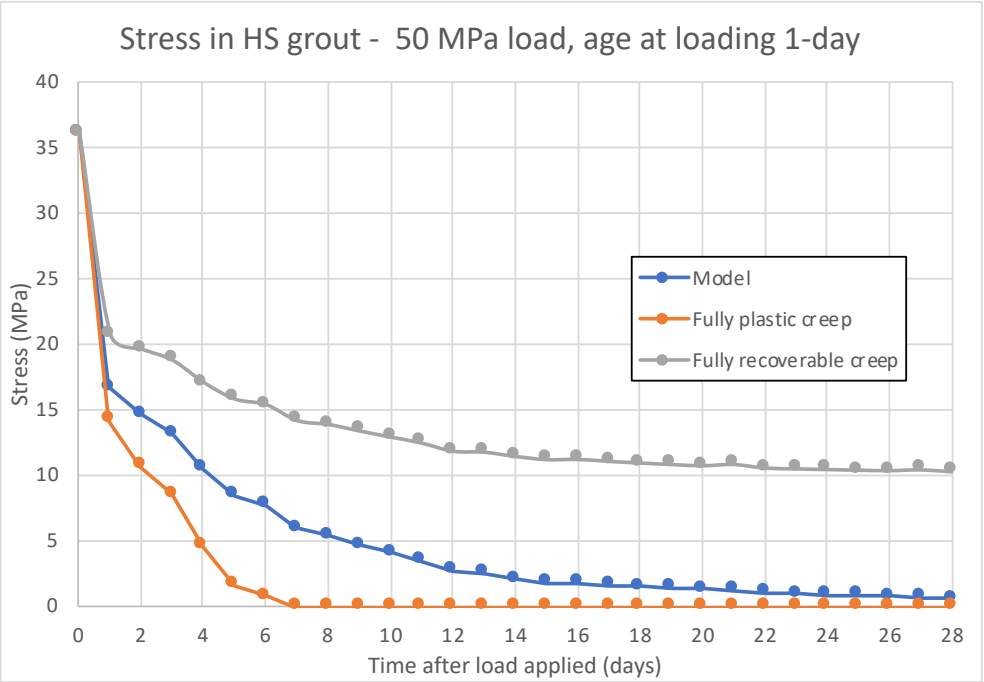

Figure 6-1: Model benchmarking by estimating stress in repair material from varying repair material creep strain assumptions

The stress in the HS grout as approximated by the model falls within the bounds of the two approximate estimates used to benchmark the model results. Thus, the model in Chapter 5, produces expected results within the assumptions taken in this research.

The benchmarking exercise, further highlights the significance of repair material creep strain assumptions in the distribution of stress in the repaired concrete element over time. This benchmarking approach may be used in future experimental research for validation of the model in Chapter 5. This may lead to a greater understanding of the creep strain behaviour of the repair material in a repaired element over time, i.e. creep recovery and creep under incremental decrease in stress.

7. Repair Simulations

7.1 Introduction

A numerical simulation was developed in Microsoft excel based on the analytical model in Chapter 5. It was used to simulate the stress and strain behaviour in a repaired concrete element under axial compression. Aspects of the simulated repair geometry, material inputs and load cases are discussed followed by the results of the simulations.

7.2 Element geometry

The repair simulations were conducted on a unreinforced square column with cross-sectional dimensions of 500mm×500mm, subjected to an axial compressive load. The cross-sectional dimensions of the patch of repair are 100mm×500mm, representing 20% of the column's total cross-sectional area. A sketch of the geometry of the repaired element is shown in Figure 7-1.

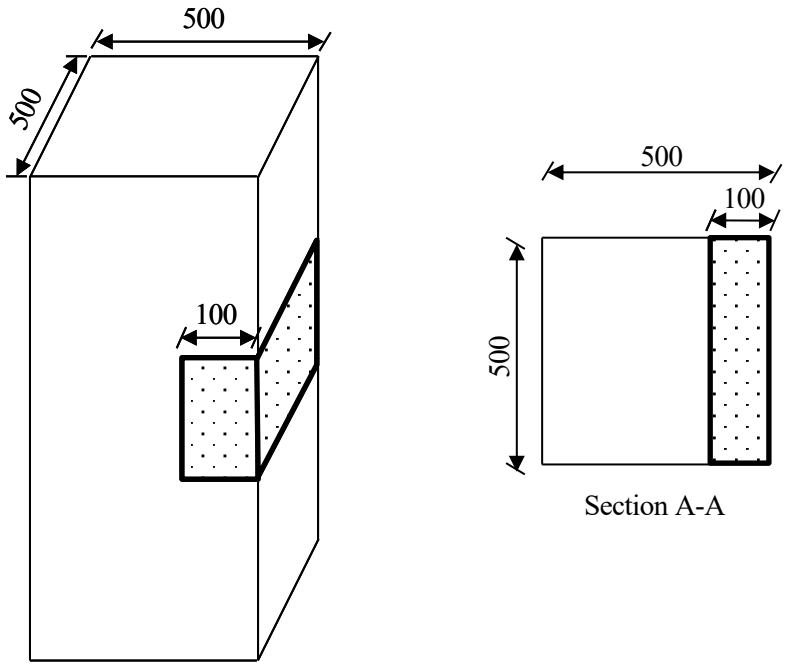

Figure 7-1: Geometry of modelled repaired concrete element

7.3 Material properties

The results obtained from the material testing in Chapter 4, were used as repair material property inputs in the model. The substrate concrete material property inputs were based on two substrate concretes of different quality, i.e. a moderate and high strength concrete, respectively. The physical material properties of each type of substrate concrete are found in Table 7-1.

Table 7-1: Modelled substrate concrete material properties

Material Property	Moderate-strength	High-strength
Compressive Strength	40 MPa	80 MPa
Elastic Modulus	25 GPa	40 GPa

7.4 Load cases

The magnitude of the load applied in the repair simulations were determined considering the mechanical properties of the substrate concrete in the repaired element from Table 7-1. These were divided into two load cases. The applied load is equal to approximately the strength of the substrate concrete divided by a factor of 1.6, representing the maximum safety factor prescribed by SANS 10100-1:2000 (2000). The applied load for each loading case is shown in Table 7-2

Table 7-2: Modelled substrate concrete material properties

	Load case 1	Load case 2
Substrate Concrete	Moderate-strength	High-strength
Applied Load	25 MPa	50 MPa

The concrete element is assumed to be propped, i.e. all imposed loading is relieved, prior to the repair application. The imposed loads are reapplied to the element after the application of the repair corresponding to the age of the repair material at loading scenario. The substrate concrete is assumed to undergo negligible creep strain recovery during the propping and reapplication of the imposed loads on the concrete element.

7.5 Model simulation results

The results of the model simulations for both load cases are presented in the sections below. The focus of the simulations is the stress in the repair material over time, and the ability of the repair material to contribute to the load-bearing resistance in the repaired concrete element.

7.5.1 Load case 1: 25 MPa load

The repair simulations for load case 1 were conducted using the three different repair materials from Chapter 4, each loaded at ages 1 and 7 days, respectively. Figure 7-2 shows the distribution of stress, over the first 14 days after the application of the load, for the concrete element repaired with the HS concrete, loaded at material age 1 day.

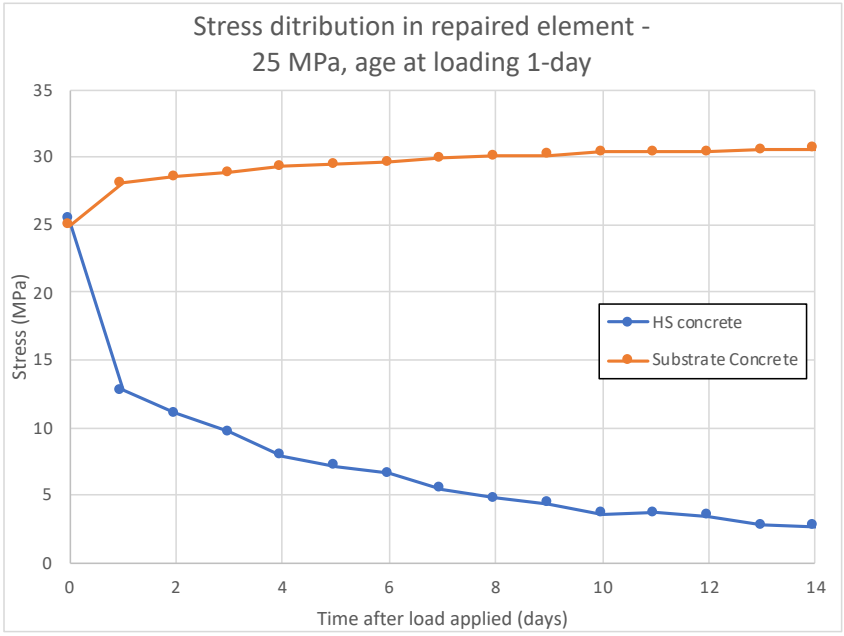

Figure 7-2: Stress distribution in repaired element - 25 MPa, HS concrete, age at loading 1-day

Figure 7-2 shows a decay of stress in the HS concrete over the first 14 days, resulting in the transfer of stress to the substrate concrete. The rate of stress decline in the repair material is sharp in the first few before it begins to flatten out slowly. This trend is associated with the high rate of shrinkage and creep strain development at earlier repair material ages after loading, resulting in a higher transfer of stress from the repair material to the substrate concrete. According to the model, after 14 days, the residual stress in the repair material is approximately 2.7 MPa, representing 11% of the original average stress in the repaired element. This illustrates a low contribution by the repair material to the externally applied loads on the repaired concrete element.

The model predicts that after 69 days of loading, the stress in the HS concrete will be less than 0.5 MPa. The repair material at this point is deemed to no longer contribute structurally to the load carrying capacity of the concrete element.

The mechanisms contributing to the transfer of stress from the repair material to the substrate concrete over time are the shrinkage and creep strain in the repair material. An analysis of the strain components in the repair material over time assist in quantifying the effect of the individual mechanisms. Figure 7-3 represents the strain components in the HS concrete over the first 14 days after loading, loaded at material age 1 day.

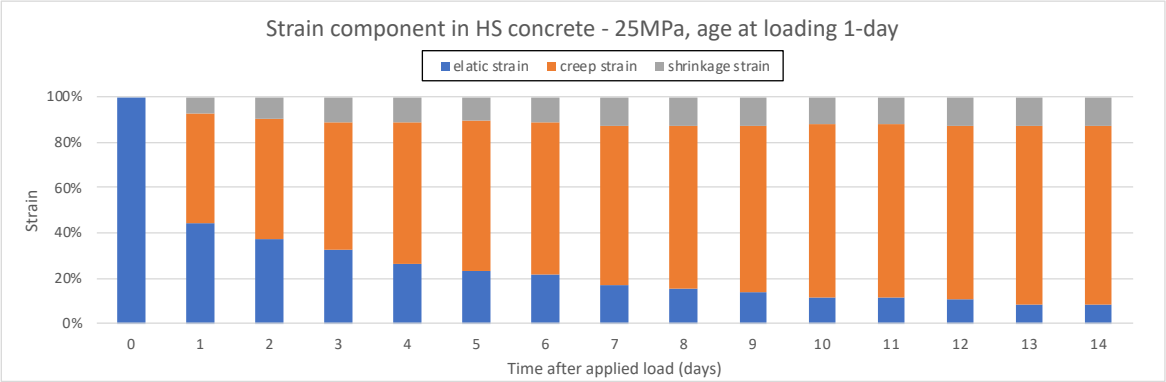

Figure 7-3: Strain component in HS concrete - 25 MPa, age at loading 1-day

From Figure 7-3, the largest component of strain in the HS concrete over time is the compressive creep strain. The large creep strains are attributed to the plastic creep strains experienced by the repair material as well as the high specific creep properties associated with cement-based materials loaded at early ages. It is indicative that the redistribution of stress from the repair material to the substrate concrete is largely owed to creep strain in the repair material. For the six repair materials tested, between 86% and 93% of the stress transferred after 14 days of loading was attributed to creep strain in the repair materials. The shrinkage strain in the repair material contributes to stress distribution to the substrate concrete at a much slower rate.

7.5.1.1 Varying repair material selection

The stress in the three repair materials for load case 1 were compared with each other, for the same material age at loading. The stress in the three repair materials, over the first 14 days, loaded at material age 1 day for load case 1 is shown Figure 7-4.

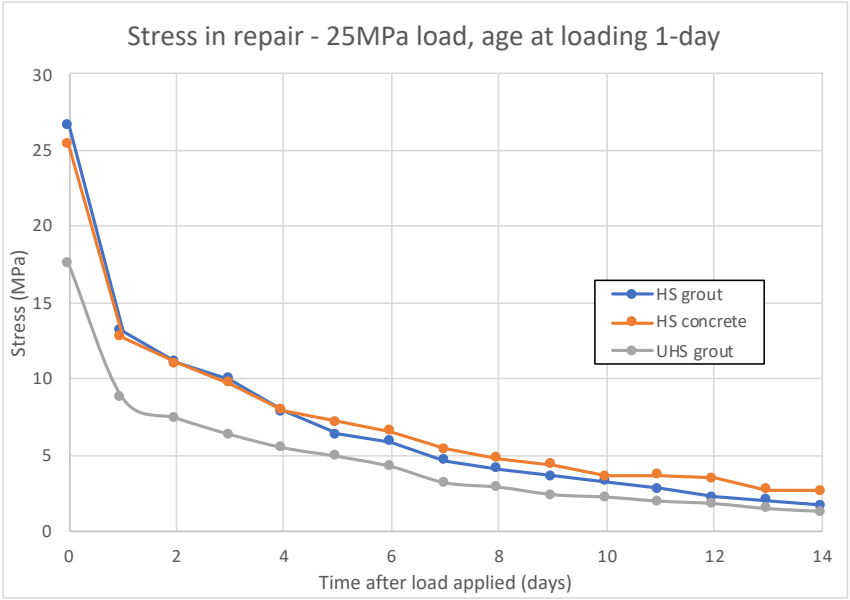

Figure 7-4: Stress in repair material - 25 MPa, age at loading 1-day

The decay of stress in all three repair materials follow a similar pattern. The stress curve associated with the UHS grout starts at a lower stress compared to the HS grout and HS concrete, due to its comparatively low elastic modulus properties resulting in the attraction of comparatively less initial stress in the composite repaired element. The similar stress decay patterns are attributed to the similar shrinkage and creep properties for all three repair materials when loaded at material age 1 day. Table 7-3 shows the percentage of residual stress remaining in the repair materials at various times within the first 28 days after loading.

Table 7-3: Residual stress in repair material – 25 MPa, age at loading 1-day

Days of loading	% of residual stress in repair material		
	HS grout	HS concrete	UHS grout
1	53%	51%	35%
3	40%	39%	25%
7	19%	22%	13%
14	7%	11%	5%
21	4%	7%	3%
28	2%	6%	3%

According to the model, the three repair materials only manage to retain 2-6% of the average stress in the repaired element after 28 days. This represents a very low contribution to load sharing by the repair materials loaded at material age 1 day for load case 1.

The stress in the three repair materials, over the first 14 days, loaded at material age 7 days for load case 1 is shown Figure 7-5.

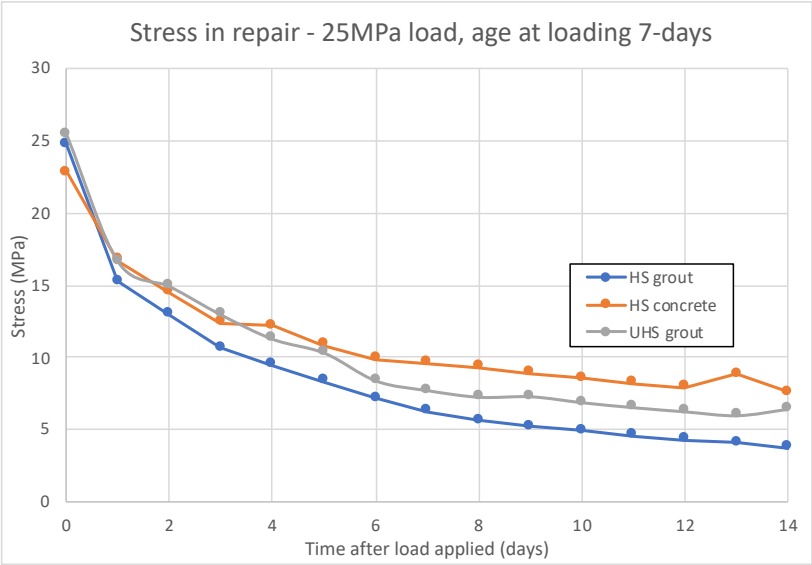

Figure 7-5: Stress in repair material - 25 MPa, age at loading 7-days

The decay of stress in the three materials loaded at material age 7 days, is more distinguishable between the respective materials after 14 days when compared to the materials loaded at age 1 day. The HS concrete manages to retain comparatively more of the stress over time. This is followed by the UHS grout and, the HS grout, which manages to retain the least stress among the three repair materials. The stress decay curves for the HS concrete and UHS grout experience an increase in stress at day 13 and day 14, respectively. This increase is as a result of lower measured specific creep properties in the repair materials comparative to the preceding day resulting, in lower total creep strains experienced by the repair material and thus in turn less redistribution of stress to the substrate concrete. This is largely attributed to the specific creep properties of the repair materials loaded at 7 day material age. The specific creep in the HS concrete is notably lower than the HS grout which is in turn lower than the UHS grout. Lower specific creep properties result in lower creep strains and thus lower transfer of stress to the substrate concrete. Table 7-4 shows the percentage of residual stress remaining in the repair materials at various times within the first 28 days after loading.

Table 7-4: Residual stress in repair material – 25 MPa, age at loading 7-days

Days of loading	% of residual stress in repair material		
	HS grout	HS concrete	UHS grout
1	61%	67%	66%
3	43%	50%	52%
7	25%	38%	31%
14	15%	30%	26%
21	13%	29%	21%
28	10%	27%	19%

The repair materials are able to retain a moderate amount of the average stress in the repaired element within the first 28 days, according to the model, with the HS concrete performing the best of the three material. However, the decay in stress in the repair materials is evident, with the repair materials contributing less to load sharing over time. The model predicts that the stress in all three repair materials will be below 0.5 MPa beyond 95 days of loading, rendering the repair materials effectively inactive in load sharing in the repaired concrete element.

7.5.1.2 Varying repair material ages at loading

The stress over time in each of the three repair materials under load case 1 was compared for varying material ages at time of loading. The stress in the repair materials for loading at 1 and 7 days of age, over the first 14 days, for the HS grout, HS concrete and UHS grout are compared in Figure 7-6, Figure 7-7 and Figure 7-8, respectively.

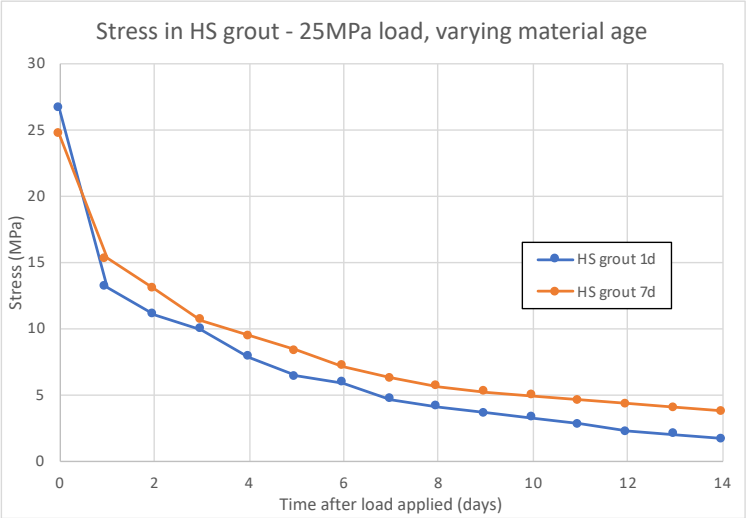

Figure 7-6: Stress in HS grout - 25 MPa, varying material age at loading

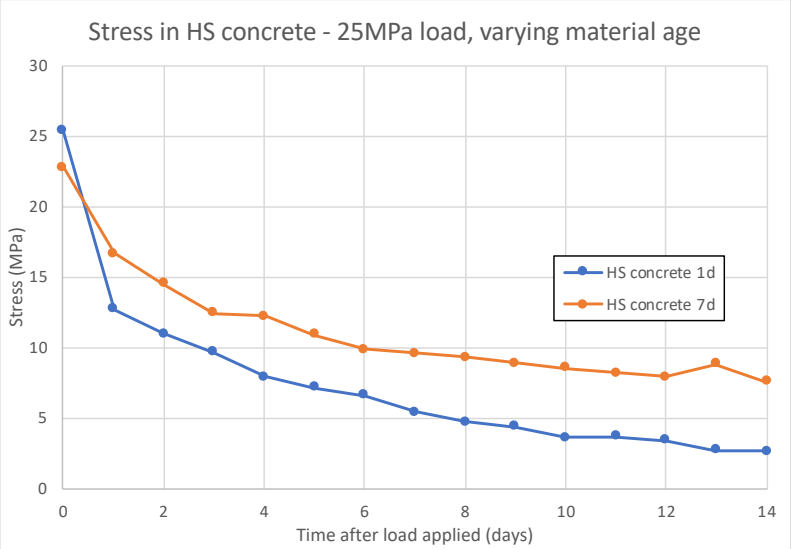

Figure 7-7: Stress in HS concrete - 25 MPa, varying material age at loading

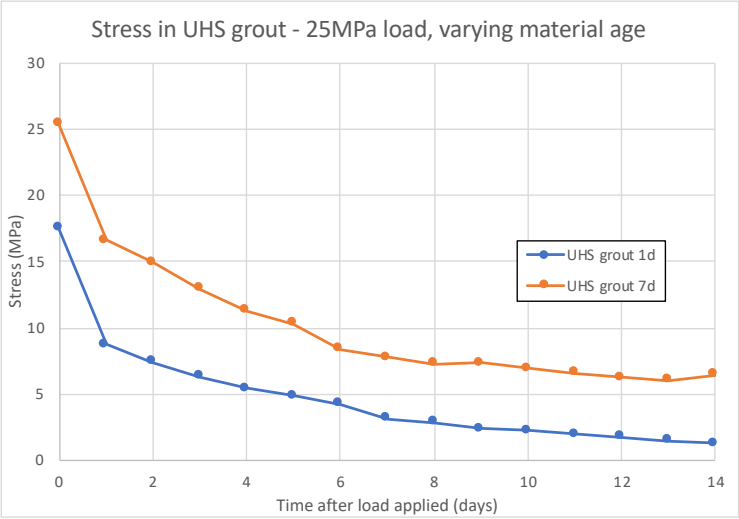

Figure 7-8: Stress in UHS grout - 25 MPa, varying material age at loading

The decay of stress in the repair materials for the different ages at loading follow a similar trend in all three repair materials, where the repair material loaded at 7 days manages to retain more residual stress compared to the material loaded at 1 day. This result is expected as it is attributed to the lower specific creep properties of the materials loaded at 7 days, thus resulting in lower creep strains. Furthermore, the difference in residual stress in the repair material is more pronounced in the HS concrete and UHS grout than in the HS grout. This is attributed to the similarities in specific creep properties for material ages 1 and 7 days in the HS grout when compared to the HS concrete and UHS grout.

7.5.2 Load case 2: 50 MPa load

Similar to load case 1, the repair simulations for load case 2 were conducted on three different repair materials, loaded at 1 and 7 days of age, respectively. Figure 7-9 shows the distribution of stress, over the first 14 days after the application of the load, for the concrete element repaired with the HS concrete, loaded at 7 days of age.

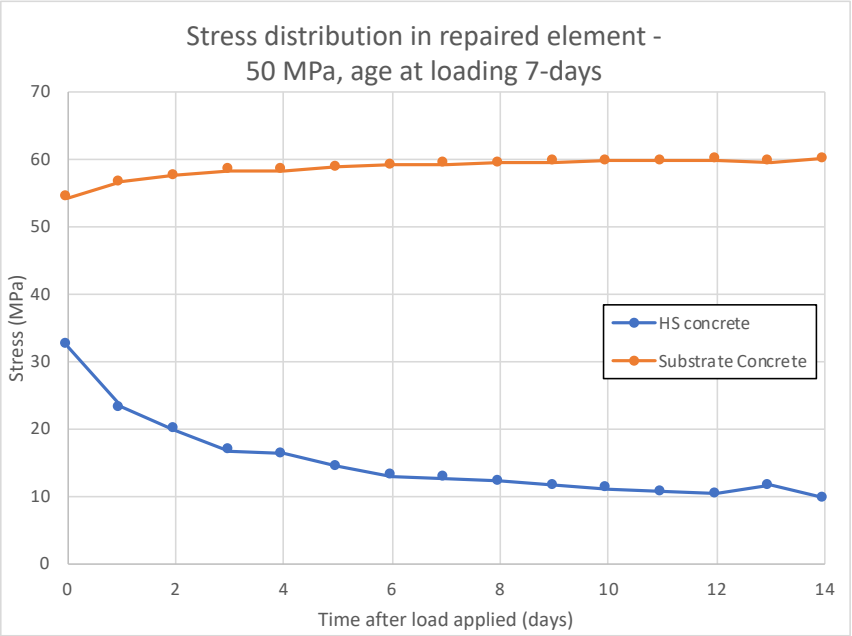

Figure 7-9: Stress distribution in repaired element - 50 MPa, HS concrete, age at loading 7-days

Figure 7-9 shows a decay of stress in the HS concrete over the first 14 days, resulting in the transfer of stress to the substrate concrete. According to the model, after 14 days, the residual stress in the repair material is approximately 9.9 MPa representing 20% of the original average stress in the repaired element, with the stress in the substrate concrete rising to 60.0 MPa. This illustrates a low contribution by the repair material to load sharing in the repaired concrete element.

The model predicts that after 95 days of loading, the stress in the HS concrete will be less than 0.5 MPa. The repair material at this point is deemed to no longer contribute to load sharing in the concrete element.

As in load case 1, an analysis of the strain components over time, in the HS concrete from Figure 7-9, is represented in Figure 7-10.

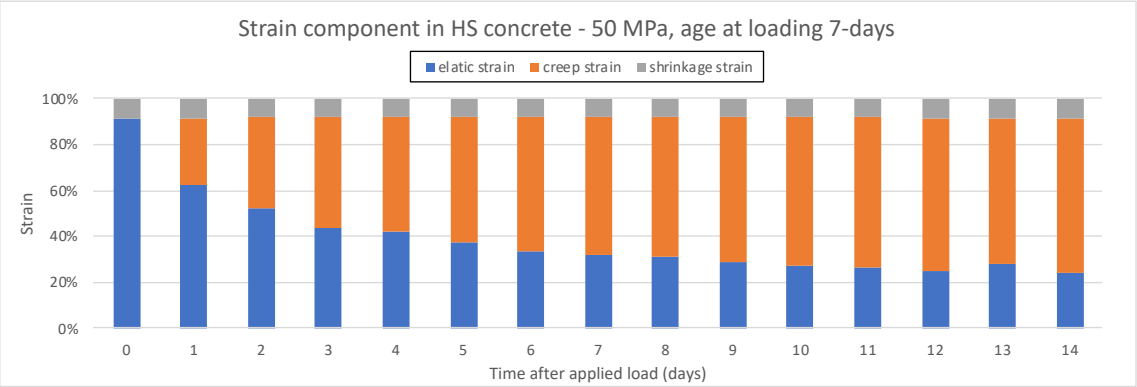

Figure 7-10: Strain component in HS concrete - 50 MPa, age at loading 7-days

The largest component of strain in the HS concrete over time is the compressive creep strain. The large creep strains are attributed to the plastic creep strains experienced by the repair material as well as the high specific creep properties associated with cement-based materials loaded at early ages. It is indicative that the redistribution of stress from the repair material to the substrate concrete is largely owed to creep strain in the repair material. For the six repair materials tested, between 86% and 93% of the stress transferred after 14 days of loading was attributed to creep strain in the repair materials. The shrinkage component of strain in the repair material is fairly constant from the time of loading as the repair material, loaded at age 7 days, has experienced a large amount of its shrinkage strain prior to the application of load.

7.5.2.1 Varying repair material selection

The stress in the three repair materials for load case 2 were compared with each other, for the same material age at loading. The stress in the three repair materials over the first 14 days, loaded at 1 day of age is shown in Figure 7-11.

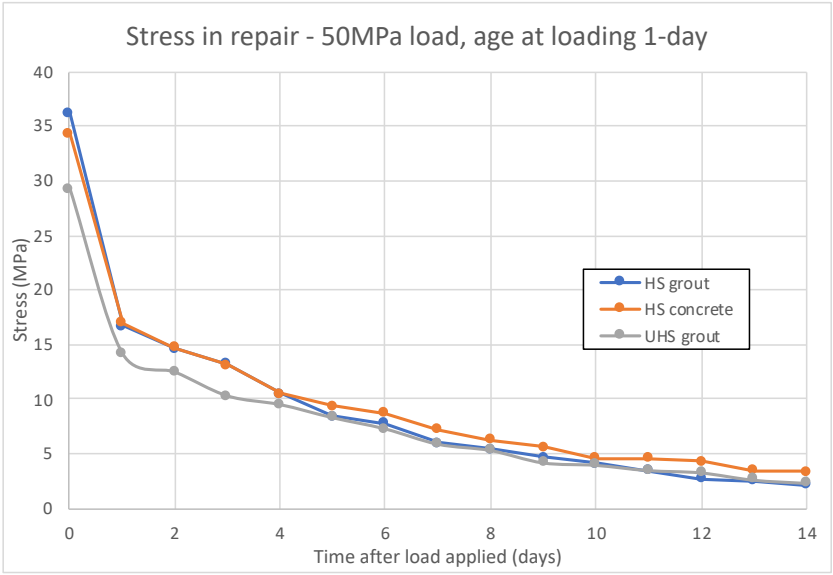

Figure 7-11: Stress in repair material - 50 MPa, age at loading 1-day

The decay of stress in all three repair materials follow a similar pattern. As in load case 1, this is attributed to the similar shrinkage and creep properties of the three repair materials when loaded at material age 1 day. Table 7-5 shows the percentage of residual stress remaining in the repair materials at various times within the first 28 days after loading.

Table 7-5: Residual stress in repair material – 50 MPa, age at loading 1-day

Days of loading	% of residual stress in repair material		
	HS grout	HS concrete	UHS grout
1	33%	34%	28%
3	27%	26%	21%
7	12%	14%	12%
14	4%	7%	5%
21	3%	4%	3%
28	1%	4%	2%

According to the model, the three repair materials only manage to retain 1-4% of the average stress in the repaired element after 28 days. This represents a very low contribution to load sharing by the repair materials loaded at 1 day of age, for load case 2.

The percentage residual stress in the repair materials under load case 2 are lower than in load case 1. This is partly attributed to the initial load sharing in load case 2. The elastic modulus of the repair materials are significantly lower than the high quality substrate concrete, thus, initially attracting a lower percentage of the average stress in the repaired element. The subsequent decay of stress results in comparatively lower percentage of average stress retained in the repair material, when compared to load case 1.

The stress in the three repair materials, over the first 14 days, loaded at 7 days of age for load case 2 are compared in Figure 7-12 to Figure 7-5.

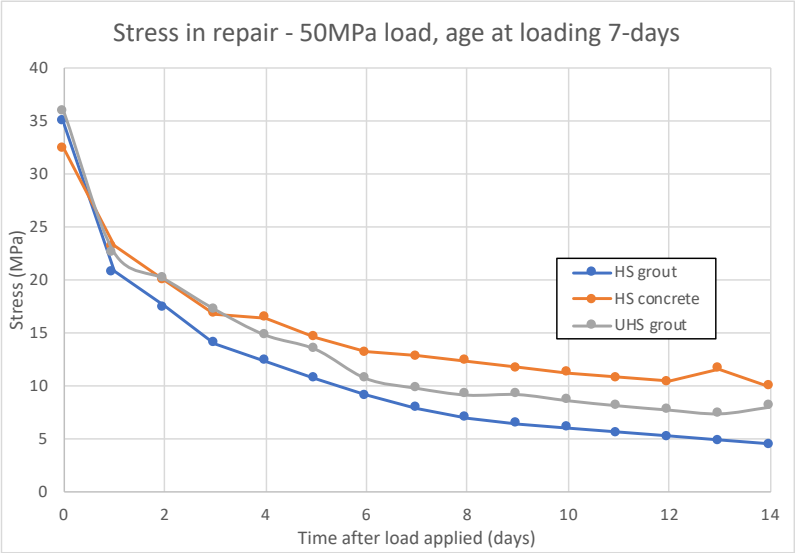

Figure 7-12: Stress in repair material - 50 MPa, age at loading 7-days

As with load case 1, the decay of stress in the three materials loaded at 7 days of age, is more distinguishable between the respective materials. This is again largely attributed to the difference in specific creep properties of the materials as previously discussed. Table 7-6 shows the percentage of residual stress remaining in the repair materials at various times within the first 28 days after loading.

Table 7-6: Residual stress in repair material – 50 MPa, age at loading 7-days

Days of loading	% of residual stress in repair material		
	HS grout	HS concrete	UHS grout
1	42%	46%	45%
3	28%	34%	34%
7	16%	25%	20%
14	9%	20%	16%
21	7%	19%	12%
28	6%	18%	12%

The repair materials are able to retain a moderate percentage of the average stress in the repaired element within the first 28 days, with the HS concrete performing the best of the three materials. However, similar to load case 1, the decay in stress in the repair materials is evident, with the repair materials contributing less to load sharing over time. The model predicts that the stress in all three repair materials will be below 0.5 MPa beyond 95 days after loading, rendering the repair materials effectively inactive in load sharing in the repaired concrete element.

The percentage of residual stress in the repair materials under load case 2, loaded at material age 7 days, are lower than in load case 1. As with the repair materials loaded at 1 day of age, this is partially attributed to the comparatively lower initial contribution of the repair material to loading sharing in the repaired element.

7.5.2.2 Varying repair material ages at loading

The stress over time in each of the three repair materials under load case 2 was compared for varying material ages at time of loading. The stress in the repair materials for varying material age at loading, over the first 14 days, for the HS grout, HS concrete and UHS grout are compared in Figure 7-13, Figure 7-14 and Figure 7-15, respectively.

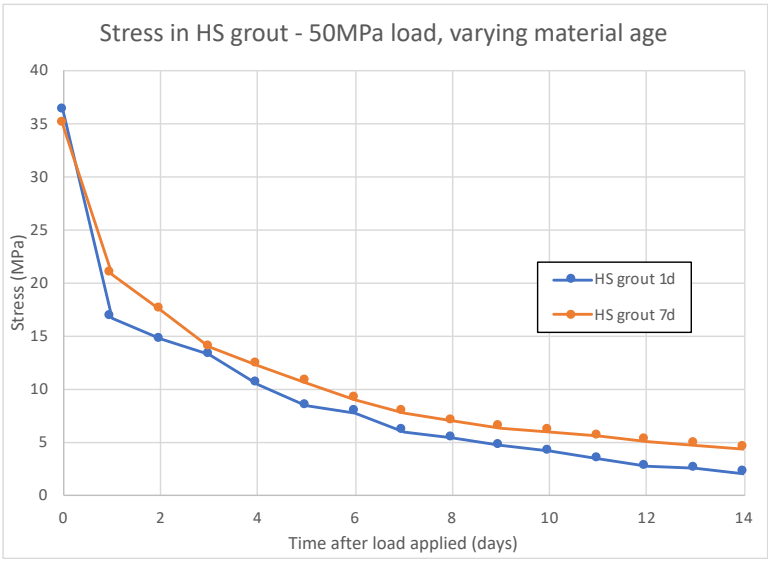

Figure 7-13: Stress in HS grout - 50 MPa, varying material age at loading

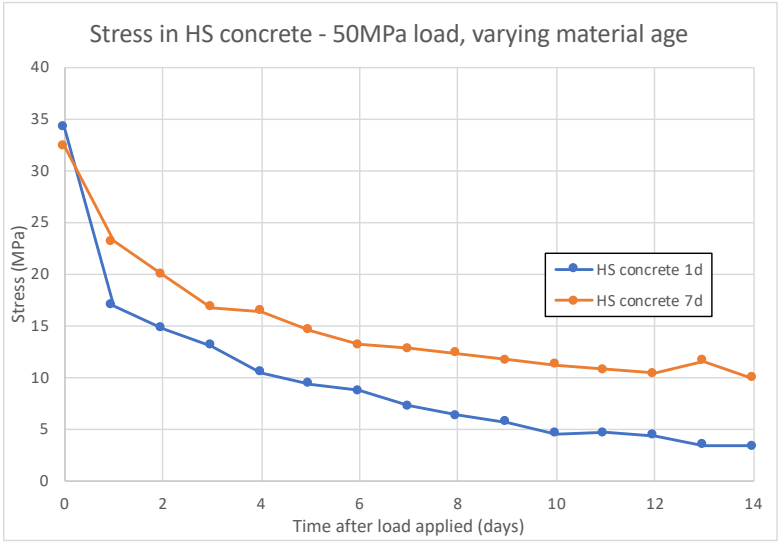

Figure 7-14: Stress in HS concrete - 50 MPa, varying material age at loading

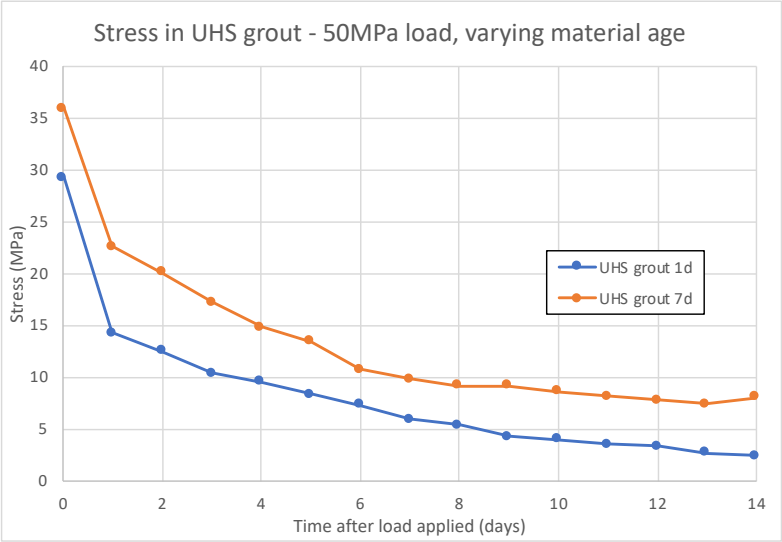

Figure 7-15: Stress in UHS grout - 50 MPa, varying material age at loading

The stress decay patterns for the three repair materials, follow distinctly similar patterns to those in load case 1 over the first 14 days. Similarly, the comparatively lower specific creep properties for materials loaded at 7 days result in a higher percentage residual stress retention in the repair material when compared to those loaded at 1 day. Furthermore, like in load case 1, the difference in residual stress in the repair material for the two ages of loading is more pronounced in the HS concrete and UHS grout than in the HS grout.

The distinct similarity in stress decay patterns between load cases 1 and 2, further shows that the stress decay pattern in the repair materials is affected very little by the magnitude of the applied load and substrate concrete properties.

7.6 Further model simulations and permutations

The model simulations conducted above were limited to a specific repair geometry subjected to two separate load cases, in order to display the application of the model. The material properties used as inputs in the simulations, were limited to the repair materials tested under the experimental component of this dissertation and the substrate concrete properties assumed above. The findings were thus limited to determining the efficacy of the specific repair materials in contributing towards load sharing in the simulated repaired concrete element. The model may, however, be further used to determine the stress distribution behaviour of structural concrete repairs under axial compression while varying the repair geometry, loading conditions, and, substrate concrete and repair material properties. Further permutations of the model inputs fall outside the scope of this research.

8. Conclusions and Recommendations

8.1 Conclusions

The conclusions of this dissertation are divided into three parts. The first part is concerned with the experimental material property tests conducted on high strength cement-based repair materials, the second part is concerned with the distribution of stress in concrete element, under axial compression, with the materials mentioned in Section 3.2.1 and based on numerical simulations using the analytical repair model in this research, and, lastly, some general conclusions on the applicability of the work done in this dissertation are discussed.

The repair material property testing was concerned with the key properties required for structural patch repair applications. The focus was primarily on the early age development of such properties in high strength cement-based repair materials. Some of the key findings are listed below:

- All four repair materials tested are suitable for structural repair applications based on their compressive strength characteristics, according to the European Standard EN 1504 for structural repair mortars, with strength values in excess of 40 MPa after 28 days. The highest values of compressive strength were associated with the HS (High Strength) grout, HS (High Strength) concrete and UHS (Ultra High Strength) concrete, which were all more than double the compressive strength of the PMRM (Polymer Modified Repair Mortar) at 1, 7 and 28 days. The tensile splitting strength of all the materials were well above 3 MPa after 28 days, typical of cement-based repair materials.
- The modulus of elasticity of the three high strength repair materials tested were relatively similar. Cement-based repair materials generally develop higher modulus of elasticity properties compared to resin-based repair materials. The 28 day elastic modulus properties of the three materials ranged between 28-34 GPa, similar to the expected properties of most moderate quality substrate concretes. Thus, on application of load to the repaired concrete member, the repair material and substrate concrete will attract a similar amount of stress. However, this is only relevant for the initial load sharing in the repaired concrete member.
- The atmospheric drying shrinkage of the three high-strength repair materials, measured under controlled environmental conditions, ranged between 250.10^{-6} and 350.10^{-6} over a 90 day measurement period. Under the shrinkage experienced, the repair material may be classified as low shrinkage repair material.
- The development of compressive specific creep was similar for all three high-strength repair materials when the load was applied at a material age of 1 day. For the three materials loaded at an age of 7 days, the specific creep values were significantly lower at the respective ages after loading when compared to the same material loaded at an age of

1 day. Furthermore, there was a noticeable difference in development rates and specific creep values between the three different repair materials. When loaded at an age of 7 days, the HS grout experienced the largest specific creep at the respective ages after loading, followed by the UHS grout and lastly the aggregate bulked HS concrete. The specific creep values of the UHS grout and HS concrete were found to be more sensitive to the age of the material at time of load application, compared to the HS grout.

The analytical model in this research approximates the stress behaviour in structural patch repairs over time, considering in particular concrete elements under axial compression. The model follows a formally complete approach, taking into account the most significant material property influences on stress distribution in the repaired element. As a result, the model has an increased level of complexity for which a modelling benchmarking exercise was conducted using simplified material assumptions to ensure the model produces expected results. A numerical simulation, using the above analytical model, was used to determine the efficacy of high strength cement-based repair materials in structural patch repair applications. The ability of the repair material to contribute to load-sharing in the repaired element was the primary focus of the simulations. The properties of repair materials tested in the experimental component of this dissertation were used as inputs to the simulation. Conclusions with respect to the model simulations are as follows:

- Repair materials with higher early age elastic moduli are able to initially attract more load in the repaired concrete element and contribute more to load sharing in the short term.
- After the repair is completed and the load reinstated on the repaired element, the stress in the repair material is transferred to the substrate concrete over time as a result of the shrinkage and creep strains experienced by the repair material.
- Creep in the repair material is responsible for the largest component of stress transfer from the repair material to the substrate concrete. For the six repair materials tested, between 86% and 93% of the stress transferred after 14 days of loading was attributed to creep strain in the repair materials.
- The calculated/modelled distribution of stress in the repaired element is highly sensitive to the assumptions made on the creep behaviour of the repair material, with regard to aspects of creep recovery and creep strain due to incremental decrease in stress. In the case where creep recovery is neglected, all the creep strain experienced by the repair material is assumed to represent permanent deformation. In reality, a component of the creep strain experienced may be viewed as a delayed elastic strain which is recoverable over time once the stress on the material is released. Accounting for this phenomenon is thus essential for the completeness of the analytical approach for calculating the distribution of stress in the repaired element.
- The age of the repair materials at loading is inconsequential to the ability of the repair material to share load in the repaired member in the long-term, as there is effectively no

remaining stress in the repair material beyond 90 days, independent of the repair material's age at loading.

- In the short-term, it is more favourable to load repaired elements at later repair material ages, to facilitate the development of lower initial specific creep strain in the repair. This results in lower initial decay of stress in repair materials, where load is applied to the repaired element at repair material age 7 days, compared to those loaded at an age of 1 day.
- The high strength cement-based materials tested in this research were unable to significantly contribute to load sharing in the repaired element in the long-term. For the simulations conducted, the model estimates that beyond 90 days, there is effectively no remaining stress in the repair material.

The findings and conclusions from the experimental tests and analytical model developed have led to practical conclusions with respect to the applicability of this research which include the following:

- Common commercially available high strength cement-based mortars and grouts, used in structural concrete repairs of elements under axial compression, do not contribute to load sharing in the repaired element in the long-term under service loads. Such materials should thus not be considered as 'structural' repair mortars or grouts, unless specific measures are taken to ensure their long-term load-bearing action.
- Despite the common conception that these structural mortars contribute to the load bearing behaviour of the structure, they can in reality and under service loads only, be considered to meet performance requirements related to aesthetic aspects and durability properties of the repaired structure.
- The contribution of structural repair mortars to the ultimate load bearing behaviour of axially loaded concrete elements needs to be considered in future research.

This research was limited to structural patch repairs conducted on axially loaded concrete elements under service loading conditions. Under ultimate loading conditions, structural repair mortars and grouts may contribute substantially to the structural behaviour of the repaired element. Furthermore, the effects of steel reinforcement were not considered in this research. In actual structures, the structural function of structural repair mortars and grouts is not limited to load-sharing but also the connection between the steel reinforcement and concrete (i.e. shear strength, etc.). In addition, the presence of steel reinforcement embedded in the patch repair may increase the structural contribution of the repair mortar or grout. This was not investigated in this research.

8.2 Recommendations for future work

The work conducted under this research forms part of the building blocks for future research within the field of structural concrete patch repairs. The analytical model shows the failure of structural patch repairs as well as structural repair mortars and grouts under the conditions and applications set out in this research (axially loaded, unreinforced concrete elements under service loads). This is provides more questions with respect to what conditions, applications and materials may result in effective structural patch repairs. The answers to these questions may be obtained through a better understanding of the stress behaviour of repaired reinforced concrete elements. Some recommendations for future work are detailed below:

- Validate the analytical model through experimental work. This entails simulating a repaired concrete element under axial compression and measuring the distribution of stress in the repair material and substrate concrete overtime.
- Develop a finite element model which may be used to approximate the stress behaviour in a repaired concrete element under axial compression, with reference to the principles of the analytical model. Further seek to validate the finite element model through experimental work as above.
- Determine the shrinkage and creep behaviour of the repair material in repair applications. This may be done through experimental work while applying the principles of the analytical model. The experimental work is to simulate a composite repaired specimen while applying controls for shrinkage and creep in the repair material.
- Conduct a sensitivity analysis to determine which of the repair material properties have the most significant effect on the distribution of stress in the repaired element over time. This may be done by conducting numerical simulations based on the analytical model, while varying the material properties of the repair material. This may inform repair material development for manufacturers as well as repair material selection for applicators and designers.
- Conduct repair material properties tests, as done in this research, on different types of repair materials. Use data as input in the analytical model to determine the efficacy of such repair materials in sharing load in structural patch repairs.
- Refine and simplify the analytical model for suitability of use in various codes of practice, to inform repair material selection for structural patch repairs. This may be done by using information gathered from repair material property sensitivity analysis and model validation through experimental work.
- Use the principles of this model to develop a model to determine the stress distribution for structurally patch repaired concrete elements under flexural loading.

9. References

ACI Committee 364. 2003. ACI 364.9T-03(11) - Cracks in a Repair. 03(11):1–3.

ACI Committee 364. 2010. *ACI364.5T-10: Importance of Modulus of Elasticity in Surface Repair Materials*. V. 1.

ACI Committee 364. 2018. ACI364.15T-18: Significance of the Shrinkage-Compensating and Non-Shrink Labels on Packaged Repair Materials. 05.

ACI Committee 546. 2014. *ACI546R-14: Guide to Materials Selection for Concrete Repair*.

Acker, P. & Ulm, F.-J. 2001. Creep and shrinkage of concrete : physical origins and practical measurements. *Nuclear Engineering and Design*. 203:143–158.

Alexander, M. & Beushausen, H. 2009. Deformation and volumen change of hardened concrete. In *Fulton's Concrete Technology*. 111–154.

Altoubat, S. & Lange, D.A. 2001. Creep, Shriankge and Cracking of Restrained Concrete at Early Age. *ACI Materials Journal*. 98(July 2001):1–31.

American Society of Civil Engineers. 2017. *2017 Infrastructure Report Card*. Available: https://www.infrastructurereportcard.org/.

Angst, U.M. 2018. Challenges and opportunities in corrosion of steel in concrete. *Materials and Structures/Materiaux et Constructions*. 51(1):1–20. DOI: 10.1617/s11527-017-1131-6.

Arito, P. 2018. Influence of Mix Design Parameters on Restrained Shrinkage Cracking in No-Structural Concrete Patch Repair Mortars. Univristy of Cape Town.

Baldwin, N.J.R. & King, E.S. 2003. *Field studies of the effectiveness of concrete repairs. Phase 1 Report: Desk study and literature review. Technical Report 175*.

Bažant, Z.P. 1975. Theory of Creep and Shrinkage in Concrete Structures: A Précis of Recent Developments. *Mechanics Today*. 2:1–93. DOI: 10.1016/b978-0-08-018113-4.50007-0.

Beushausen, H. 2005. Long-term performance of bonded concrete overlays subjected to differential shrinkage. University of Cape Town.

Beushausen, H. & Alexander, M. 2006. Failure mechanisms and tensile relaxation of bonded concrete overlays subjected to differential shrinkage. *Cement and Concrete Research*. 36(10):1908–1914. DOI: 10.1016/j.cemconres.2006.05.027.

Beushausen, H. & Alexander, M. 2007. Localised strain and stress in bonded concrete overlays subjected to differential shrinkage. *Materials and Structures/Materiaux et Constructions*. 40(2):189–199. DOI: 10.1617/s11527-006-9130-z.

Beushausen, H. & Arito, P. 2018. The influence of mix composition, w/b ratio and curing on restrained shrinkage cracking of cementitious mortars. *Construction and Building Materials*. 174:38–46. DOI: 10.1016/j.conbuildmat.2018.04.099.

Birkeland, H.W. 1960. Differential Shrinkage in Composite Beams. *ACI Journal Proceedings*. 56(5). DOI: 10.14359/8133.

Brooks, J.J. 2005. 30-Year Creep and Shrinkage of Concrete. *Magazine of Concrete Research*. 57(9):545–556. DOI: 10.1680/macr.2005.57.9.545.

Brooks, J.J. & Neville, A.M. 1978. Predicting long-term creep and shrinkage from short-term tests. *Magazine of Concrete Research*. 30(103):51–61.

Cabrera, J.G. & Al-Hasan, A.S. 1997. Performance properties of concrete repair materials. *Construction and Building Materials*. 11(5–6):283–290.

Cairns, J. 1993. Load relief during structural repairs to reinforced concrete beams. *Proceedings of the Institution of Civil Engineers: Structures and Buildings*. 99(4):417–427. DOI: 10.1680/istbu.1993.25335.

Canisius, T.D.G. & Waleed, N. 2004. Concrete patch repairs under propped and unpropped implementation. *Proceedings of the Institution of Civil Engineers: Structures and Buildings*. 157(2):149–156. DOI: 10.1680/stbu.2004.157.2.149.

Chilwesa, M. 2012. Assessing the age at cracking of concrete repair moratrs/overlays subjected to restrained drying shrinkage. Univeristy of Cape Town. Available: http://open.uct.ac.za/handle/11427/5054.

Cusson, D. & Mailvaganam, N. 1996. Durability of repair materials NRCC-38817. *Concrete international: Design and Construction*. 18(3):34–38.

Decter, M.H. & Keeley, C. 1997. Durable Concrete Repair - Importance of Compatibility and Low Shrinkage. *Construction and Building Materials*. 11:267–273.

Dilger, W.H., Wang, C. & Niitani, K. 1996. Experimental studies on shrinkage and creep of high-performance concrete. In *BHP '96, 4th International symposium on utilisatoin of high strength/high performance concrete*. Paris. 311–319.

Dilger, W.H., Niitani, K. & Wang, C. 1997. A creep and shrinkage prediction model for high-performance concrete. In *International Conference on Engineering Materials*. V. 1. Ottawa. 615–630.

Emberson, N.K. & Mays, G.C. 1990a. Significance of property mismatch in the patch repair of structural concrete Part 1: Properties of repair systems. *Magazine of Concrete Research*. 42(152):147–160. DOI: 10.1680/macr.1990.42.152.147.

Emberson, N.K. & Mays, G.C. 1990b. Significance of property mismatch in the patch repair of structural concrete Part 2: Axially loaded reinforced concrete members. *Magazine of Concrete Research*. 42(152):161–170. DOI: 10.1680/macr.1990.42.152.161.

Emberson, N.K. & Mays, G.C. 1996. Significance of property mismatch in the patch repair of structural concrete . Part 3 : Reinforced concrete members in flexure. *Magazine of Concrete Research*. 48(174):45–57.

Emmons, P.H. & Sordyl, D. 2006. The state of the concrete repair industry, and a vision for its future. *Concrete Repair Bulletin*. 7–14. Available: http://scholar.google.com/scholar?hl=en&btnG=Search&q=intitle:The+State+of+the+Concrete+Repair+Industry+,+and+a+Vision+for+its+Future#0.

Emmons, P.H. & Vaysburd, A.M. 1993. Compatibility considerations for durable concrete repairs. In *Transportation Research Board Annual Meeting*. Washington DC.

Emmons, P.H. & Vaysburd, A.M. 1994. Factors affecting the durability of concrete repair : the contractor 's viewpoint. *Construction & Building Materials*. 8(1):5–16.

Emmons, P.H., McDonald, J.E. & Vaysburd, A.M. 1983. Some compatability problems in

repair of concrete structures –a fresh look. In *"Proceedings of the third international colloqium on materials science and restauration", Technische Akademie Esslingen*. 837–853.

Emmons, P.H., Vaysburd, A.M. & McDonald, J.E. 1993. A rational approach to durable concrete repairs. *Concrete International*. 15(9):40–45.

Glass, G.K. 2003. *Reinforcement corrosion*. Woodhead Publishing Limited. DOI: 10.1016/B978-075065686-3/50256-1.

Harrison, T.A. 2003. Concrete properties: setting and hardening. In *Advanced concrete technology - Concrete properties*. J. Newman & B.S. Choo, Eds. Oxford: Elsevier.

ISO Technical Committee 71. 2014. *ISO 16311-1:2014 - Maintenance and repair of concrete structures. Part 1: General principles*. V. 1. International Organization for Standardization.

Kesner, K. & Conroy, K. 2017. ACI 562-16 - The ACI concrete repair code. *High Tech Concrete: Where Technology and Engineering Meet - Proceedings of the 2017 fib Symposium*. (June):1566–1572. DOI: 10.1007/978-3-319-59471-2_180.

Kesner, K., Conroy, K. & Kahn, L.F. 2014. ACI 562 - Requirements for Evaluation, Repair and Rehabilitation of Concrete Buildings. *Structures Magazine*. (September):18–21.

Kim, M.O., Bordelon, A., Lee, M.K. & Oh, B.H. 2016. Cracking and failure of patch repairs in RC members subjected to bar corrosion. *Construction and Building Materials*. 107:255–263. DOI: 10.1016/j.conbuildmat.2016.01.017.

Kocab, D., Kucharczykova, B., Misak, P., Zitt, P. & Kralikova, M. 2017. Development of the Elastic Modulus of Concrete under Different Curing Conditions. *Procedia Engineering*. 195:96–101. DOI: 10.1016/j.proeng.2017.04.529.

Kovler, K. & Roussel, N. 2011. Properties of fresh and hardened concrete. *Cement and Concrete Research*. 41(7):775–792. DOI: 10.1016/j.cemconres.2011.03.009.

Kristiawan, S.A. 2006. Strength, shrinkage and creep of concrete in tension and compression. *Civil Engineering Dimension*. 8(2):73–80.

Kristiawan, S.A., Supriyadi, A., Sangadji, S., Anggraeni, T. & Pattiwael, M.M. 2019. Experimental investigation on the behaviour of patched reinforced concrete column under eccentric loading: a case of compression failure. *International Journal of Advanced Structural Engineering*. 11(1):31–43. DOI: 10.1007/s40091-019-0214-8.

Lee, H.K., Lee, K.M. & Kim, B.G. 2003. Autogenous shrinkage of high-performance concrete containing fly ash. *Magazine of Concrete Research*. 55(6):507–515. DOI: 10.1680/macr.2003.55.6.507.

Mangat, P.S. & Limbachiya, M.K. 1994. Repair material properties which influence long-term performance of concrete structures. *Construction and Building Materials*. 9(2):81–90.

Mangat, P.S. & O'Flaherty, F.J. 1999a. Serviceability characteristics of flowing repairs to propped and unpropped bridge structures. *Materials and Structures/Materiaux et Constructions*. 32(9):663–672. DOI: 10.1007/bf02481704.

Mangat, P.S. & O'Flaherty, F.J. 1999b. Long-term performance of high-stiffness repairs in highway structures. *Magazine of Concrete Research*. 51(5):325–339. DOI: 10.1680/macr.1999.51.5.325.

Mangat, P.S. & O'Flaherty, F.J. 2000. Influence of elastic modulus on stress redistribution

and cracking in repair patches. *Cement and Concrete Research*. 30:125–136. DOI: 10.1016/S0008-8846(99)00217-3.

Manita, T. & Triantafillou, C.P. 2011. Influence of the design materials on the mechanical and physical properties of repair mortars of historic buildings. *Materials and Structures*. 44:1671–1685. DOI: 10.1617/s11527-011-9726-9.

Matthews, S. 2007. CONREPNET: Performance-based approach to the remediation of reinforced concrete structures: Achieving durable repaired concrete structures. *Journal of Building Appraisal*. 3(1):6–20. DOI: 10.1057/palgrave.jba.2950063.

Mays, G.C. 1999. Materials for the protection and repair of concrete: Progress towards European standardisation. *Concrete Durability and Repair Technology*. 481–491.

Mays, G.C. & Barnes, R.A. 1995. The structural effectiveness of large volume patch repairs to concrete structures. *Proceedings of the Institution of Civil Engineers: Structures and Buildings*. 110(4):351–360. DOI: 10.1680/istbu.1995.28053.

Mays, G.C. & Wilkinson, W.B. 1987. Polymer Repairs to Concrete: Their Influence on Structural Performance. *ACI Symposium Publication*. 100:351–375. DOI: 10.14359/2618.

Mehta, P.K. & Monteiro, P.J.M. 2014. *Concrete: Microstructure, Properties, and Materials*. Fourth ed. McGraw-Hill Education.

Mihashi, H. 2013. JCI guidelines for assessment of existing concrete structures. *Sustainable Construction Materials and Technologies*. 2013-Augus.

Morgan, D.R. 1996. Compatibility of concrete repair materials and systems. *Construction and Building Materials*. 10(I):57–67.

Nahlawi, K. & Paul, J.H. 2017. Evolution of ACI 562 Code—Part 9 Interface bond provisions in ACI 562-16. *Concrete International*. 38(May).

Oluokun, F.A., Burdette, E.G. & Deatherage, J.H. 2010. Rates of Development of Physical Properties of Concrete at Early Ages. *Transportation Research Record*. 16–22.

Ortega, A.I., Pellicer, T.M., Calderón, P.A. & Adam, J.M. 2018a. An experimental study on RC columns repaired on all four sides with cementitious mortars. *Construction and Building Materials*. 161:53–62. DOI: 10.1016/j.conbuildmat.2017.11.126.

Ortega, A.I., Pellicer, T.M., Calderón, P.A. & Adam, J.M. 2018b. Axially loaded RC columns repaired on one side with cement-based mortars. *Construction and Building Materials*. 177:1–9. DOI: 10.1016/j.conbuildmat.2018.05.102.

Ortega, A.I., Pellicer, T.M., Calderón, P.A. & Adam, J.M. 2018c. Cement-based mortar patch repair of RC columns . Comparison with all-four-sides and one-side repair. *Construction and Building Materials*. 186:338–350. DOI: 10.1016/j.conbuildmat.2018.07.148.

Pan, Z. & Meng, S. 2016. Three-level experimental approach for creep and shrinkage of high-strength high-performance concrete. *Engineering Structures*. 120:23–36. DOI: 10.1016/j.engstruct.2016.04.009.

Pane, I. & Hansen, W. 2002. Early age creep and stress relaxation of concrete containing blended cements. *Materials and Structures/Materiaux et Constructions*. 34(246):92–96. DOI: 10.1617/13800.

Pellegrino, C., Porto, F. da & Modena, C. 2009. Rehabilitation of reinforced concrete axially

loaded elements with polymer-modified cementicious mortar. *Construction and Building Materials*. 23(10):3129–3137. DOI: 10.1016/j.conbuildmat.2009.06.025.

Pellegrino, C., Da Porto, F. & Modena, C. 2011. Experimental behaviour of reinforced concrete elements repaired with polymer-modified cementicious mortar. *Materials and Structures/Materiaux et Constructions*. 44(2):517–527. DOI: 10.1617/s11527-010-9646-0.

Plum, D. 1991. Materials - what to specify. *Construction Maintenance and Repair*. 5(4):3–7.

Da Porto, F., Stievanin, E. & Pellegrino, C. 2012. Efficiency of RC square columns repaired with polymer-modified cementitious mortars. *Cement and Concrete Composites*. 34(4):545–555. DOI: 10.1016/j.cemconcomp.2011.11.020.

Raupach, M. & Büttner, T. 2014. *Concrete Repair to EN 1504*. DOI: 10.1201/b16852.

Revie, R.W. & Uhlig, H.H. 2008. *Corrosion and corrosion control: An introduction to corrosion science and engineering*. Fourth Edi ed. John Wiley & Sons, Inc.

Río, O., Andrade, C., Izquierdo, D. & Alonso, C. 2005. Behavior of patch-repaired concrete structural elements under increasing static loads to flexural failure. *Journal of Materials in Civil Engineering*. 17(2):168–177. DOI: 10.1061/(ASCE)0899-1561(2005)17:2(168).

Robery, P. & Shaw, J. 1997. Materials for the Repair and Protection of Concrete. *Construction & Building Materials*. 11(97):275–281.

SANS 10100-1:2000. 2000. *Code of preactice for the structural use of concrete*. Pretoria: South African Bureau of Standards.

Shambira, M.V. & Nounu, G. 2000. On the effect of time-dependent deformations on the behaviour of patch-repaired reinforced concrete short columns. *Construction and Building Materials*. 14(8):425–432. DOI: 10.1016/S0950-0618(00)00048-9.

Shambira, M.V. & Nounu, G. 2001. Numerical simulation of shrinkage and creep in patch-repaired axially loaded reinforced concrete short columns. *Computers and Structures*. 79(29–30):2491–2500. DOI: 10.1016/S0045-7949(01)00132-8.

Sharif, A., Rahman, M.K., Al-Gahtani, A.S. & Hameeduddin, M. 2006. Behaviour of patch repair of axially loaded reinforced concrete beams. *Cement and Concrete Composites*. 28(8):734–741. DOI: 10.1016/j.cemconcomp.2006.05.013.

South African Institute for Civil Engineers. 2017. *South African Infrastructure Report Card 2017*.

Sprinkel, M.M., Hossain, M.S. & Ozyildirim, C. 2019. *Premature Failure of Concrete Patching: Reasons and Resolutions*.

Termkhajornkit, P., Nawa, T., Nakai, M. & Saito, T. 2005. Effect of fly ash on autogenous shrinkage. *Cement and Concrete Research*. 35(3):473–482. DOI: 10.1016/j.cemconres.2004.07.010.

Tilly, G. & Jacobs, J. 2007. Concrete Repairs: Observations on Performance in Service and Current Practice. *CONREPNET Project Report*. (IHS BRE Press, Watford, UK, (in press)).

Trost & H. 1967. Auswirkungen des Superpositionsprinzips auf Kriech-und Relaxationsprobleme bei Beton und Spannbeton. *Beton-und stahlbetonbau*. 10:230-238,261-269. Available: http://ci.nii.ac.jp/naid/10002938330/en/ [2021, March 16].

Vaysburd, A.M. 2006. Holistic system approach to design and implementation of concrete repair. *Cement & Concrete Composites*. 28:671–678. DOI: 10.1016/j.cemconcomp.2006.05.008.

Vaysburd, A.M. 2016. Specifying Concrete Repair Materials. *Materiały Budowlane*. 1(3):44–47. DOI: 10.15199/33.2016.03.13.

Vaysburd, A.M. & Emmons, P.H. 2006. Concrete repair - A composite system: Philosophy, engineering and practice. *Concrete Repair, Rehabilitation and Retrofitting - Proceedings of the International Conference on Concrete Repair, Rehabilitation and Retrofitting, ICCRRR 2005*. 12(5):9–11.

Vaysburd, A.M., Bissonnette, B. & von Fay, K.F. 2014. *Compatibility Issues in Design and Implementation of Concrete Repairs and Overlays*.

Wood, J.G.M., King, E.S. & Leek, D.S. 1990. Concrete Repair Materials for Effective Structural Application. *Construction & Building Materials*. 4(2):64–67. DOI: 10.1016/0950-0618(90)90002-I.

Yuan, Y.-S. & Marosszeky, M. 1994. Restrained shrinkage in repaired reinforced concrete elements. *Materials and Structures*. 27:375–382.

Zewdu, W., Sistonen, E. & Taffese. 2013. Service Life Prediction of Repaired Structures Using Concrete Recasting Method : State-Of-The-Art. In *Procedia Engineering*. V. 57. 1138–1144. DOI: 10.1016/j.proeng.2013.04.143.

Appendix A : Material Datasheets

BUILDING TRUST

PRODUCT DATA SHEET

Sika MonoTop®-615 HB

R4 High build repair and re-profiling mortar

DESCRIPTION

Sika MonoTop®-615 HB is a high build cementitious, polymer modified, one component repair and reprofiling mortar containing silica fume and Ferrogard corrosion inhibitor.

USES

- Suitable for restoration work (Principle 3, method 3.1 & 3.3 of EN 1504-9). Repair of spalling and damaged concrete in buildings, bridges, infrastructure and superstructure works.
- Suitable for structural strengthening (principle 4, method 4.4 of EN 1504-9). Increasing the bearing capacity of the concrete structure by adding mortar.
- Suitable for preserving or restoring passivity (principle 7, method 7.1 and 7.2 of EN 1504-9). Increasing cover with additional mortar and replacing contaminated or carbonated concrete.

CHARACTERISTICS / ADVANTAGES

- Polymer modified for increased durability
- Superior workability and finishing
- Suitable for hand and machine application
- Can be applied up to 70 mm thick per layer
- Class R4 of EN 1504-3
- Structural repair
- Very low shrinkage behaviour
- Contains corrosion inhibitor
- Low permeability

PRODUCT INFORMATION

Chemical Base	Cement and crystaline free silica aggregate
Packaging	25kg bag
Appearance / Colour	Powder Grey when Mixed
Shelf Life	12 Months in original, unopened packaging

Storage Conditions	Store properly in undamaged original sealed packaging, in dry cool conditions.
Density	Fresh mortar density ~1, 65kg/litre
Maximum Grain Size	D_{max}: 1.1 mm
Compressive Strength	Class R4 (EN 12190)

24 Hours	7 days	28 days
~18 MPa	~38 MPa	~46 MPa

SYSTEM INFORMATION

System Structure

Sika MonoTop®-615 HB is part of the range of Sika mortars complying with the relevant part of European Standard EN 1504 and comprising of:

Bonding Primer / Reinforcement Corrosion Protection

Sika® MonoTop® 610	Low demand requirements
SikaTop® Armatec® 110 EpoCem®	Demanding requirements

Repair Mortar	
Sika MonoTop®-615 HB	Class R4 concrete repair hand and & machine applied

Levelling Mortar	
Sikagard®-720 EpoCem®	Demanding requirements

APPLICATION INFORMATION

Mixing Ratio	3.5 to 4.0 litres of water for 25 kg powder
Consumption	This depends on the substrate roughness and thickness of layer applied. As a guide, ~ 19 kg of powder per cm thick per m²
Yield	25 kg of powder yields approximately 15.0 litres of mortar
Layer Thickness	min. 5 mm / max. 70 mm
Ambient Air Temperature	Min.5°C - Max.35°C
Substrate Temperature	Min.5°C - Max.30°C

BASIS OF PRODUCT DATA

All technical data stated in this Product Data Sheet are based on laboratory tests. Actual measured data may vary due to circumstances beyond our control.

LIMITATIONS

Freshly applied Sika® MonoTop® -615 HB should be protected from damp, condensation and water for at least 12 hours.
When spray applying Sika® MonoTop® products, water jet blasting is the preferred method of surface preparation and the surface profile should be greater than 2mm.
Sika® MonoTop®-610 should be used as bonding slurry for hand and spray applied applications.
When curing with polythene sheets, ensure all edges are fastened down and that air movement/circulation over the surface of the fresh mortar cannot occur.
Once Sika® MonoTop®-615HB has started to set, it should be discarded. Do not add more water to improve workability.
Concrete should be a minimum of 28 days old.

ECOLOGY HEALTH AND SAFETY

APPLICATION INSTRUCTIONS

SUBSTRATE QUALITY / PRE-TREATMENT

Concrete:
The concrete shall be thoroughly clean, free from dust, loose material, surface contamination and materials which reduce bond or prevent suction or wetting by repair materials. De-laminated, weak, damaged and deteriorated concrete and where necessary sound concrete shall be removed by suitable means.
Steel Reinforcement:
Rust, scale, mortar, concrete, dust and other loose and deleterious material which reduces bond or contributes to corrosion shall be removed. Surfaces shall be prepared using abrasive blast cleaning techniques or

high pressure water-blasting to Sa 2 (ISO 8501-1) Reference shall be made to EN1504-10 for specific requirements.

MIXING

Sika MonoTop®-615 HB can be mixed with a low speed (< 500 rpm) hand drill mixer or for machine application, using a force action mixer 2 to 3 bags or more at once depending the type and size of mixer.
Pour the recommended water in a suitable mixing container. While stirring slowly, add the powder to the water and mix thoroughly at least for 3 minutes adding additional water if necessary within the mixing time to the maximum specified amount and adjust to the required consistency.

APPLICATION

Bonding Primer:
Refer to the **System Information** above for compatible Sika products and refer to the relevant Product Data Sheet for instructions. Any bonding primer shall be applied on a pre-wet substrate and subsequent application of the repair mortar shall be applied wet on wet with the bonding primer.
Reinforcement Corrosion Protection:
Where a reinforcement coating is required the application of a repair mortar shall be applied wet on dry with the reinforcement corrosion protection. Refer to the **System Information** above for compatible Sika products and refer to the relevant Product Data Sheet for more detailed information about the reinforcement corrosion product.
Sika MonoTop®-615 HB can be applied either manually using traditional techniques or mechanically using wet spray equipment. Thoroughly pre-wet the prepared substrate a recommended 2 hours before application. Keep the surface wet and do not allow to dry. Before application remove excess water e.g. with a clean sponge. The surface shall appear a dark matt appearance without glistening and surface pores and pits shall not contain water.
Build up layers from bottom to top by pressing mortar well into the repair area. The surface can be finished according to the requirements using a float while wet or with a relevant rough-cast tool as soon as the mortar has started to stiffen.

CLEANING OF TOOLS

Application and mixing tools should be cleaned with water immediately after use. Hardened material must be removed mechanically.

LOCAL RESTRICTIONS

Please note that as a result of specific local regulations the performance of this product may vary from country to country. Please consult the local Product Data Sheet for the exact description of the application fields.

LEGAL NOTES

The information, and, in particular, the recommendations relating to the application and end-use of Sika products, are given in good faith based on Sika's current knowledge and experience of the products when properly stored, handled and applied under normal conditions in accordance with Sika's recommendations. In practice, the differences in materials, substrates and actual site conditions are such that no warranty in respect of merchantability or of fitness for a particular purpose, nor any liability arising out of any legal relationship whatsoever, can be inferred either from this information, or from any written recommendations, or from any other advice offered. The user of the product must test the product's suitability for the intended application and purpose. Sika reserves the right to change the properties of its products. The proprietary rights of third parties must be observed. All orders are accepted subject to our current terms of sale and delivery. Users must always refer to the most recent issue of the local Product Data Sheet for the product concerned, copies of which will be supplied on request. It may be necessary to adapt the above disclaimer to specific local laws and regulations. Any changes to this disclaimer may only be implemented with permission of Sika® Corporate Legal in Baar.

Sika South Africa (Pty) Ltd
9 Hocking Place,
Westmead, 3608
South Africa
Phone +27 31 792 6500
www.sika.co.za

BUILDING TRUST

PRODUCT DATA SHEET

SikaGrout®-212

High Strength shrinkage compensated cementitious grout

DESCRIPTION

SikaGrout®-212 is a 1-component, ready to mix, free flowing, low shrinkage expanding cementitious grout.

USES

- General purpose grouting
- Machine and base plates
- Dowling reinforcing bars
- Bedding joints in pre-cast concrete sections
- Filling cavities, voids, gaps and recesses
- Post fixings

CHARACTERISTICS / ADVANTAGES

- Easy to use (ready to mix powder)
- Shrinkage compensated properties
- Pre-batched for quality
- Good flow characteristics
- Good bond to concrete
- Non-corrosive
- No segregation or bleeding
- Can be pumped or poured

APPROVALS / STANDARDS

PRODUCT INFORMATION

Chemical Base	Cement, selected fillers and aggregates, special additives	
Packaging	25 kg bags	
Appearance / Colour	Grey powder	
Shelf Life	12 months from date of production	
Storage Conditions	Store properly in dry conditions in undamaged and unopened original sealed packaging.	
Maximum Grain Size	D_{max}: 2.4 mm	
Soluble Chloride Ion Content	≤ 0.05%	(EN 1015-17)

TECHNICAL INFORMATION

Compressive Strength	Ambient temperature 25ºC			
	1 days	**7 days**	**28 days**	(EN 196-1)
	~31 MPa	~80 MPa	~95 MPa	
Tensile Strength in Flexure	Ambient temperature +24ºC			
	1 day	**7 days**	**28 days**	
	~5.8 N/mm²	~8.3 N/mm²	~10.2 N/mm²	
Tensile Strength	Ambient temperature 24ºC			
	1 day	**7 day**	**28 day**	
	~2.6 N/mm²	~4.7 N/mm²	~5.4 N/mm²	

APPLICATION INFORMATION

Mixing Ratio	16% by weight - Max. 4.0 litres of water per 25 kg bag
Fresh mortar density	~2.3kg/l (density of fresh mortar)
Consumption	As a guide, ~20 kg of powder per 10 mm thickness for each m²
Yield	1 bag yields approximately ~12.5 l of mortar
Layer Thickness	Minimum 10 mm/ maximum 100 mm
Ambient Air Temperature	+5°C min. / +35°C max.
Substrate Temperature	+5°C min. / +30°C max.
Pot Life	~45 minutes at 24 °C

BASIS OF PRODUCT DATA

All technical data stated in this Product Data Sheet are based on laboratory tests. Actual measured data may vary due to circumstances beyond our control.

LIMITATIONS

- Not to be used as an overlay in unconfined spaces
- Not to be used as a hand applied patch repair
- Refer to the Sika Method Statement for more information
- Avoid application in direct sun and/or strong wind
- Do not add water over recommended dosage
- Apply only to sound, prepared substrate
- Do not add additional water after application as this may cause cracking
- Protect freshly applied material from freezing and frost
- Keep exposed surfaces to a minimum
- Do not vibrate

ECOLOGY HEALTH AND SAFETY

For information and advice on the safe handling, storage and disposal of chemical products, users shall refer to the most recent Safety Data Sheet (SDS) containing physical, ecological, toxicological and other safety-related data.

APPLICATION INSTRUCTIONS

SUBSTRATE QUALITY / PRE-TREATMENT

The concrete shall be thoroughly clean, free from dust, loose material, surface contamination and materials which reduce bond or prevent suction.

MIXING

Pour the water in the recommended proportion into a suitable mixing container. While stirring slowly, add the powder to the water. Mix with low speed (< 500 rpm) hand drill mixer to avoid entraining too much air. Mix thoroughly at least for 3 minutes until homogenous with no lumps. Mix only full bags for best results.

APPLICATION

Stand the grout for ~2-3 minutes; stir with a trowel and then pour into the prepared openings.
For more information on pouring techniques refer to Sika Method Statement

CURING TREATMENT

Protect the fresh material from premature drying using an appropriate curing method e.g. curing compound, moist geotextile membrane etc.

CLEANING OF TOOLS

Clean all tools and application equipment with water

immediately after use.

LOCAL RESTRICTIONS

Please note that as a result of specific local regulations the performance of this product may vary from country to country. Please consult the local Product Data Sheet for the exact description of the application fields.

LEGAL NOTES

The information, and, in particular, the recommendations relating to the application and end-use of Sika products, are given in good faith based on Sika's current knowledge and experience of the products when properly stored, handled and applied under normal conditions in accordance with Sika's recommendations. In practice, the differences in materials, substrates and actual site conditions are such that no warranty in respect of merchantability or of fitness for a particular purpose, nor any liability arising out of any legal relationship whatsoever, can be inferred either from this information, or from any written recommendations, or from any other advice offered. The user of the product must test the product's suitability for the intended application and purpose. Sika reserves the right to change the properties of its products. The proprietary rights of third parties must be observed. All orders are accepted subject to our current terms of sale and delivery. Users must always refer to the most recent issue of the local Product Data Sheet for the product concerned, copies of which will be supplied on request. It may be necessary to adapt the above disclaimer to specific local laws and regulations. Any changes to this disclaimer may only be implemented with permission of Sika® Corporate Legal in Baar.

Sika South Africa (Pty) Ltd
9 Hocking Place,
Westmead, 3608
South Africa
Phone +27 31 792 6500
www.sika.co.za

BUILDING TRUST

PRODUCT DATA SHEET

SikaGrout®-295 ZA

Fatigue tested, ultra-high strength cementitious grout

DESCRIPTION

SikaGrout®-295 ZA is a one component, ultra-high strength, cement based grout, with high mechanical strengths, specifically designed and fatigue tested for use in the renewable energy field, under metal bases and concrete structures.

USES

SikaGrout®-295 ZA may be used in areas where high mechanical strengths
are required, such as :

- Under Wind turbine bases
- Under bearing plates
- Between precast concrete segments
- Anchors in bases, concrete posts and precast construction columns.
- Cracks, gaps and large voids.

CHARACTERISTICS / ADVANTAGES

- Easy mixing and placing
- Rapid strength development
- Fatigue tested
- Good flow properties
- Pumpable
- Free from chlorides and metallic particles
- Protects metallic parts against corrosion, due to its high pH level.
- Expansive properties
- Very high mechanical strengths.
- Not corrosive or toxic

APPROVALS / STANDARDS

Fatigue tested according to fib Model code 2010

PRODUCT INFORMATION

Chemical Base	Cement, selected fillers, aggregates and special additives
Packaging	25kg bags
Appearance / Colour	Grey powder
Shelf Life	6 months from date of production
Storage Conditions	Store properly in dry conditions, in undamaged, original unopened bags
Density	~ 2.3 kg/l (density of fresh mortar)
Maximum Grain Size	Dmax: ~3 mm

TECHNICAL INFORMATION

Compressive Strength	Ambient temperature +20°C (water curing) (40 x 40 x 160mm prisms) **24 hours** ~ 35 N/mm²; **48 hours** ~ 50 N/mm²; **7 days** ~ 80 N/mm²; **28 days** ~95 N/mm²	(EN 12190)
Modulus of Elasticity in Compression	~30GPa	
Tensile Strength in Flexure	Ambient temperature: +20°C (water curing) **1 day** ~ 6.0 N/mm²; **7 days** ~ 8.0 N/mm²; **28 days** ~ 10.0 N/mm²	(EN12190)
Tensile Strength	Ambient temperature: +25°C (Splitting tensile) **1 day** ~ 2.6 N/mm²; **7 days** ~ 3.8 N/mm²; **28 days** ~ 4.8 N/mm²	(EN12190)

APPLICATION INFORMATION

Mixing Ratio	11.5 -12.0% or 2.87 - 3.0 litres per 25 kg bag / 57.5 - 60 litres per 500 kg
Consumption	*For 1 mm thickness per m²* ~ 2.05 kg of powder
Yield	*~12.0 ltr per 25kg bag*
Layer Thickness	10 mm min. / 150 mm max
Ambient Air Temperature	+5º C min / +35º C max.
Substrate Temperature	+5º C min / +35º C max.
Pot Life	**Conditions**: +20°C / 50% r.h.; **Time**: 90 minutes Temperature will affect the pot life. Application at temperatures above +23°C will reduce the pot life and the working time. Temperatures below +23ºC will increase the pot life and extend the working time.

BASIS OF PRODUCT DATA

All technical data stated in this Product Data Sheet are based on laboratory tests. Actual measured data may vary due to circumstances beyond our control.

ECOLOGY HEALTH AND SAFETY

For information and advice on the safe handling, storage and disposal of chemical products, users shall refer to the most recent Safety Data Sheet (SDS) containing physical, ecological, toxicological and other safety related data.

APPLICATION INSTRUCTIONS

SUBSTRATE QUALITY / PRE-TREATMENT

The concrete shall be thoroughly clean, free from dust, loose material, surface contamination and materials which reduce bond or prevent suction or wetting by the grout. Delaminated, weak, damaged and deteriorated concrete and where necessary sound concrete shall be removed by suitable means. It is recommended the concrete surface shall be continuously saturated with clean water for at least 2 hours before grouting.

MIXING

SikaGrout®-295 ZA can be mixed with a low speed (<500rpm) hand drill mixer to avoid entraining too much air.Mix only full bags for best results.
Pour the minimum recommended water in a suitable mixing container. While stirring slowly, add the powder to the water and mix thoroughly at least for 3 minutes adding additional water if necessary to the maximum specified amount to adjust the grout to the required consistency

APPLICATION

SikaGrout®-295 ZA is applied manually using traditional pouring techniques or for large applications using suitable pumping device. (refer to Sika technical department for advice). It is recommended to check the material after pumping.
Remove excess water from substrate surface e.g. with clean sponge, until surface is dark matt in appearance without glistening (saturated surface dry) . Surface pores and pits shall not contain water. Let the grout stand for ~5 minutes to release air entrained by mixing. Pour grout into the prepared openings using a sufficient pressure head to maintain a continuous flow of grout. Ensure air displaced by the mortar can easily escape. For optimum use of the expansion properties apply the grout within ~10 minutes after mixing.
Cure exposed surfaces immediately with protective sheet or membrane. Shield the fresh mortar from direct sun, wind and frost.
Finish exposed surface as desired as soon as the mortar has started to stiffen. Do not add additional water on surface. Do not over work surface as this may cause surface cracking.

CURING TREATMENT

Keep visible exposed grout surfaces to a minimum. Protect the fresh material from premature drying using appropriate curing method e.g. curing compound, moist textile membrane, polythene sheet etc.

CLEANING OF TOOLS

Clean all tools and application equipment with water immediately after use. Hardened/cured material can only be mechanically removed.

LOCAL RESTRICTIONS

Please note that as a result of specific local regulations the performance of this product may vary from country to country. Please consult the local Product Data Sheet for the exact description of the application fields.

LEGAL NOTES

The information, and, in particular, the recommendations relating to the application and end-use of Sika products, are given in good faith based on Sika's current knowledge and experience of the products when properly stored, handled and applied under normal conditions in accordance with Sika's recommendations. In practice, the differences in materials, substrates and actual site conditions are such that no warranty in respect of merchantability or of fitness for a particular purpose, nor any liability arising out of any legal relationship whatsoever, can be inferred either from this information, or from any written recommendations, or from any other advice offered. The user of the product must test the product's suitability for the intended application and purpose. Sika reserves the right to change the properties of its products. The proprietary rights of third parties must be observed. All orders are accepted subject to our current terms of sale and delivery. Users must always refer to the most recent issue of the local Product Data Sheet for the product concerned, copies of which will be supplied on request. It may be necessary to adapt the above disclaimer to specific local laws and regulations. Any changes to this disclaimer may only be implemented with permission of Sika® Corporate Legal in Baar.

Sika South Africa (Pty) Ltd
9 Hocking Place,
Westmead, 3608
South Africa
Phone +27 31 792 6500
www.sika.co.za

Appendix B: Material Test Results

Table B - 1: 1-day compressive strength test results

Sample ID		Cube mass (g)	Density (kg/m^3)	Failure load (kN)	Compressive strength (MPa)	Avg. compressive strength (MPa)
HS-G	1	2115	2115	390	39.0	39.4
	2	2195	2195	395	39.5	
	3	2160	2160	397	39.7	
HS-C	1	2275	2275	416	41.6	41.7
	2	2319	2319	417	41.7	
	3	2307	2307	419	41.9	
UHS-G	1	2179	2179	360	36.0	36.3
	2	2204	2204	358	35.8	
	3	2196	2196	371	37.1	
PMRM	1	1770	1770	171	17.1	16.9
	2	1748	1748	173	17.3	
	3	1759	1759	164	16.4	

Table B - 2: 7-day compressive strength test results

Sample ID		Cube mass (g)	Density (kg/m^3)	Failure load (kN)	Compressive strength (MPa)	Avg. compressive strength (MPa)
HS-G	1	2166	2166	596	59.6	59.3
	2	2140	2140	588	58.8	
	3	2117	2117	596	59.6	
HS-C	1	2285	2285	642	64.2	66.8
	2	2306	2306	674	67.4	
	3	2295	2295	688	68.8	
UHS-G	1	2221	2221	600	60.0	61.7
	2	2211	2211	670	67.0	
	3	2224	2224	580	58.0	
PMRM	1	1733	1733	271	27.1	30.9
	2	1799	1799	327	32.7	
	3	1781	1781	328	32.8	

Table B - 3: 28-day compressive strength test results

Sample ID		Cube mass (g)	Density (kg/m^3)	Failure load (kN)	Compressive strength (MPa)	Avg. compressive strength (MPa)
HS-G	1	2150	2150	682	68.2	70.7
	2	2176	2176	720	72.0	
	3	2154	2154	718	71.8	
HS-C	1	2294	2294	870	87.0	77.0
	2	2220	2220	720	72.0	
	3	2296	2296	720	72.0	
UHS-G	1	2190	2190	840	84.0	79.3
	2	2188	2188	780	78.0	
	3	2162	2162	760	76.0	
PMRM	1	1686	1686	376	37.6	38.2
	2	1701	1701	350	35.0	
	3	1762	1762	420	42.0	

Table B - 4: 1-day tensile splitting strength test results

Sample ID		Cube mass (g)	Density (kg/m^3)	Failure load (kN)	Tensile splitting strength (MPa)	Avg. tensile splitting strength (MPa)
HS-G	1	2200	2178	57	3.6	3.5
	2	2250	2162	55	3.5	
	3	2200	2187	55	3.5	
HS-C	1	2350	2309	70	4.5	4.2
	2	2350	2283	58	3.7	
	3	2350	2281	70	4.5	
UHS-G	1	2300	2191	64	4.1	3.7
	2	2300	2201	50	3.2	
	3	2300	2195	62	3.9	
PMRM	1	1850	1785	31	2.0	2.1
	2	1800	1731	34	2.2	
	3	1750	1745	31	2.0	

Table B - 5: 7-day tensile splitting strength test results

Sample ID		Cube mass (g)	Density (kg/m^3)	Failure load (kN)	Tensile splitting strength (MPa)	Avg. tensile splitting strength (MPa)
HS-G	1	2150	2159	65	4.1	4.4
	2	2250	2198	78	5.0	
	3	2200	2200	64	4.1	
HS-C	1	2350	2280	71	4.5	4.8
	2	2350	2279	75	4.8	
	3	2350	2293	78	5.0	
UHS-G	1	2250	2187	67	4.3	4.1
	2	2300	2222	62	3.9	
	3	2350	2206	64	4.1	
PMRM	1	1800	1770	40	2.5	2.6
	2	1800	1767	41	2.6	
	3	1850	1795	42	2.7	

Table B - 6: 28-day tensile splitting test results

Sample ID		Cube mass (g)	Density (kg/m^3)	Failure load (kN)	Tensile splitting strength (MPa)	Avg. tensile splitting strength (MPa)
HS-G	1	2250	2186	66	4.2	4.6
	2	2300	2206	74	4.7	
	3	2250	2176	75	4.8	
HS-C	1	2350	2266	73	4.6	4.7
	2	2350	2287	78	5.0	
	3	2300	2270	71	4.5	
UHS-G	1	2300	2154	71	4.5	4.3
	2	2300	2235	67	4.3	
	3	2300	2207	65	4.1	
PMRM	1	1750	1728	57	3.6	3.4
	2	1800	1727	53	3.4	
	3	1800	1770	52	3.3	

Table B - 7: 1-day static elastic modulus test results

Sample ID		Elastic modulus (GPa)	Avg. elastic modulus (MPa)	Std. Dev
HS-G	1	25.7	27.1	1.49
	2	27.1		
	3	28.6		
HS-C	1	26.5	25.5	1.37
	2	23.9		
	3	26.0		
UHS-G	1	21.0	21.2	2.58
	2	18.8		
	3	23.9		

Table B - 8: 7-day static elastic modulus test results

Sample ID		Elastic modulus (GPa)	Avg. elastic modulus (MPa)	Std. Dev
HS-G	1	27.4	27.9	0.48
	2	28.1		
	3	28.4		
HS-C	1	32.5	33.0	2.84
	2	36.1		
	3	30.4		
UHS-G	1	27.7	28.8	1.01
	2	29.7		
	3	29.1		

Table B - 9: 28-day static elastic modulus test results

Sample ID		Elastic modulus (GPa)	Avg. elastic modulus (MPa)	Std. Dev
HS-G	1	32.6	33.5	1.20
	2	34.8		
	3	33.1		
HS-C	1	28.6	28.3	0.89
	2	27.3		
	3	29.0		
UHS-G	1	30.7	31.0	0.24
	2	31.2		
	3	31.1		

Table B - 10: Shrinkage strain test results for HS grout measured from age 1 day

Age (days)	Shrinkage (microstrains)			Average Shrinkage (microstrains)
	HS-G S1	HS-G S2	HS-G S3	
0	0	0	0	0
1 hr	0	0	0	0
6 hr	-5	5	15	5
1	10	-5	20	8
2	100	170	125	132
3	135	130	200	155
4	170	175	230	192
5	215	175	260	217
6	220	195	250	222
7	230	190	250	223
8	235	210	290	245
9	240	205	295	247
10	215	225	290	243
11	220	220	305	248
12	220	230	300	250
13	235	235	300	257
14	235	240	310	262
15	240	240	310	263
21	245	245	315	268
27	255	245	315	272
29	255	250	325	277
34	260	255	325	280
37	265	260	330	285
42	270	265	335	290
47	275	270	345	297
65	280	275	345	300
72	285	280	350	305
79	290	280	350	307
90	290	285	355	310

Table B - 11: Shrinkage strain test results for HS concrete measured from age 1 day

Age (days)	Shrinkage (microstrains)			Average Shrinkage (microstrains)
	HS-C S1	HS-C S2	HS-C S3	
0	0	0	0	0
1 hr	100	5	40	55
6 hr	135	30	100	95
1	190	105	170	167
2	255	125	230	210
3	290	190	220	250
4	300	195	220	255
5	295	205	150	247
6	295	225	210	267
7	330	230	260	293
8	320	250	260	298
9	315	235	240	292
10	315	240	240	292
11	335	230	240	288
12	335	240	250	293
13	345	240	260	303
19	350	240	270	307
25	355	245	270	312
27	355	240	270	308
32	365	245	270	315
35	365	245	270	315
40	370	245	280	318
45	375	255	280	325
63	385	255	280	330
70	385	270	280	335
77	385	285	290	340
88	385	285	290	340

Table B - 12: Shrinkage strain test results for UHS grout measured from age 1 day

Age (days)	Shrinkage (microstrains)			Average Shrinkage (microstrains)
	UHS-G S1	UHS-G S2	UHS-G S3	
0	0	0	0	0
1 hr	20	20	20	20
6 hr	35	30	20	28
1	50	105	50	68
2	110	170	120	133
3	120	140	75	112
4	150	220	150	173
5	145	215	130	163
6	115	245	170	177
7	125	310	215	217
8	110	295	250	218
9	130	270	240	213
10	155	270	230	218
11	165	265	235	222
12	170	270	240	227
13	170	275	240	228
14	180	285	230	232
20	175	285	240	233
26	175	290	240	235
28	190	280	230	233
33	190	285	235	237
36	195	280	240	238
41	195	290	245	243
46	200	295	245	247
64	195	295	255	248
71	205	295	255	252
78	215	295	265	258
89	215	295	265	258

Table B - 13: Creep test results for HS grout loaded at age 1 day @ 11 MPa

Age (days)	Cumulative strain		Avg. cumulative strain (μ-ε)	Control strain (μ-ε)	Net creep strain (μ-ε)	Specific creep (μ-ε/MPa)
	HS-G C1-1	HS-G C2-1				
0	460*	487*	473*	0	-	-
1 hr	550	603	577	0	103	9
6 hr	657	750	703	5	225	20
1	803	863	833	8	352	32
2	923	1030	977	132	372	34
3	973	1097	1035	155	407	37
4	1070	1230	1150	192	485	44
5	1177	1313	1245	217	555	50
6	1203	1353	1278	222	583	53
7	1297	1447	1372	223	675	61
8	1297	1530	1413	245	695	63
9	1350	1570	1460	247	740	67
10	1390	1617	1503	243	787	72
11	1500	1610	1555	248	833	76
12	1533	1717	1625	250	902	82
13	1553	1727	1640	257	910	83
14	1580	1787	1683	262	948	86
15	1613	1820	1717	263	980	89
21	1680	1883	1782	268	1040	95
27	1740	1967	1853	272	1108	101
29	1790	1977	1883	277	1133	103
34	1783	2020	1902	280	1148	104
37	1810	2067	1938	285	1180	107
42	1830	2073	1952	290	1188	108
47	1833	2093	1963	297	1193	108
65	1883	2163	2023	300	1250	114
72	1900	2163	2032	305	1253	114
79	1950	2223	2087	307	1307	119
90	1957	2227	2092	310	1308	119

* initial elastic strain at loading instant

Table B - 14: Creep test results for HS concrete loaded at age 1 day @ 11 MPa

Age (days)	Cumulative strain		Avg. cumulative strain (μ-ε)	Control strain (μ-ε)	Net creep strain (μ-ε)	Specific creep (μ-ε/MPa)
	HS-C C1-1	HS-C C2-1				
0	370*	403*	387*	0	-	-
1 hr	473	577	525	55	83	8
6 hr	597	717	657	95	175	16
1	770	963	867	167	313	28
2	843	1080	962	210	365	33
3	937	1147	1042	250	405	37
4	1030	1247	1138	255	497	45
5	1077	1287	1182	247	548	50
6	1100	1343	1222	267	568	52
7	1187	1427	1307	293	627	57
8	1243	1477	1360	298	675	61
9	1290	1507	1398	292	720	65
10	1373	1573	1473	292	795	72
11	1347	1593	1470	288	795	72
12	1350	1630	1490	293	810	74
13	1407	1723	1565	303	875	80
19	1510	1797	1653	307	960	87
25	1617	1873	1745	312	1047	95
27	1597	1870	1733	308	1038	94
32	1647	1933	1790	315	1088	99
35	1667	1960	1813	315	1112	101
40	1680	1963	1822	318	1117	102
45	1683	1987	1835	325	1123	102
63	1767	2077	1922	330	1205	110
70	1770	2067	1918	335	1197	109
77	1787	2107	1947	340	1220	111
88	1787	2110	1948	340	1222	111

* initial elastic strain at loading instant

Table B - 15: Creep test results for UHS grout loaded at age 1 day @ 11 MPa

Age (days)	Cumulative strain		Avg. cumulative strain (μ-ε)	Control strain (μ-ε)	Net creep strain (μ-ε)	Specific creep (μ-ε/MPa)
	UHS-G C1-1	UHS-G C2-1				
0	527*	567*	547*	0	-	-
1 hr	713	783	748	20	182	17
6 hr	673	810	742	28	167	15
1	987	1073	1030	68	415	38
2	1117	1203	1160	133	480	44
3	1200	1300	1250	112	592	54
4	1293	1377	1335	173	615	56
5	1367	1423	1395	163	685	62
6	1420	1497	1458	177	735	67
7	1443	1630	1537	217	773	70
8	1493	1643	1568	218	803	73
9	1570	1707	1638	213	878	80
10	1593	1713	1653	218	888	81
11	1620	1757	1688	222	920	84
12	1627	1780	1703	227	930	85
13	1687	1837	1762	228	987	90
14	1727	1850	1788	232	1010	92
20	1800	1917	1858	233	1078	98
26	1847	2037	1942	235	1160	105
28	1837	2047	1942	233	1162	106
33	1877	2057	1967	237	1183	108
36	1900	2083	1992	238	1207	110
41	1910	2090	2000	243	1210	110
46	1907	2097	2002	247	1208	110
64	1943	2127	2035	248	1240	113
71	1963	2130	2047	252	1248	113
78	1997	2157	2077	258	1272	116
89	2000	2140	2070	258	1265	115

* initial elastic strain at loading instant

Table B - 16: Creep test results for HS grout loaded at age 7 day @ 19.8 MPa

Age (days)	Cumulative strain		Avg. cumulative strain (μ-ε)	Control strain (μ-ε)	Net creep strain (μ-ε)	Specific creep (μ-ε/MPa)
	HS-G C1-7	HS-G C2-7				
0	600*	647*	623*	0	-	-
1 hr	837	890	863	0	240	12
6 hr	933	927	930	2	305	15
1	1037	1083	1060	13	423	21
2	1223	1191	1207	23	561	28
3	1353	1393	1373	25	725	37
4	1450	1463	1457	22	812	41
5	1553	1560	1557	27	907	46
6	1647	1673	1660	28	1008	51
7	1730	1777	1753	35	1095	55
8	1807	1850	1828	40	1165	59
9	1870	1903	1887	42	1222	62
15	1977	2037	2007	47	1337	68
21	2143	2230	2187	50	1513	76
23	2153	2260	2207	55	1528	77
28	2213	2303	2258	58	1577	80
31	2243	2337	2290	63	1603	81
36	2257	2357	2307	68	1615	82
41	2260	2390	2325	75	1627	82
59	2347	2473	2410	78	1708	86
66	2370	2483	2427	83	1720	87
73	2440	2553	2497	85	1788	90
84	2447	2577	2512	88	1800	91

* initial elastic strain at loading instant

Table B - 17: Creep test results for HS concrete loaded at age 7 day @ 19.8 MPa

Age (days)	Cumulative strain		Avg. cumulative strain (μ-ε)	Control strain (μ-ε)	Net creep strain (μ-ε)	Specific creep (μ-ε/MPa)
	HS-C C1-7	HS-C C2-7				
0	637*	617*	627*	0	-	-
1 hr	733	813	773	10	137	7
6 hr	807	880	843	20	197	10
1	917	980	948	27	295	15
2	1070	1100	1085	32	427	22
3	1230	1203	1217	25	565	29
4	1247	1227	1237	25	585	30
5	1347	1307	1327	22	678	34
6	1400	1403	1402	27	748	38
7	1423	1450	1437	37	773	39
13	1493	1543	1518	40	852	43
19	1627	1680	1653	45	982	50
21	1657	1673	1665	42	997	50
26	1697	1743	1720	48	1045	53
29	1740	1787	1763	48	1088	55
34	1780	1817	1798	52	1120	57
39	1780	1833	1807	58	1122	57
57	1860	1877	1868	63	1178	60
64	1867	1920	1893	68	1198	61
71	1920	1967	1943	73	1243	63
82	1920	1983	1952	73	1252	63

* initial elastic strain at loading instant

Table B - 18: Creep test results for UHS grout loaded at age 7 day @ 19.8 MPa

Age (days)	Cumulative strain		Avg. cumulative strain (μ-ε)	Control strain (μ-ε)	Net creep strain (μ-ε)	Specific creep (μ-ε/MPa)
	UHS-G C1-7	UHS-G C2-7				
0	627*	613*	620*	0	-	-
1 hr	887	887	887	5	262	13
6 hr	947	957	952	30	302	15
1	1010	1053	1032	40	372	19
2	1100	1150	1125	42	463	23
3	1213	1247	1230	37	573	29
4	1313	1367	1340	42	678	34
5	1373	1440	1407	45	742	37
6	1560	1563	1562	50	892	45
7	1607	1630	1618	52	947	48
8	1650	1680	1665	55	990	50
14	1743	1767	1755	57	1078	54
20	1847	1880	1863	58	1185	60
22	1860	1903	1882	57	1205	61
27	1937	1950	1943	60	1263	64
30	1973	1990	1982	62	1300	66
35	2017	2023	2020	67	1333	67
40	2023	2027	2025	70	1335	67
58	2080	2083	2082	72	1390	70
65	2087	2117	2102	75	1407	71
72	2113	2147	2130	82	1428	72
83	2123	2160	2142	82	1440	73

* initial elastic strain at loading instant

Appendix C : Creep Modelling

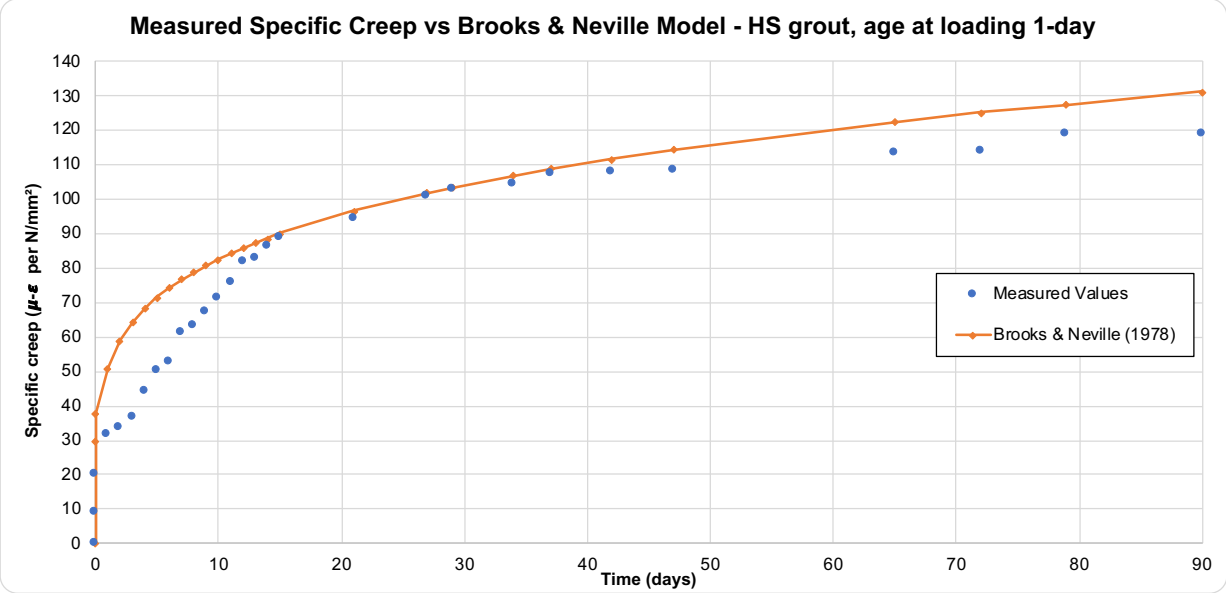

Figure C - 1: Measured specific creep vs Brooks & Neville (1978) – HS grout, age at loading 1-day

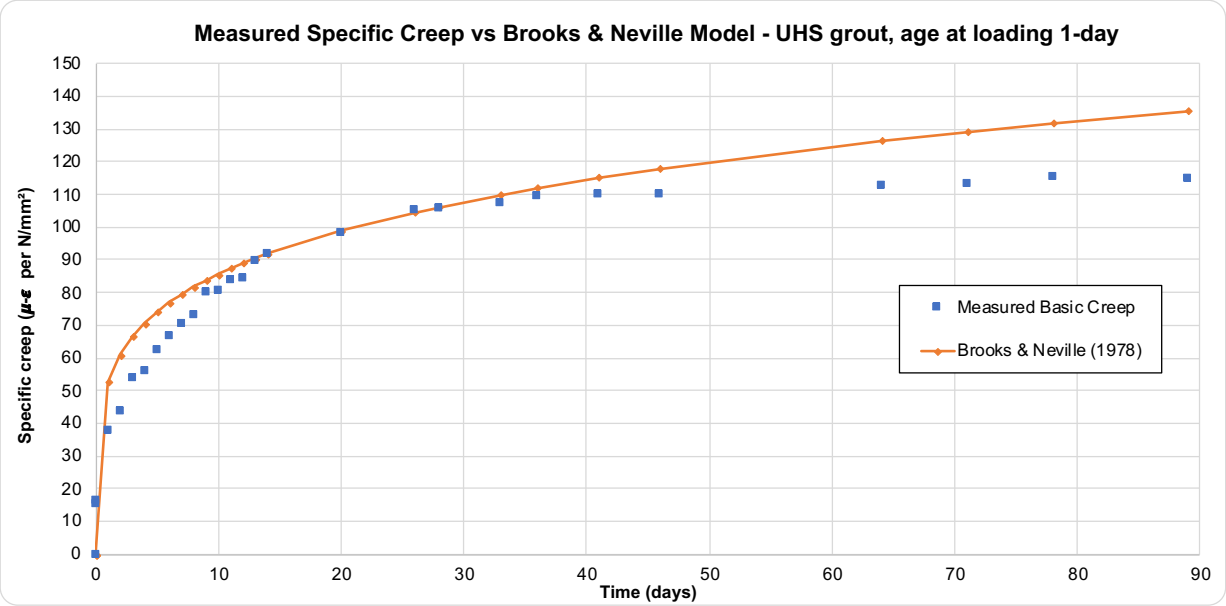

Figure C - 2: Measured specific creep vs Brooks & Neville (1978) – UHS grout, age at loading 1-day

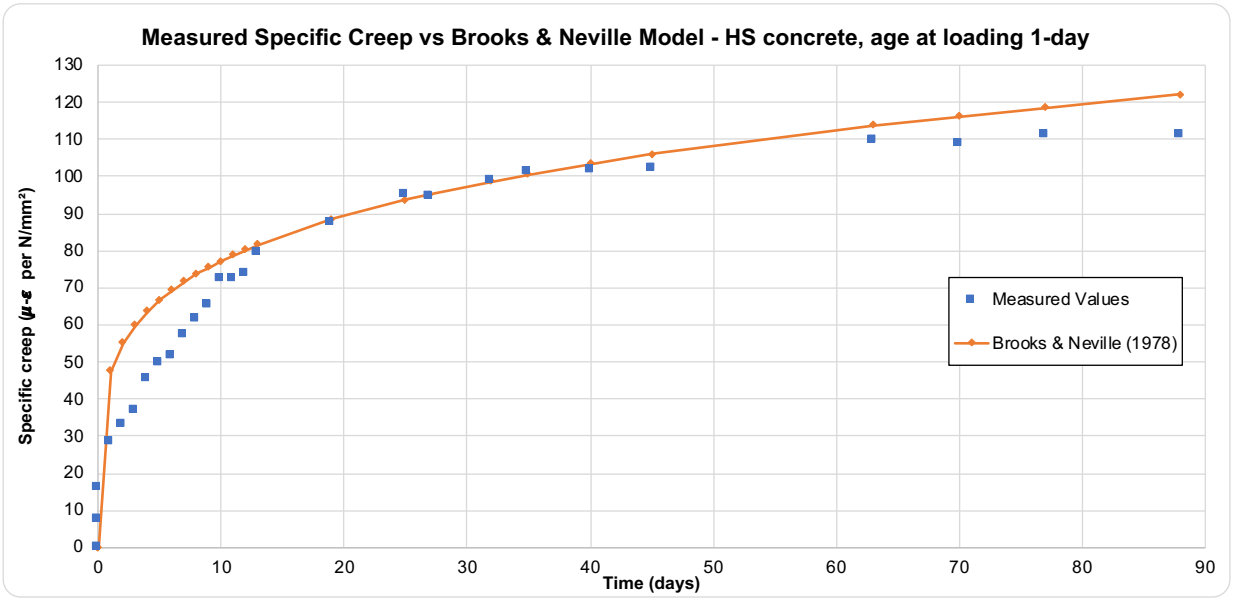

Figure C - 3: Measured specific creep vs Brooks & Neville (1978) – HS concrete, age at loading 1-day

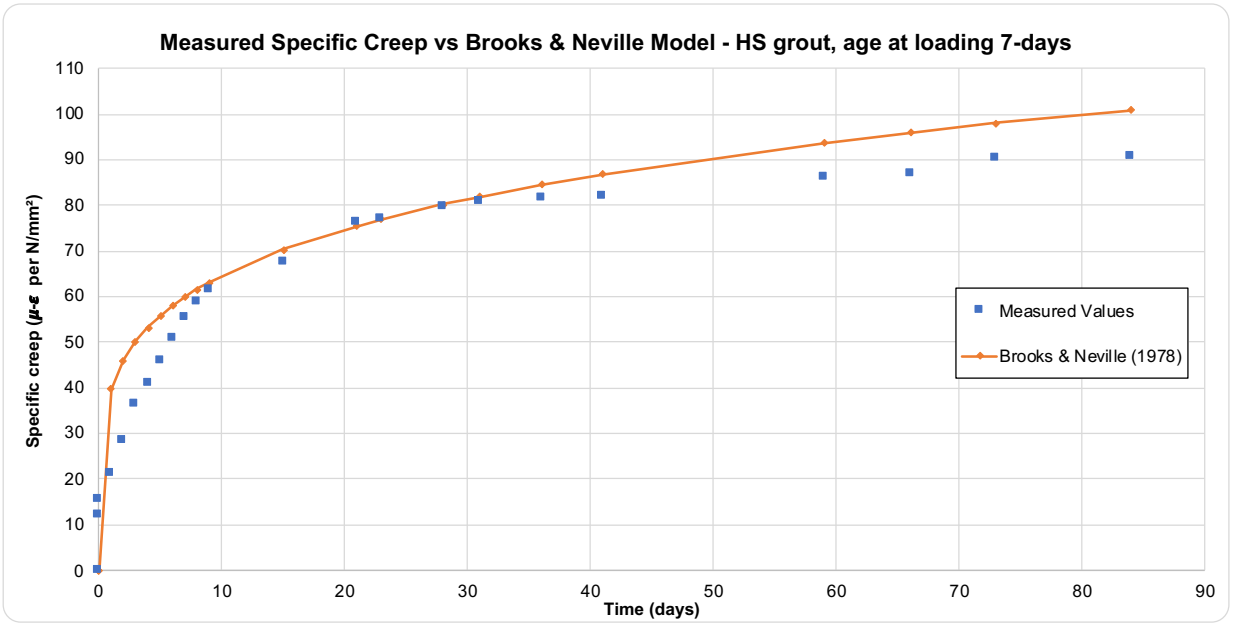

Figure C - 4: Measured specific creep vs Brooks & Neville (1978) – HS grout, age at loading 7-days

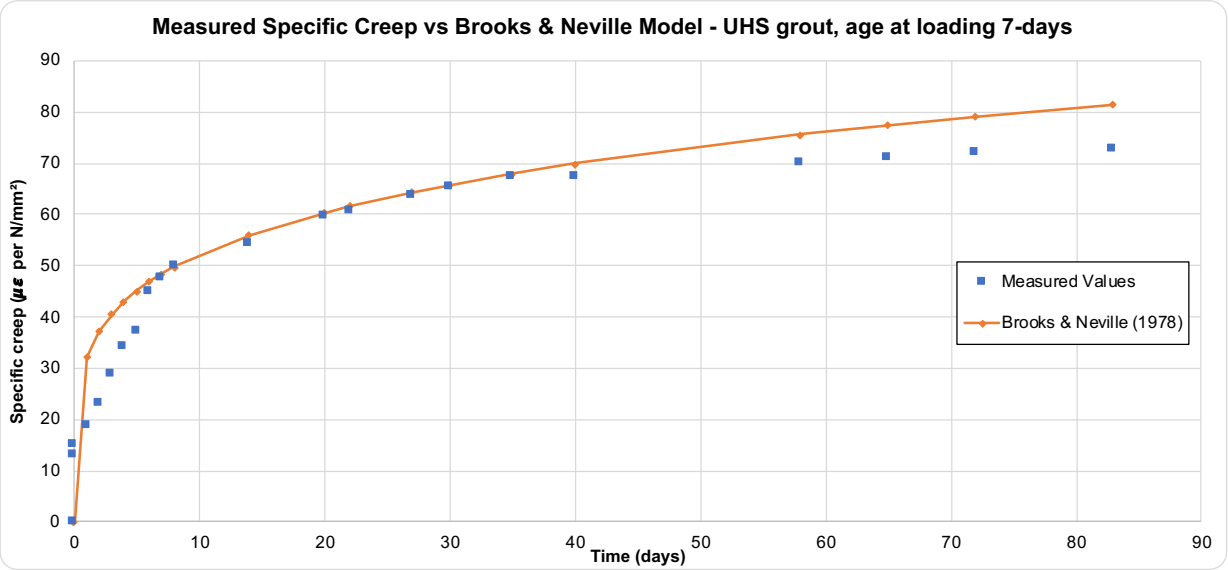

Figure C - 5: Measured specific creep vs Brooks & Neville (1978) – UHS grout, age at loading 7-days

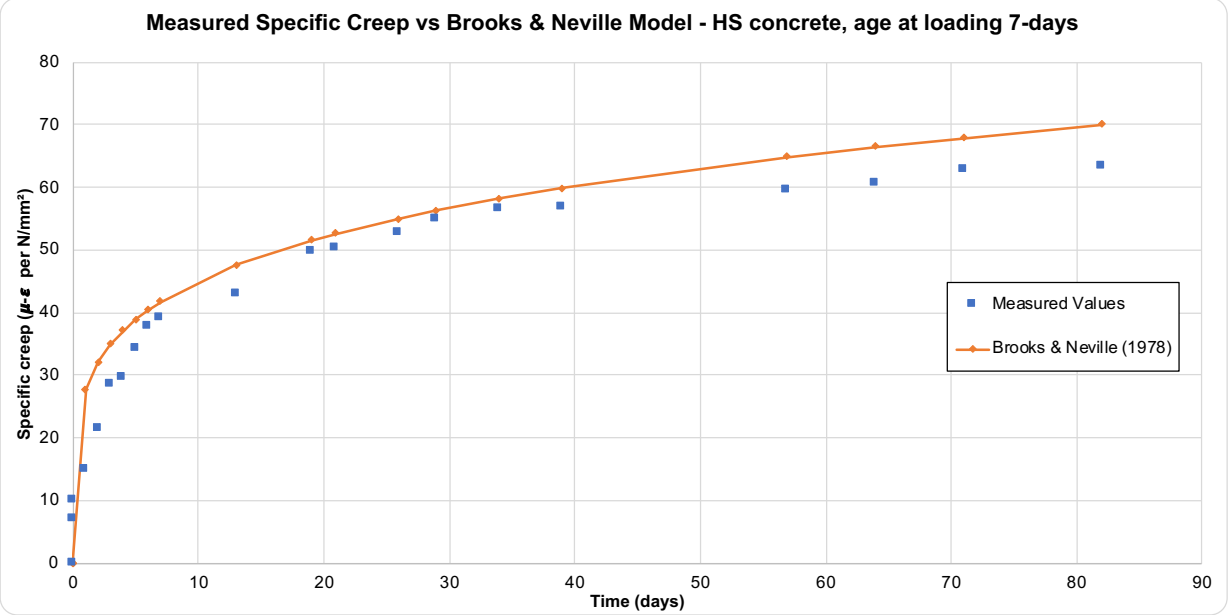

Figure C - 6: Measured specific creep vs Brooks & Neville (1978) – HS concrete, age at loading 7-days